Flue gas cleaning by pulse corona streamer

tu/e
Research Report
ISSN 0167-9708
Coden: TEUEDE

Eindhoven
University of Technology
Netherlands

Faculty of Electrical Engineering

Flue Gas Cleaning by Pulse Corona Streamer

by
Yan Keping
E.M. van Veldhuizen

EUT Report 93-E-272
ISBN 90-6144-272-9
March 1993

Eindhoven University of Technology Research Reports

EINDHOVEN UNIVERSITY OF TECHNOLOGY

Faculty of Electrical Engineering
Eindhoven, The Netherlands

ISSN 0167-9708 Coden: TEUEDE

FLUE GAS CLEANING BY PULSE CORONA STREAMER

by

Yan Keping
E.M. van Veldhuizen

EUT Report 93-E-272
ISBN 90-6144-272-9

Eindhoven
March 1993

CIP-GEGEVENS KONINKLIJKE BIBLIOTHEEK, DEN HAAG

Yan, Keping

Flue gas cleaning by pulse corona streamer / by Yan Keping, E.M. van Veldhuizen. - Eindhoven : Eindhoven University of Technology, Faculty of Electrical Engineering. - Fig. - (EUT report, ISSN 0167-9708 ; 93-E-272)
Met lit. opg., reg.
ISBN 90-6144-272-9
NUGI 832
Trefw.: rookgasreiniging / corona / hoogspanningspulsen.

Flue gas cleaning by pulse corona streamer
Yan Keping and E.M. van Veldhuizen

Abstract

Currents of upto 600 A are obtained on a corona wire of 1 m length by applying DC and pulse voltage. The energy input is upto 6 J/pulse. The current duration is between 100 and 600 ns, and depends strongly on the DC voltage, the stray inductance and resistance of the circuit. Breakdown can be avoided by choosing the appropriate values for the components in the pulse circuit.

Average electron energies resolved in space and in time are obtained by means of optical spectroscopy for corona discharge streamers in a wire-cylinder reactor in air and in flue gas. It was found that the electron energy for primary streamers in air is in the order of 10 eV, it increases slightly with the pulse voltage and is almost constant during the streamer propagation. The electron energy for the secondary streamer is about a factor two lower near the anode where its optical emission is strong. In the gap and near the cathode its emission is much less and the electron energy is another three times lower. The secondary streamer is limited in length, because it must satisfy the stability field requirement. The larger attachment coefficient of flue gas in the low field region explains that in flue gas the secondary streamer is shorter than in air. The ratio of the electrical energy input into primary and secondary streamers is controlled by the length of the electrical pulse. Measurements of NO removal from flue gas indicate that a pulse duration equal to the time required by the primary streamer to cross the gap gives the highest cleaning efficiency.

Keywords: pulsed corona, streamer discharge, flue gas, NOx removal, spectroscopy

- Yan Keping and E.M. van Veldhuizen
Flue gas cleaning by pulse corona streamer.
Eindhoven: Faculty of Electrical Engineering, Eindhoven University of Technology, 1993
EUT Report 93-E-272

- Adresses of the authors:

Yan Keping
Department of Applied Physics
Beijing Institute of Technology
Beijing 100081, China

E.M. van Veldhuizen
Division of Electrical Energy Systems
Faculty of Electrical Engineering
Eindhoven University of Technology
PO Box 513, 5600 MB Eindhoven, The Netherlands

CONTENTS

Preface

-------to my wife-------

During this period, the main research is focused on the influence of pulse voltage generator on the streamer structure in order to optimise the energization processes, and to create the possibility to investigate the chemical reactivity of pulse corona streamer. It has been found that with modifying the electric circuit, different streamer structures can be produced with different active electrons production.

By means of local light emission near the emitting wire and near the cathode, it has been observed that with increasing applied voltage, the primary streamer could cross the gap, while the secondary streamers usually stop between the electrodes. The propagation speed for the primary streamer increases with increasing the applied voltage.

With the time-resolved spectrum measurements, it can be concluded that the mean electron energy releated to the primary streamer is much larger than that for the secondary streamers. The mean electron energy for the primary streamer is supposed to be almost constant along the channel; however, the energy for the secondary streamer it will decrease from the anode to the cathode.

Two type of energization has been proposed in order to optimise the energization processes. The main point to influence the energy conversion process from the pulse voltage generator to reactor is the rise rate of pulse voltage and the available stored energy in the circuit, which lead to different effects of DC bias level, pulse voltage level and the circuit parameters. New criterian for designing the pulse voltage generator are also presented based on the limitation of secondary streamers.

I am very grateful for Dr. van Veldhuizen to receive me to study on this project in Eindhoven and I do appreciate our invaluabe discussions and his promotions for each step of the investigation. I would also like thank Dr. Creyghton, Prof. Rutgers for the invaluable discussions and promotions, and the helpful assitance by Dr. Creyghton on the data processing. I especially like thank Mr. Baede for the successful cooperation and discussions, and all these effects together make this experimental investigation be realized within this period.

I would also like thank NWO for the fianicial support for my visitation.

Keping Yan

LIST OF SYMBOLS

DeNOx	removal of NO and NO_2 (from flue gas)
DeSOx	removal of SO_2 and SO_3 (from flue gas)
E-beam	electron beam (800 keV energy)
EMI	electromagnetic interference
ESP	electrostatic precipitator
<E>	average electron energy
FNS	first negative system (emission of N_2 ions, maximum at 391.4 nm)
Li	series inductance in pulse forming loop
NOx	mixture of NO and NO_2
R	series resistance in pulse forming loop
RH	relative humidity
SPS	second positive system (emission of N_2 neutrals, max. at 337.1 nm)
Vdc	DC bias voltage on corona wire
Vp	maximum of voltage pulse on corona wire
$B\ ^3\Pi_g$	lower level of SPS transition
$B\ ^2\Sigma_u^+$	upper level of FNS transition
$C\ ^3\Pi_u$	upper level of SPS transition
$X\ ^2\Sigma_g^+$	lower level of FNS transition

1. INTRODUCTION

Up to date, we have collected quite a lot of information on pulsed corona streamer properties and chemical kinetics on the processes for flue gas cleaning by pulse corona or by E-beam. There are also lots of publications on these tecniques [1,2].

In this section, I just like to emphasis some points, I suppose, which are very important for further study and to describe the main purposes of this investigation.

1.1 Current status of De-SOx and De-NOx by pulse corona streamer

Both pilot and experimental investigations have indicated that the technique by pulse corona for flue gas cleaning seems a very competitive method in the future and also shown that the main problem for the applications of this technique is the global energy consumption.

Current study on reducing the global energy consumption seem to be focused on two points:

- from chemical point of view, to enhance the heterogeneous reactions before and after corona streamer and to enhance the mass growing process during and after discharging period.

- from energization point of view, the main point is to optimise streamer structure in order to increase active electrons productions per unit energy injection.

As we have noticed that both E-beam and pulse corona streamer can enhance the global chemical reaction rate and it is also possible to obtain a very larger global G value by experiments [3]. However, the operations are based on experiences. As for as the physical and chemical models, current comprehensive schemes are based on combustion chemistry and atmospheric chemistry and it is still unable to expain or to predicate many experimental phenomena in terms of the model.

In contrasting E-beam with pulse corona streamer, the energy dissipation processes are completely different and the initial physical and chemical processes are supposed to be able to play a different role in the initial radical production. However, the main chemical and physical elementary process and the mass growing process are supposed to be very similar to the acid rain formation processes.

The key point for evaluation of the possible techniques for removal of SOx and NOx in industry is which techniques, E-beam or pulse corona, can effectively enhance the heterogeneous reactions and to obtain an acceptable energy consumption. Based on current investigations, to clean SO2 together with removing a large amount of NO seems to be the biggest challenge for both techniques.

For the development of these techniques, investigation on corona techniques seem very few. However, many investigation have indicated that the next cost effective generation for De-SOx and De-NOx is the technique to combine current ESP with pulsed corona streamer. And a big promotion for study pulse corona is the possibility to reform the current ESP to remove SOx, NOx and fly ash simultaneously in a single stage dry process. To enhance the efficiency and to reduce the cost of current chemical techniques by pulse corona streamer are also very significant goals for the technical development.

1.2 Streamer properties and optimization of energization

Up to date, quite a lot of study on streamer model and experiments have been reported. Generally speaking, the subjects of the model can be divided into two groups [4,5]; streamer model for heads propagation and channel model.

Broadly speaking, according to the streamer heads and channel, discharging can be divided into two different regions:

- active region, defined as the space around streamer tip, in which because the electric field is very higher, the net ionisation phenomena take place.

Active phenomena such as ionization, collision detachment and photoization are predominant.

- passive region, which represents the low conductive connection between the streamer tip and the high voltage electrode.

Due to the smaller electric field in this region passive phenomena such as attachment and recombination are predominant.

Therefore, it can be concluded that active electrons with larger average energy are only produced by the streamer heads. Concerning the two parts of streamer, head and channel, in principle it is possible to seperate the energy dissipation for streamer heads propagation and the energy dissipation after streamer heads stopping propagation. This means that in order to increase the active electrons production per unit injected energy, after streamer heads stop propagation, the voltage level should be very small in order to prohibit the continuous current flow through the formed channel.

Regarding the practical situations, due to the limited rise rate of pulse voltage and the unavoidable stray inductance of the electric circuit, the obtained voltage waveforms are not so perfect to limit the current continuous flow.

The energy consumption of the process and energy conversion can be divided into several steps and the optimization can be realized by means of modifing the matching of the generator and corona streamer as indicated in figure 1 [6].

(see figure 1)

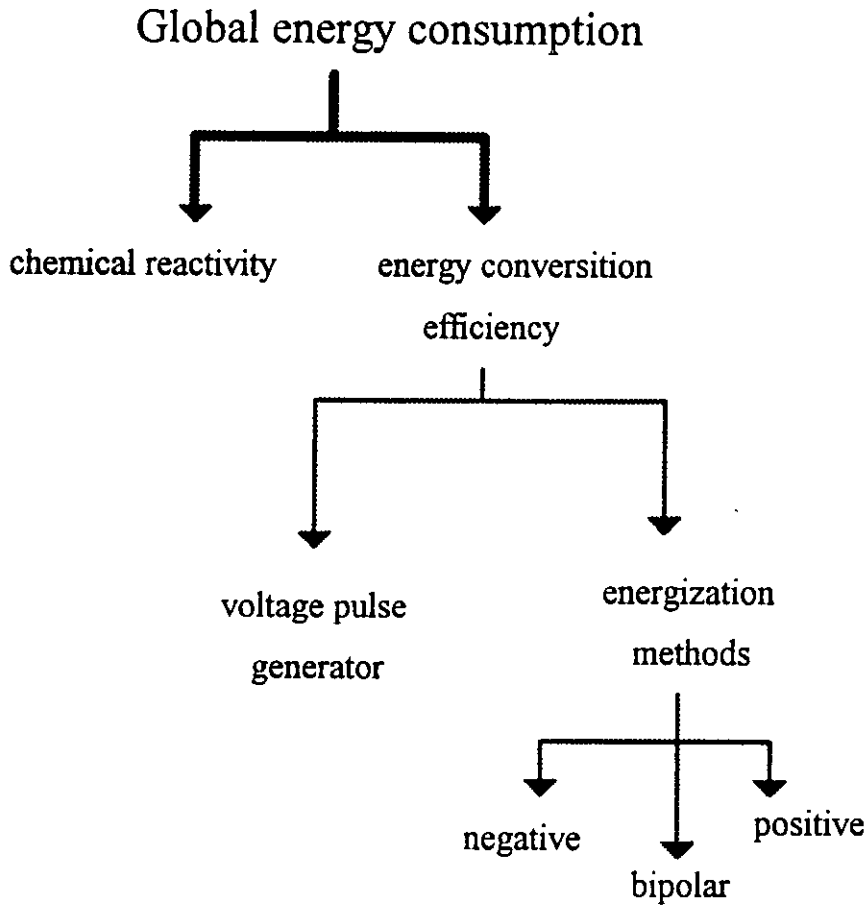

Figure 1a: General indication of the energization process for pulsed corona with respect to optimization.

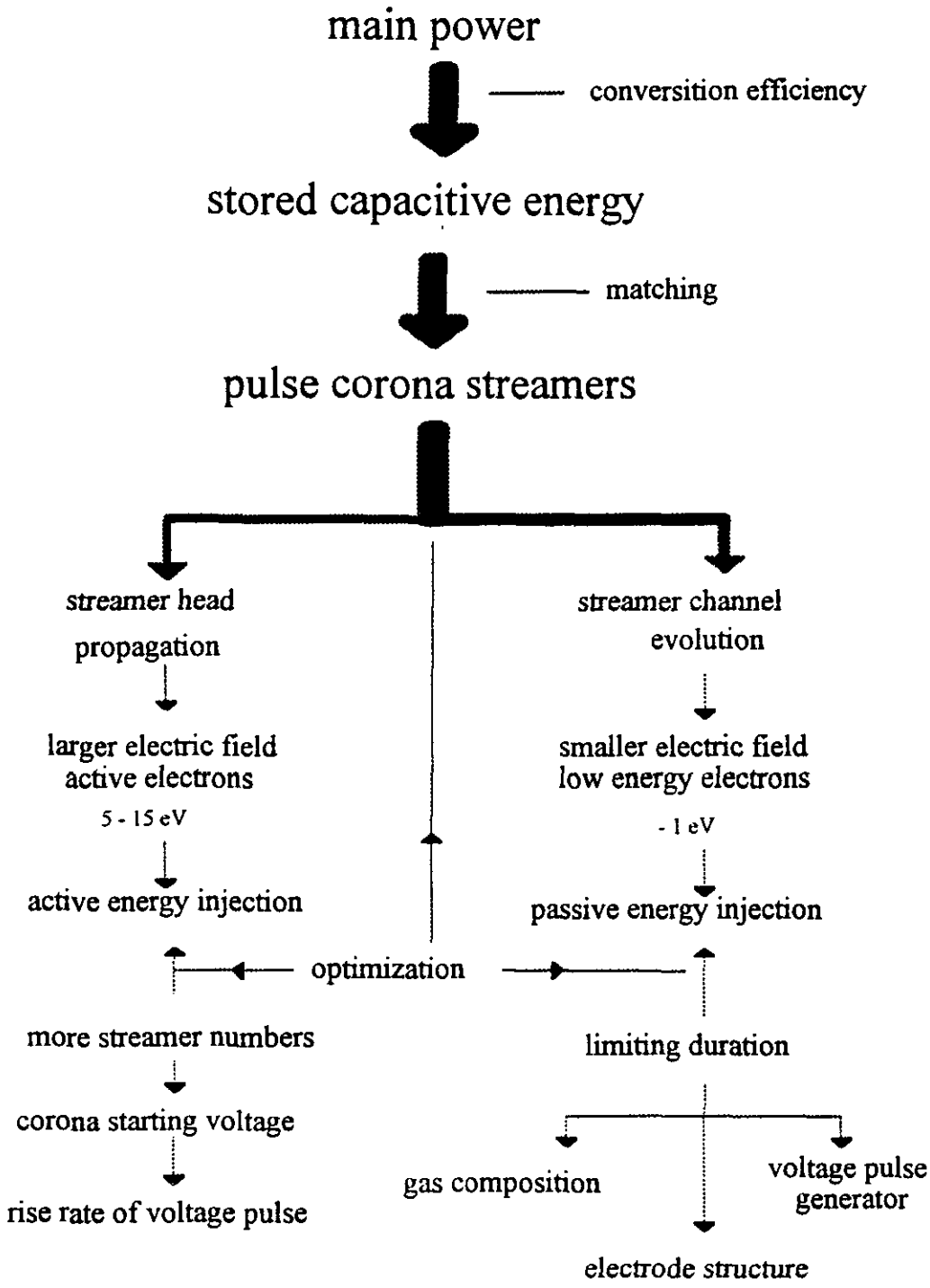

Figure 1b: Detailed steps in the optimization of the energy conversion for pulsed corona discharge.

1.3 Objective of this investigation

There are lots of physical and chemical questions related to the processes which are not very clear and the optimal energization are still unknown even just considering the active electrons production per unit energy injection and per unit discharging volume. The chemical activity of pulsed corona streamer is still a very big open question. The main objects of this investigation can be summarized as following:

- the influence of pulse voltage generator on the streamer
- streamer distribution along the emitting wire
- energy and charge dispersion during different discharge periods
- observation of the secondary streamers
- comparison of pulsed corona streamer in air and in flue gas
- evaluation of electron energy during the discharging
- streamer heads propagation speed
- optical properties of pulsed corona streamer
- time resolved spectroscopy of corona streamer
- relation between corona streamer and chemical reactivity
- removal of SO2 and NOx by pulse corona

The final objects of this investigation is to understand streamer structure in time and in space and to optimise the energization process in order to reduce the overall energy consumption.

In order to investigate the above mentioned points, experiments were conducted with wire-cylinder type reactor [1000 mm length, 155 mm diameter and 3 mm emitting wire]. Following techniques are also adopted:

- for increasing streamer intensity and avoding spark breakdown, pulse voltage is coupled to a DC bias level;

- in order to evaluate streamer distribution along the emitting wire, streamer current is measured both from the emitting wire and from a sample part of the grounding electrode;

- in order to investigate the influence of the pulse voltage generator on streamer structure, a damping resistor and a additional inductance are used to modify the shape of applied voltage;

- in order to evaluate the propagation speed of the primary streamer, local light emission near the anode and near the cathode are observed by means of two quarts fibres;

- in order to evaluate the eletron energy, time-resolved light emission from nitrogen [so called SPS/337.1 nm] and from positive nitrogen ions [so called FNS/391.4 nm] are recorded with a 0.5 m monochromator;

- for investigating the relation of chemical reactivity and corona streamer, SO_2 and NO are injected before the reactor, and the removal efficiency is used to evaluate it.

2. EXPERIMENTAL SET UP AND MEASUREMENT SYSTEM

Very detailed description on the experimental set up and measuring system have been described before [7]. The experiments were conducted in flue gas and in air.

Room temperature is about 15-21 C
RH is about about 40 %

In this section only two points are discussed for this investigation. The first is the pulse voltage generator, and the second is the techniques and problems of EMI for voltage and current measuring systems.

2.1 Pulse forming circuit and limitation of operation

The pulse voltage generator developted here is based on the capacitor type discharge circuit with a trigger spark gap and the pulse voltage is capacitively coupled to a DC base supply.

Figure 2 indicates the priciple of the circuit. The fixed spark gap is continuously refreshed with a constant gas flow and can be operated at different pressure. It has been noticed that with increasing the gas pressure in the spark gap system, the operation voltage can be increased with a reduction of the switch time.

(see figure 2)

Figure 2 shows the experimental set up and electrical circuit

By modifying the damping resistor R or changing the additional inductance Li, the rise rate of pulse voltage can be changed.

Because the pulse forming capacitor is charged with a resistor in this generator, the energy conversion efficiency for charging the capacitor is at most 50%.

Therefore, the maximum output of the pulse generator is about half of the DC power supply (300 W = 600 W x 50%).

The other point is the limitation of pulse frequency. It can be easily seen from the circuit that the frequency is limited by the charging resistor. With 1 M ohm charging resistor, the pulse voltage can be generated at 50 Hz with 80 KV peak value.

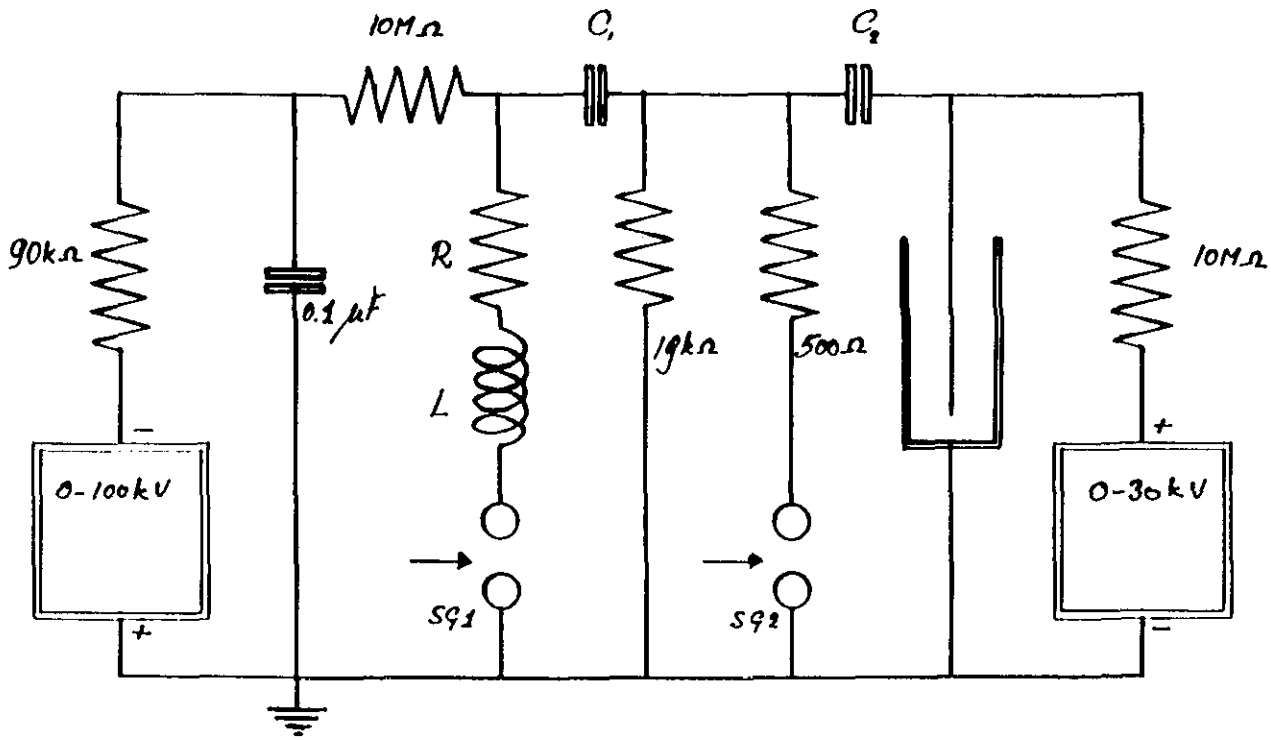

Figure 2: Electric circuit of the pulse generator, SG1 is the spark gap that switches the pulse on, SG2 can be used to switch it off.

As for the limitation of the peak voltage and the rise time of the pulse voltage, it depends on the electric circuit and the two DC power sources.

The DC bias voltage is usually coupled to the pulse voltage by means of a larger inductance or resistor in order to limit the DC current and to avoid its breakdown caused by the pulse voltage. The bias level is usually limited to be below the DC corona onset.

The main specification of the circuit is listed as following

pulse forming capacitor	Cp = 1.7, 3.3 nf
coulping capacitor	C = 1.7, 2.5, 5 nf
DC bias voltage	Vdc = 0 - 30 KV
pulse voltage	Vp = 20 - 80 KV
damping resistor	R = 0 - 100 ohm
additional inductance	Li = 0 - 55 uH
pulse voltage rise rate	dV/dt = 0.3 - 2.6 KV/ns
total peak volatge	V = 20 - 110 KV
pulse frequency	f = 2 - 50 Hz
pulse duration	T = 100 ns - 2 us
wire-cylinder	800 mm X 155mm + 200 mm X 200 mm
emitting wire	3 mm

2.2 Measurement systems and EMI protection

In this experimental investigation, in order to investigate the energy and charge injection and the streamer distribution along the emitting wire, pulse voltage, corona current from emitting wire and from the grounding wire are measured. The light emission at different position is also measured with photomultiplier and monochromator.

Because larger streamer current (can be up to 600 A) is produced with a larger rise rate, and the measurement system should also work well for the signal in the range of 2 or 3 mV, very serious EMI problems are supposed.

Generally speaking, the measuring system consists of sample sensor or probe and cable to transmit the signal to the oscilloscope. For many cases, the electrical noise in the discharging environments can be divided into two types, one is releated to the grounding loop, and the second is due to the cable is exposed to the discharging noise.

In priciple, in order to elimate the influence of the grounding wire, the grounding loop should be as small as possible and a common grounding point is often adopted to avoid the oscillation in the loop.

As for as the electrical noise, under discharging conditions, the noise frequency is around 20 MHz-50 MHz, therefore the cable or the power line are recommended to be shielded.

When using Pearson current transfomer, the main points are that the current transformer should only be grounded at the terminal of the oscilloscope and should be isolated from the discharging circuit.

If discharging current is also measured from the high voltage wire, the transformer will be also required to be electrically shielded in order to avoid the breakdown and to reduce the potential difference between the different grounding wire connected together in the oscilloscope. The potential difference can lead to typical L-C oscillation.

If the current is measured from the sample grounding wire, the main point for obtaining a good signal is to reduce the potential difference between the sample electrode and the remaining part of the cathode. The suggested way is to reduce the grounding loop size together with adding an acceptable damping resistor.

The size of the current sample electrode should be designed according to the streamer intensity and the electrode arrangements. Supposing the reactor is a wire - cylinder with diameter from 100 mm to 200 mm, the suggested size of the sample electrode can be about 2.5 cm, 5 cm and 10 cm for different streamer intensity. In order to have a very good measurement, smaller size of electrode is recommeded when streamer intensity is larger.

For the voltage measurements, the Tek high voltage probe p6015 was modified in order to measure much higher voltage and the pulse voltage is measured just before the coupling capacitor due to the limitation of the spark voltage.

The applied voltage on the emitting wire can be easily calculated in terms of the releation of the current and the capacitance of the DC coupling capacitor.

For measuring each signal, the analog bandwidth of the measuring system should be as large as possible in order to reduce the influence of the limitation of the bandwidth. However, for the evaluation of energy injection, the suggesed bandwidths for voltage and current measurements should be very similiar in order to reduce integration error due to the modification of the shapes of the voltage and current oscillograms.

3. EXPERIMENTAL RESULTS AND DISCUSSIONS

In principle, the measured current consists of two parts, capacitive current for charging the electrode arrangements and the corona current once the applied voltage is larger than the inception value. However, these two parts of current may not be graphically separated in the current oscillograms. Two parts may be overlapped together in the current oscillograms.

In principle, it is possible to derive the capacitive current based on the obtained voltage waveform and the capacitance of the electrode arrangement. However, due to the limited and different bandwidths of the voltage and current measuring systems, it is very hard to seperate the two parts exactly.

In this report, the injected charge is obtained by means of integration of the measured current, and the power can be calculated by multiplying the current and voltage waveforms. The associated energy is calculated by the integration of the power. The energy related to streamer development can be obtained by means of subtracting the capacitive energy of the electrode arrangements from the total energy.

Once streamer is produced, the voltage waveforms are strongly dependant on the streamer intensity and it is not very easy to use the characteristic value of the pulse voltage, such as the rise time, peak value and decay rate, to describe the streamer conditions. Therefore, the main parameters used in this report are the DC bias voltage Vdc, the initial voltage Vp on the pulse forming capacitor and the parameters of the electric circuit.

When investigating or comparing the effects of a single parameter, the experiments were often conducted at the same time in order to eliminate the influence of changing of temperature, humidity, operation procedures and the stability of the system.

When measuring the nitrogen ions emission, because the light intensity is very small, the measurements were often conducted in two steps. The first one is to record all signal including the noise; the second step is just record the noise after closing the monochromator. The light emission can be perfectly obtained if the measurments were conducted with the same trigger. In this test, the recording were conducted by using pulse voltage as a trigger source.

3.1 Determination of circuit parameters and the limitation of experiments

The main parameters to limit the experimental possibility are the stray inductance of the circuit and the capacitance of the electrode arrangements. These two parameters would limit the rise time or the rise rate of pulse voltage.

The other parameters are the breakdown voltage and the maximum peak voltage and corona current, which would limit the investigation possiblity.

In order to determine the capacitance of the electrode arrangements of the system and avoid the influence of the measuring system, the test were conducted under lower pulse voltage only (20 KV) with a additional inductance about 17.5 uH for reducing the rise rate. The obtained current and voltage oscillograms are indicated in figure 3. It can be easily seen that in this case the obtained current is only capacitive current.

(see figure 3 from data c-5)

Figure 3 indicates the voltage and current response without corona discharge. Vp=20 KV, Li=17.5 uH, Vdc=0, R=0

Based on the releation of the current and voltage, the capacitance of the electrode arrangements and the time delay between the two measurement systems can be obtained. The derived capacitance of the electrode arrangements is 42.5 pf, which includes the capacitance of the reactor and the capacitance of the high voltage wire.

With respect to the voltage probe the time delay of the current measurement system from the emitting wire is 24.5 ns.

In order to evaluate the stray inductance of the arrangements and to check the maximum total voltage and peak current, the test were conducted under the following conditions:

Vdc = 30 KV
Vp = 80 KV
R = 0
Li = 0

The pressure in the spark gap : 4 atm

The obtained minimum rise time is about 30 ns, and the peak value of total current is about 600 A. The total value of voltage can reach about 110 KV. In this case, the half width of corona current is about 150 ns.

Therefore, the equivalent stray inductance of this set up, which includes the elelctrode arrangements and the spark gap system, is about 8 uH. The maximum pulse voltage rise rate is about 2.6 KV/ns.

Generally speaking, for a spark gap of 10 cm seperation, the switching time is about 20 ns at 1 atmosphere. It is also supposed that the obtained minimum rise time is mainly limited by the spark system and the stray inductance.

Considering the value of the equivalent stray inductance, it can be concluded that with a additional inductance of several or several tens uH, the pulse voltage waveforms can be easily modified.

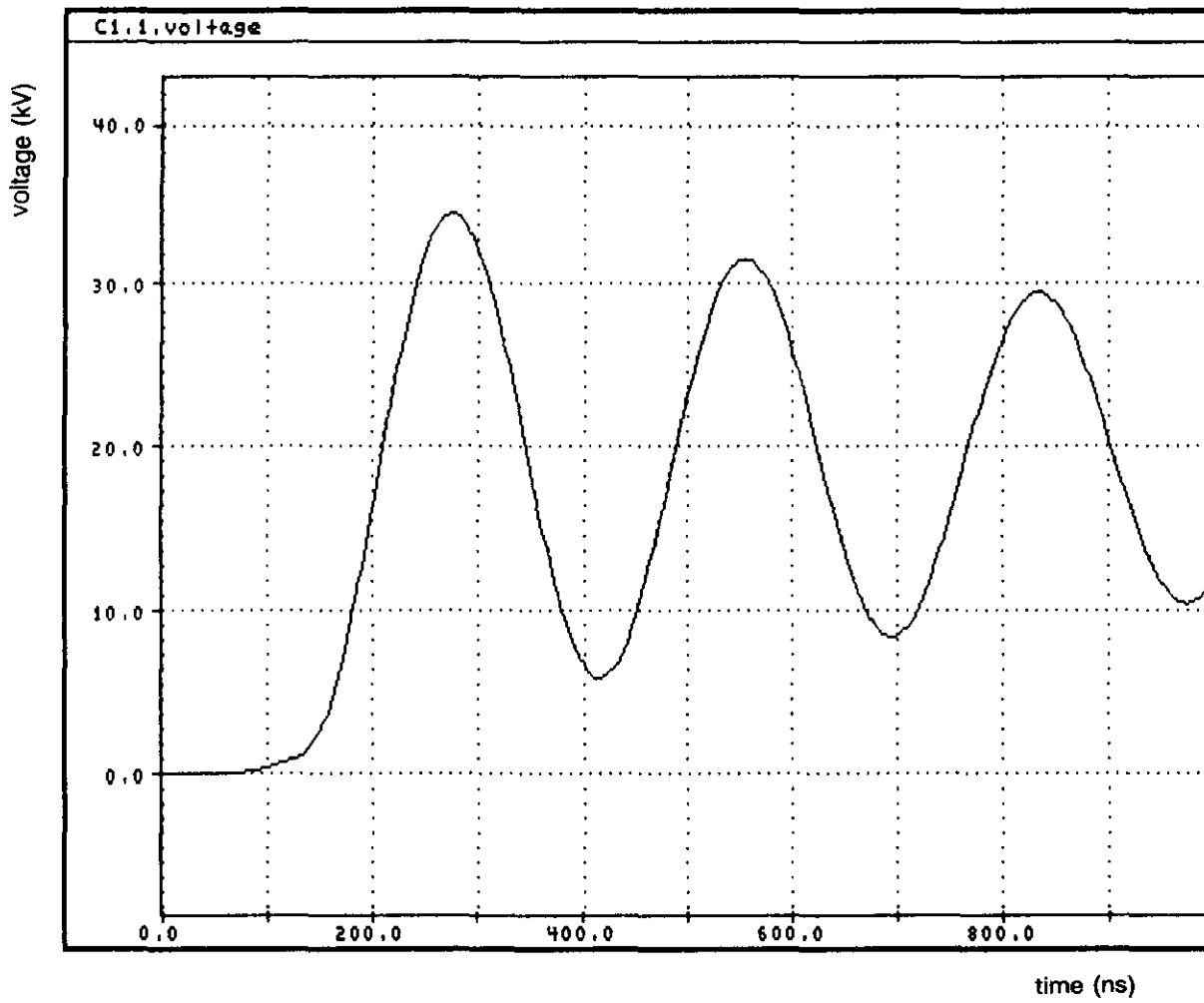

Figure 3a: Voltage waveform of the pulse circuit without corona discharge. Vp = 20 kV, Vdc = 0, Li = 0 and R = 0.

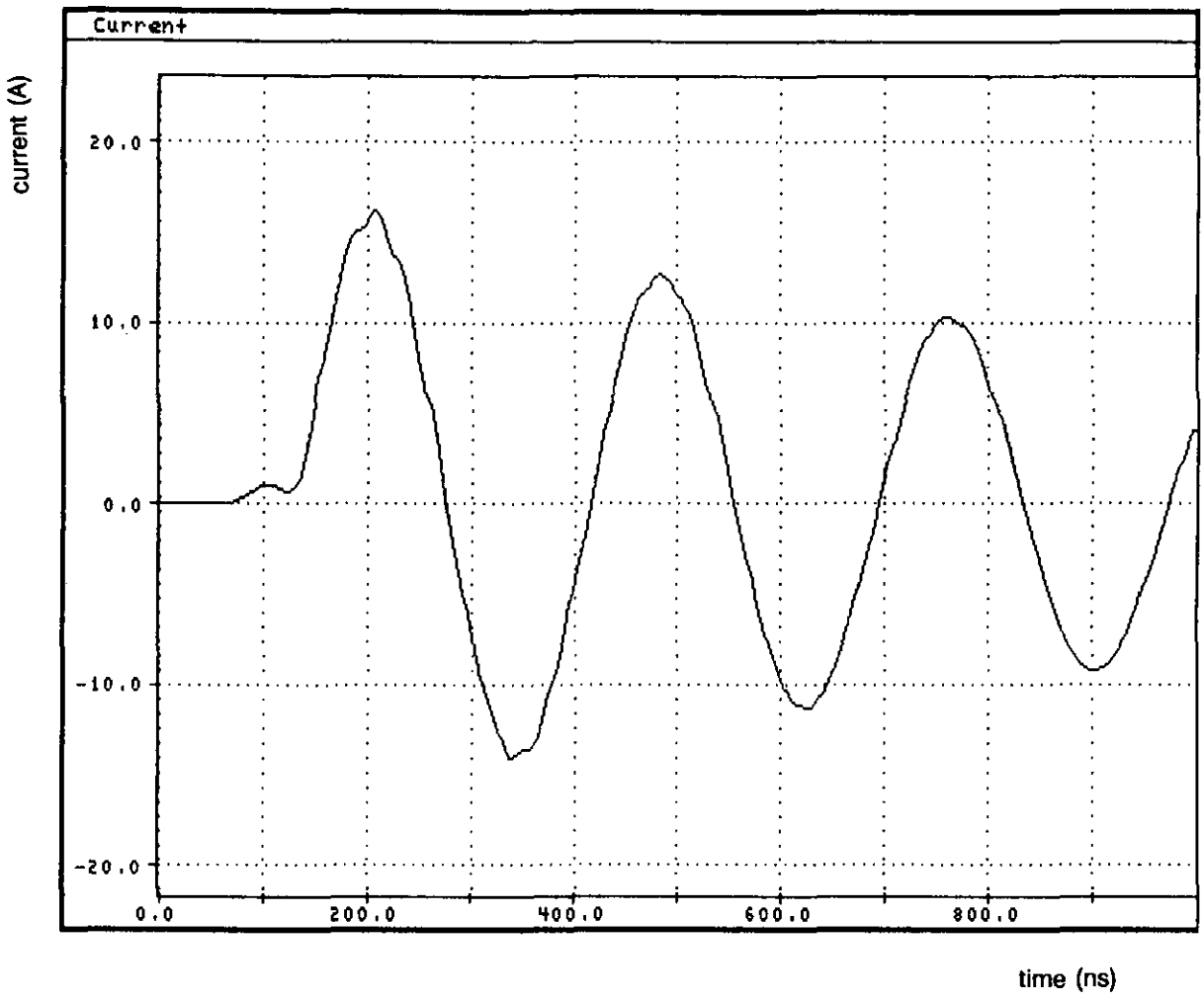

Figure 3b: Current waveform of the pulse circuit without corona discharge. Vp = 20 kV, Vdc = 0, Li = 0 and R = 0.

3.2 Effects of the damping resistor R

With adding a damping resistor in the circuit, two effects can become important for energization.

The first one is the damping resistor will reduce the rise rate of the pulse voltage which may influence streamer starting voltage due to the statistic time lag.

The second effect is that when streamer occurs, a big voltage drop on the damping resistor may be formed due to the larger streamer current. The capacitive current for charging the electrode can also lead to a big voltage drop on the resistor if the rise rate of pulse voltage becomes larger.

Regarding the energy efficiency of the circuit, the voltage drop across the resistor will completely become thermal losses. As for as the streamer intensity, the voltage drop will lead to reduce the pulse voltage level on the emitting wire and limit current flow from power supply to the reactor.

Therefore, it can be concluded that in any case, the damping resistor in the circuit of the pulse voltage generator will limit the streamer intensity and reduce the energy conversion efficiency from the pulse generator to the reactor.

Figure 4 graphically indicates the influence of the resistor on the current and voltage oscillograms. Figure 5 shows the effects on the energy and charge conversion. It should also be remarked that the effects of limitation on streamer intensity become very obvious with increasing corona current.

(see figure 4 from data c-1)

Figure 4 indicates the typical voltage and current oscillograms with different damping resistor; Vdc=30 KV, Vp=80 KV, a: R=0, b: R=40 ohm.

(see figure 5 from data c-1)

Figure 5 indicates the influence of the damping resistor on the energy injection with different pulse voltage and different Vdc bias level. a: Vdc=30 KV, b: Vdc=80 KV

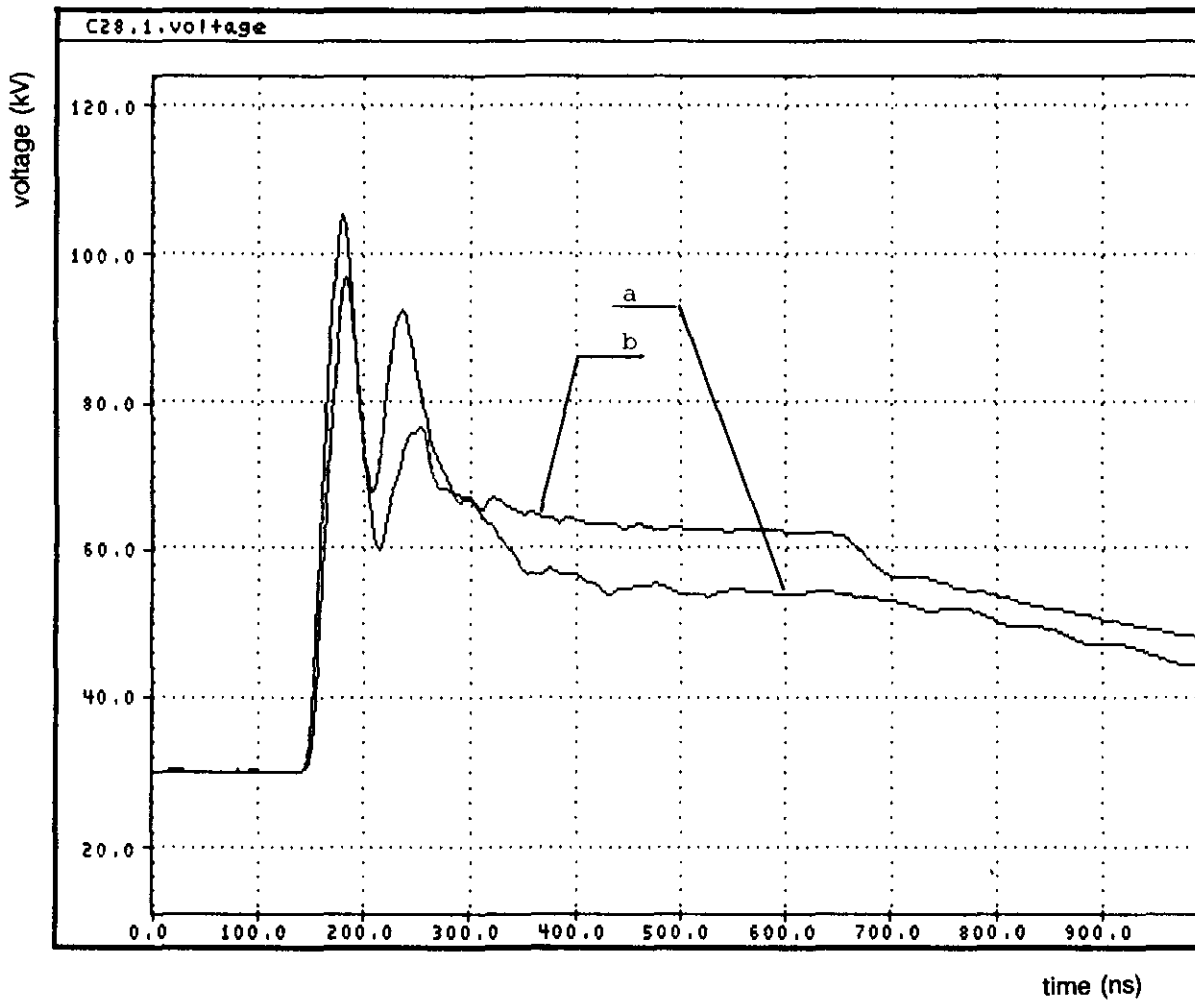

Figure 4a: Voltage waveform of the corona discharge in air.
a: R = 0 Ω, b: R = 40 Ω, Vdc = 30 kV and Vp = 80 kV.

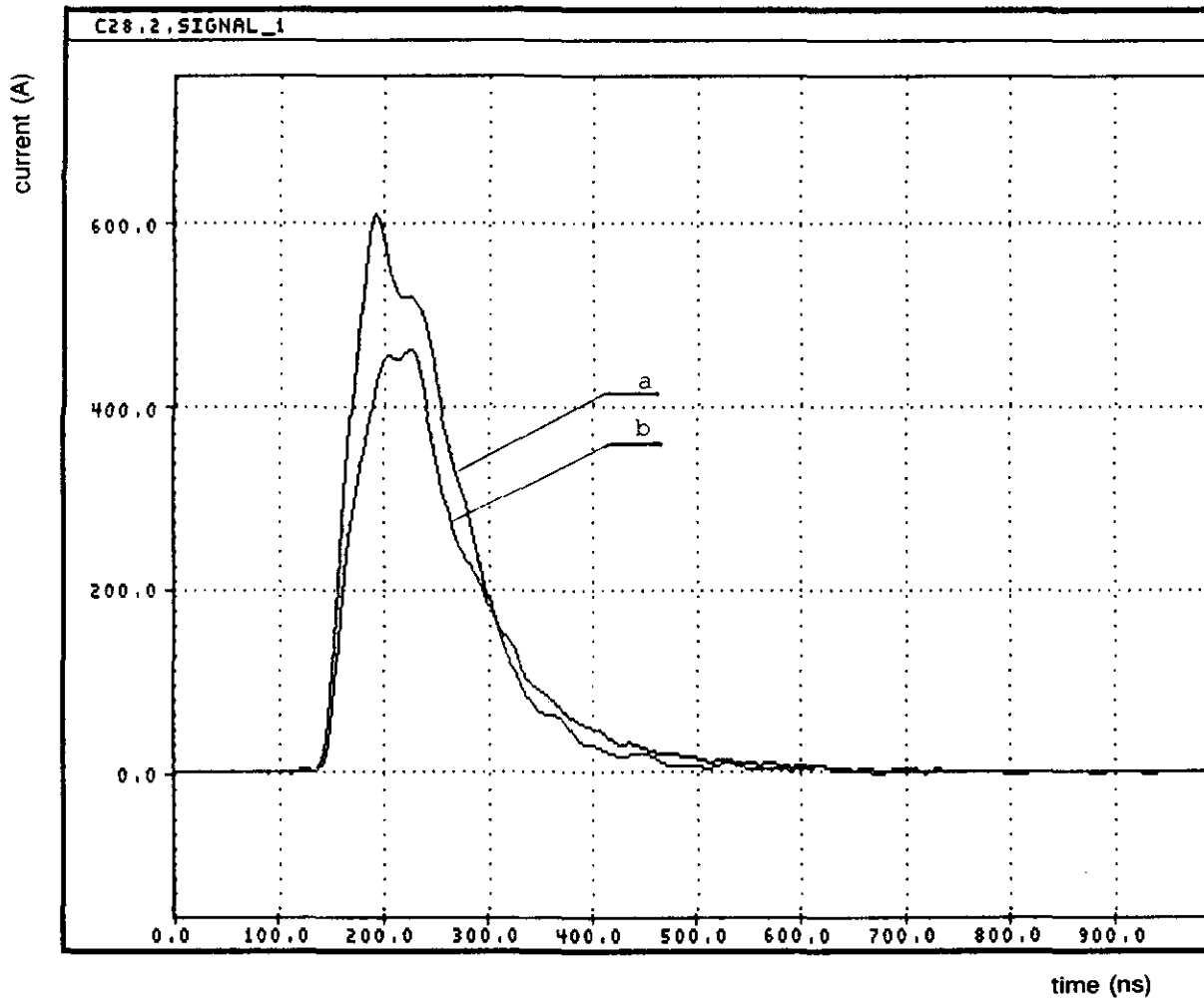

Figure 4b: Current waveform of the corona discharge in air.
a: R = 0 Ω, b: R = 40 Ω, Vdc = 30 kV and Vp = 80 kV.

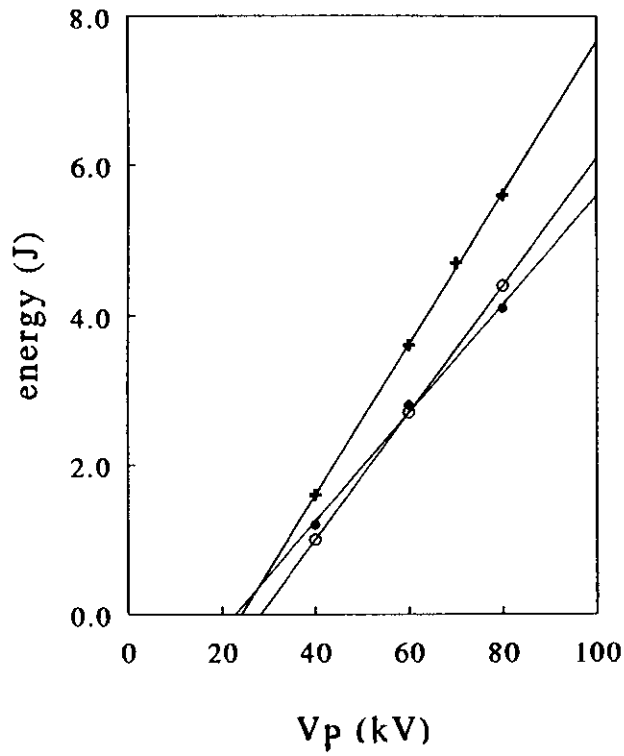

Figure 5a: Energy per pulse of corona discharge in air versus peak voltage, +: R = 0 Ω, ○ : R = 40 Ω, ● : R = 100 Ω and Vdc = 30 kV

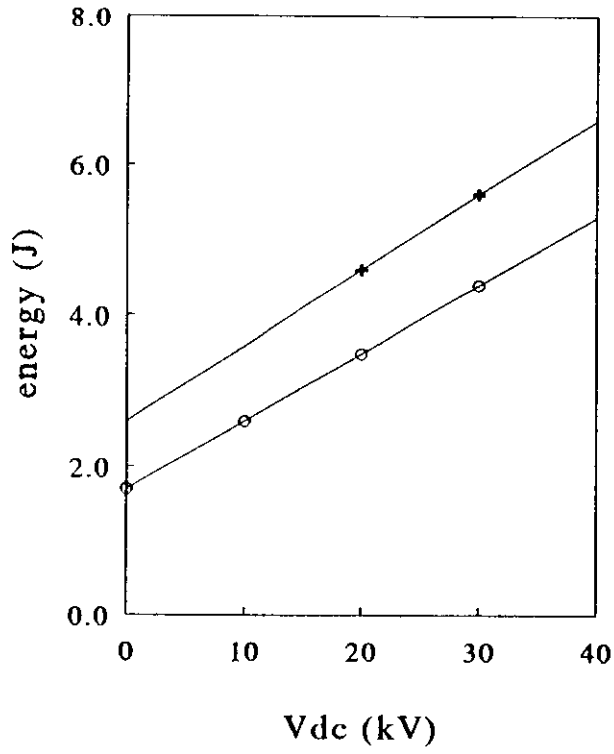

Figure 5b: Energy per pulse of corona discharge in air versus DC bias, +: R = 0 Ω, ○ : R = 40 Ω and Vdc = 30 kV

3.3 Influence of the additional inductance Li

Comparing the effects of the damping resistor, the additional inductance Li also shows two effects on the output of the pulse voltage generator.

The first is that the rise rate of pulse voltage is decreased with increasing the inductance. However, in contrast to the damping resistor, its second effect is that after streamer current reaches its peak value, the inductance may lead to the pulse voltage increase again as indicated in fig 6.

(see figure 6 from data c-5)

Figure 6 shows typical current and voltage correspondence with different additional inductance. R=0, Vdc=30 KV, Vp=80 KV, a: Li=0, b: Li=17.5 uH, c: Li= 55 uH

It can be noticed that with increasing the inductance, pulse rise rate becomes smaller which leads to a reduction of the streamer starting voltage. The associated peak current is decreased but its duration becomes longer. Within test conditions, the corona current could last from 100 ns to 600 ns with different inductance. It also indicates that the obtained corona current not only depends on the streamer itself but also on the pulse voltage generator.

As for as the total energy and charge dissipation, it has been found that the injected charge and energy can be very similar for different inductance under the same power source as indicated in figure 7.

(see figure 7 from data c-5)

Figure 7 illustrates the dependence of energy injection on the inductance (0, 17.5 uH, 55 uH) under different applied voltage. a: Vdc = 30 KV; b: Vp = 80 KV

However, it is supposed that the produced streamer shows different structure in time and in space. It is supposed that changing the additional inductance would lead to modify the inception voltage, which may correspond to various number and intensity of the first primary streamers; and the voltage level for secondary streamer evaluation just after the primary streamer reaching the cathode.

Therefore, in principle different kinds of streamer structure in time and in space can be produced just by modifying the inductance of the electric circuit. In fact, it is also very important to known the relation between the impendance of the pulse voltage generator and streamer structure. From the point view of experimental investigation, it is also very useful to be able to produce different streamer structure in order to investigate its corresponded chemical reactivity.

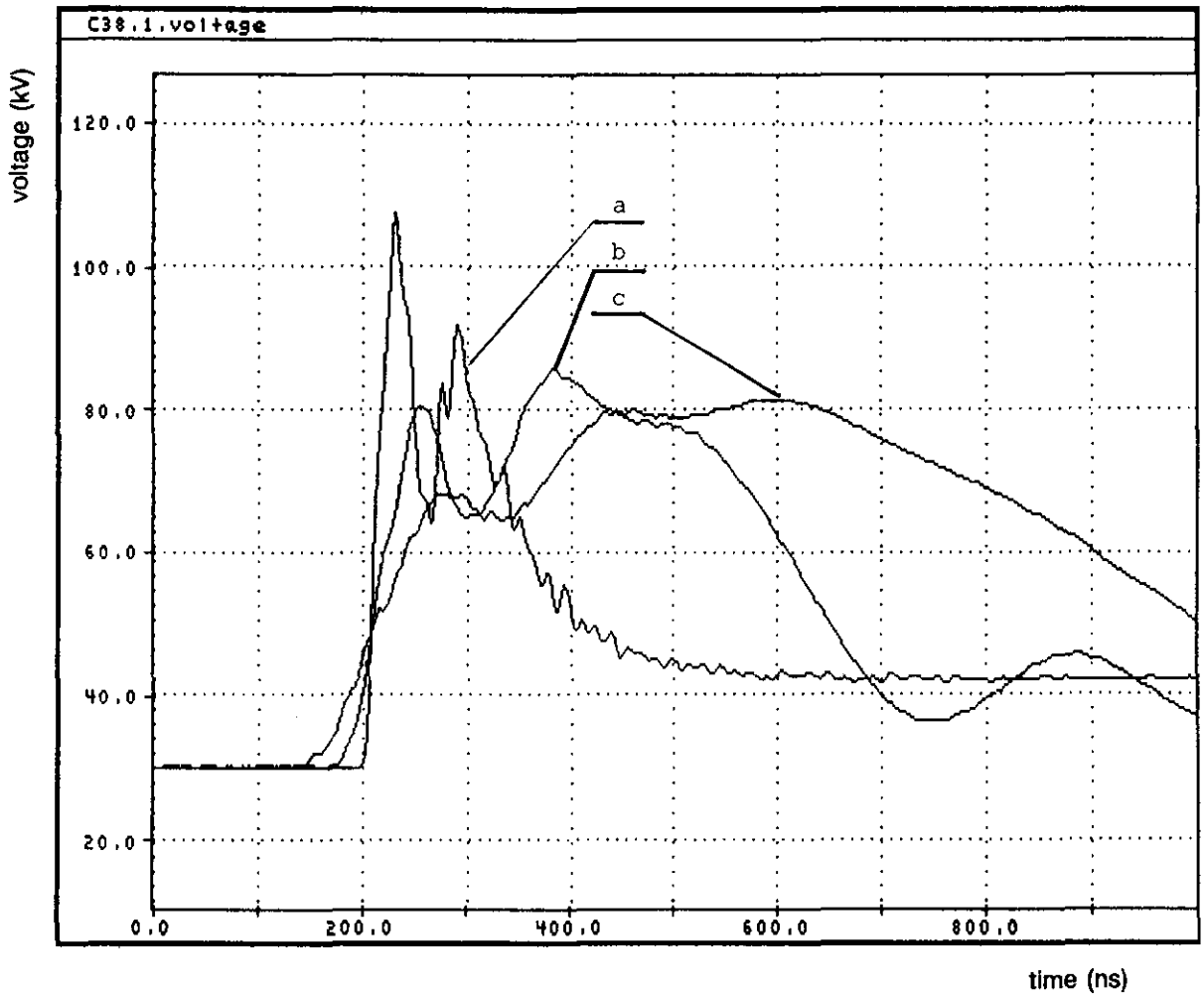

Figure 6a: Voltage waveform of the corona discharge in air for different series inductances.
a: Li = 0 uH, b: Li = 17.5 uH, c: Li = 55 uH, Vdc = 30 kV and Vp = 80 kV.

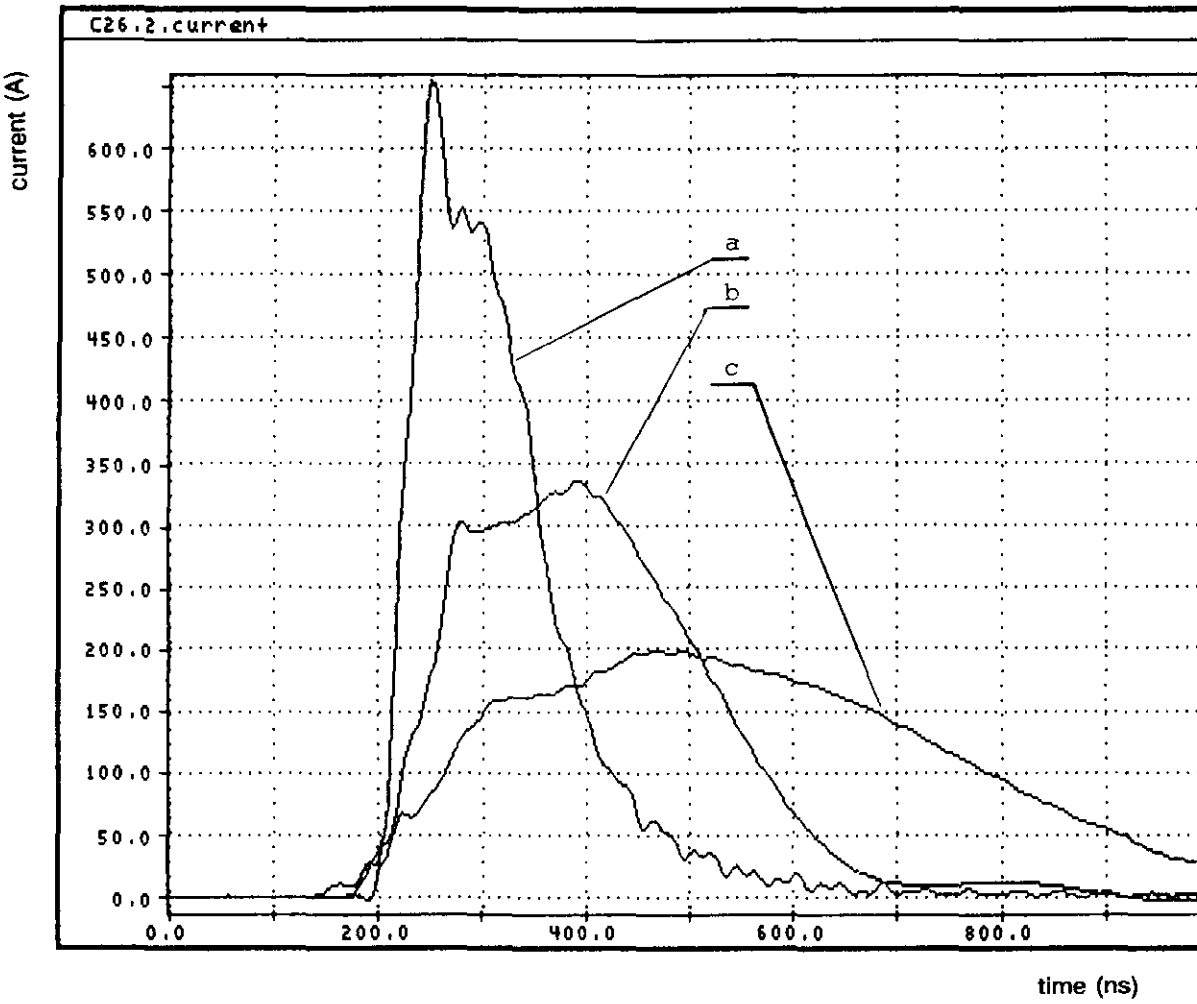

Figure 6b: Current waveform of the corona discharge in air for different series inductances.
a: Li = 0 uH, b: Li = 17.5 uH, c: Li = 55 uH, Vdc = 30 kV and Vp = 80 kV.

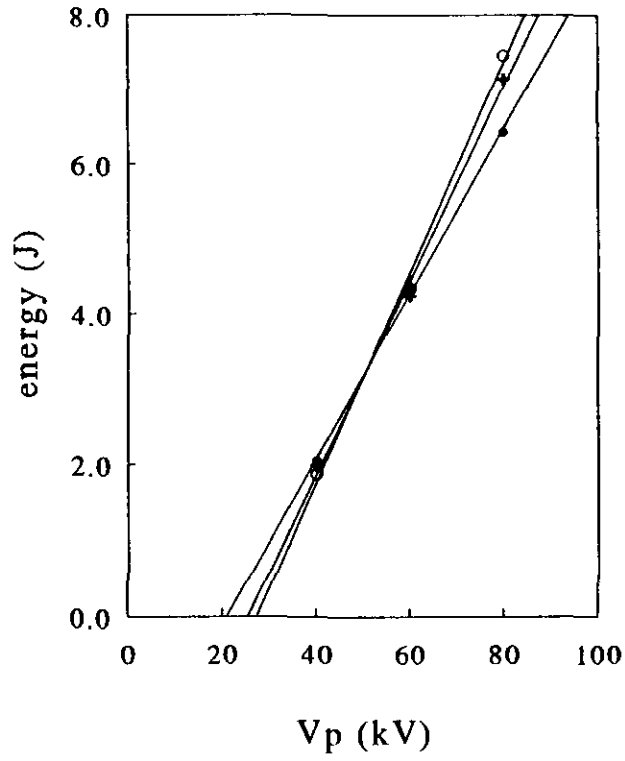

Figure 7a: Energy per pulse of corona discharge in air for different series inductances versus peak voltage.
+: Li = 17.5 uH, ○ : Li = 55 uH, ● : Li = 0 uH and Vdc = 30 kV

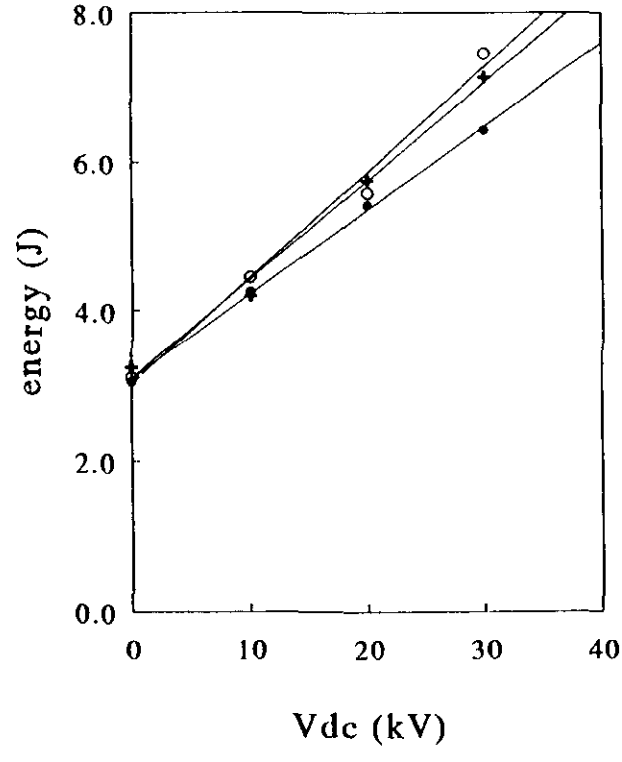

Figure 7b: Energy per pulse of corona discharge in air for different series inductances versus DC bias.
+: Li = 17.5 uH, ○ : Li = 55 uH, ● : Li = 0 uH and Vp = 80 kV

3.4 Effects of pulse voltage level on corona streamer

Generally speaking, when the fixed spark gap system is in the state of 'switch-on', the applied pulse voltage on the electrode arrangements is increased almost linearly until streamer occurs.

Once the total applied voltage on the emitting wire is beyound its inception value, corona streamers occur, the current and voltage show a very complticated relation. Figure 8 and figure 9 indicate the influence of pulse voltage level on discharging current with different rise rates.

(see figure 8 from data c-1)

Figure 8 indicates the influence of pulse voltage level on streamer current under fast rise rate. Vdc=30 KV, R=40 ohm, a: Vp=80 KV, b: Vp= 60 KV, c: Vp=40 KV

(see figure 9 from data c-5)

Figure 9 indicates the influence of pulse voltage level on streamer intensity under slow rise rate. Li=55uH.

From the current and voltage waveforms, it can be seen that in any case with increasing the pulse voltage, the level of corona streamer current and its duration will be continuously increased and corona current and capacitive current tend to be overlapped.

However, If roughly dividing the current flow into two regions at the time of its first peak value, it can be remarked that under larger rise rate, with increasing the pulse voltage, all of the two parts increase simultaneously with a very similiar increasing rate. Under the slow rise rate, increasing the initial voltage level on the pulse forming capacitor mainly enhance the second part of streamer current. It is supposed that with larger additional inductance the secondary streamer can be strongly increased with larger stored energy in the pulse generator.

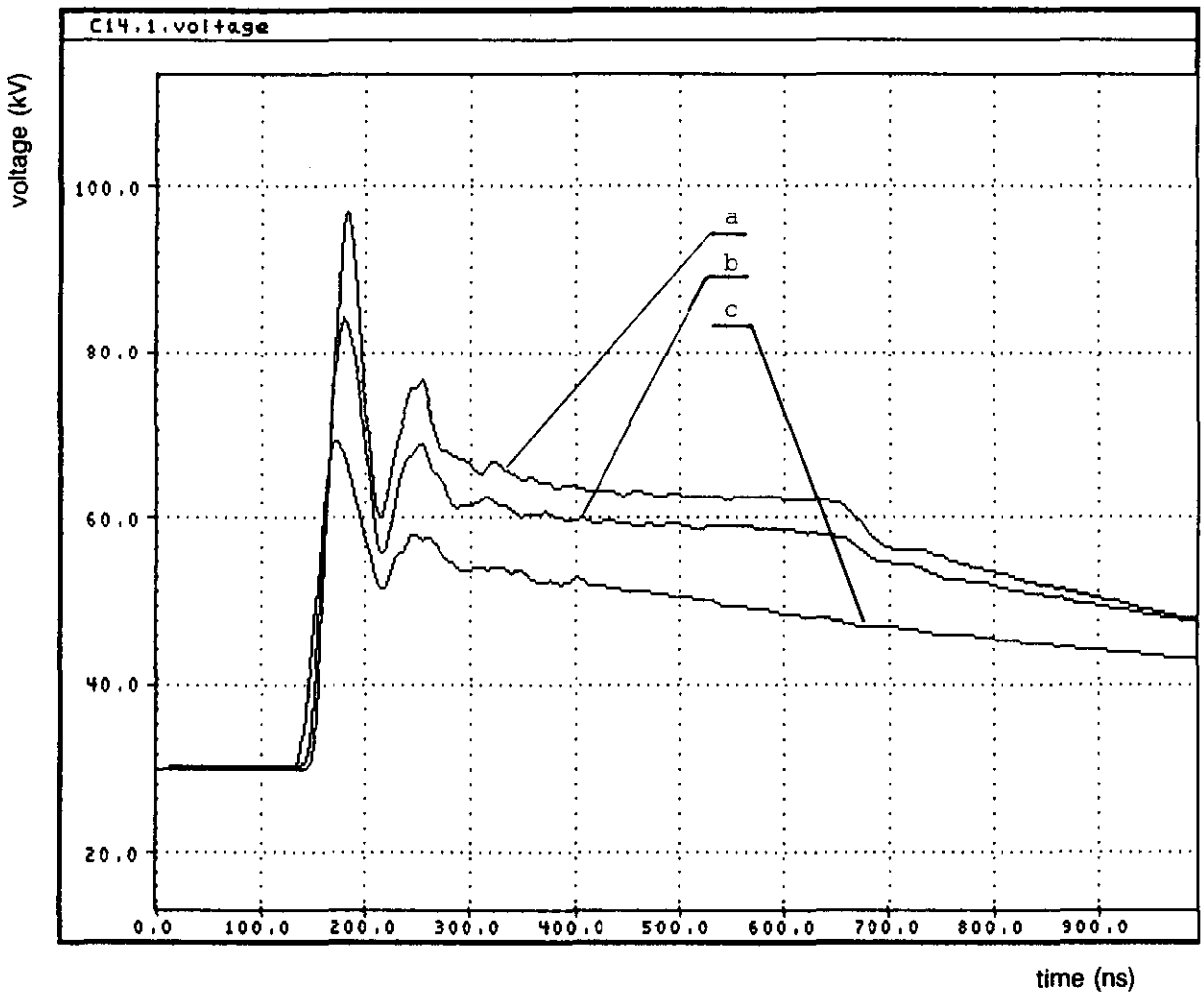

Figure 8a: Voltage waveform of the corona discharge in air for different peak voltages and a series resistor.
a: Vp = 80 kV, b: Vp = 60 kV, c: Vp = 40 kV, R = 40 Ω and Vdc = 30 kV.

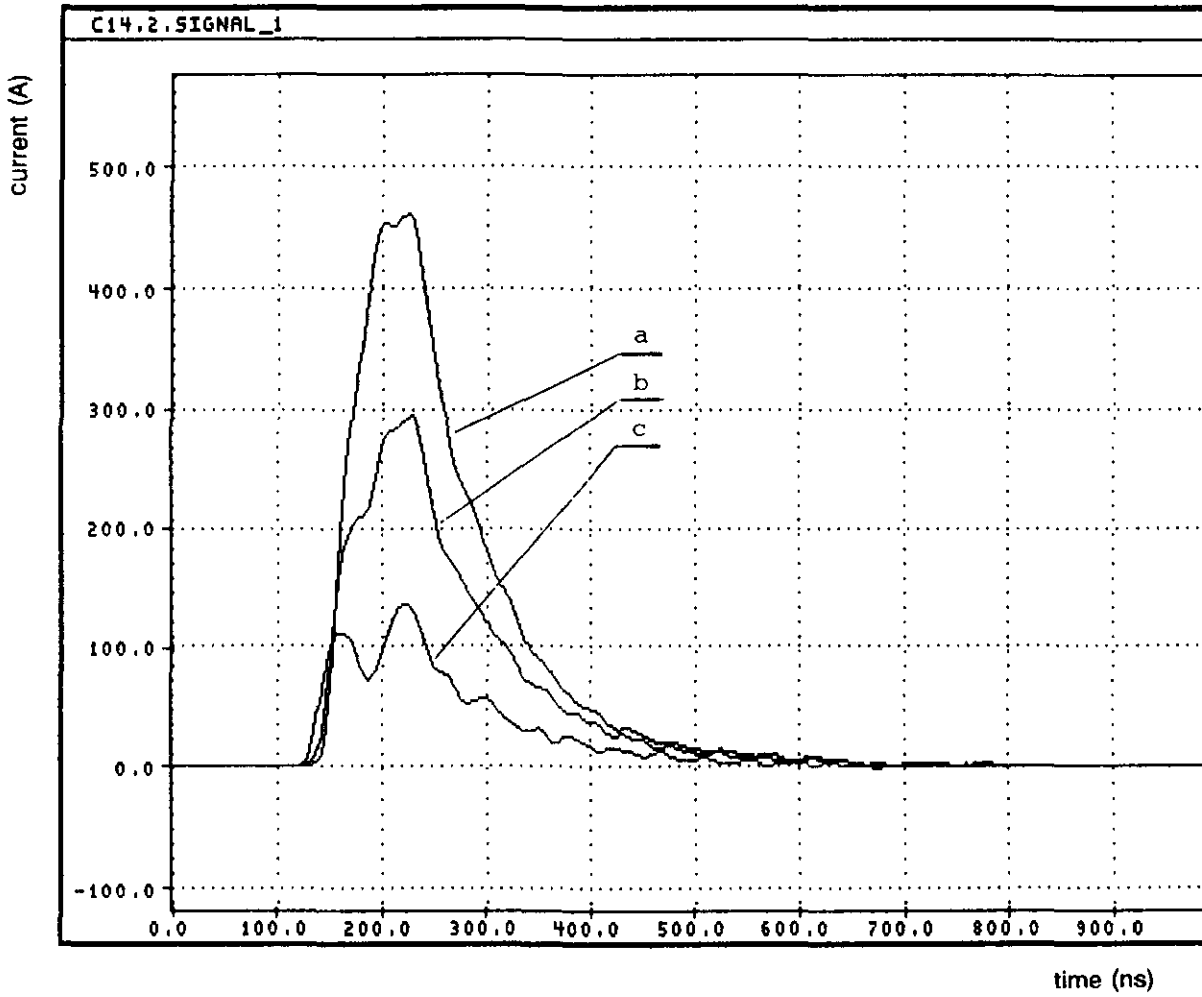

Figure 8b: Current waveform of the corona discharge in air for different peak voltages and a series resistor. a: Vp = 80 kV, b: Vp = 60 kV, c: Vp = 40 kV, R = 40 Ω and Vdc = 30 kV.

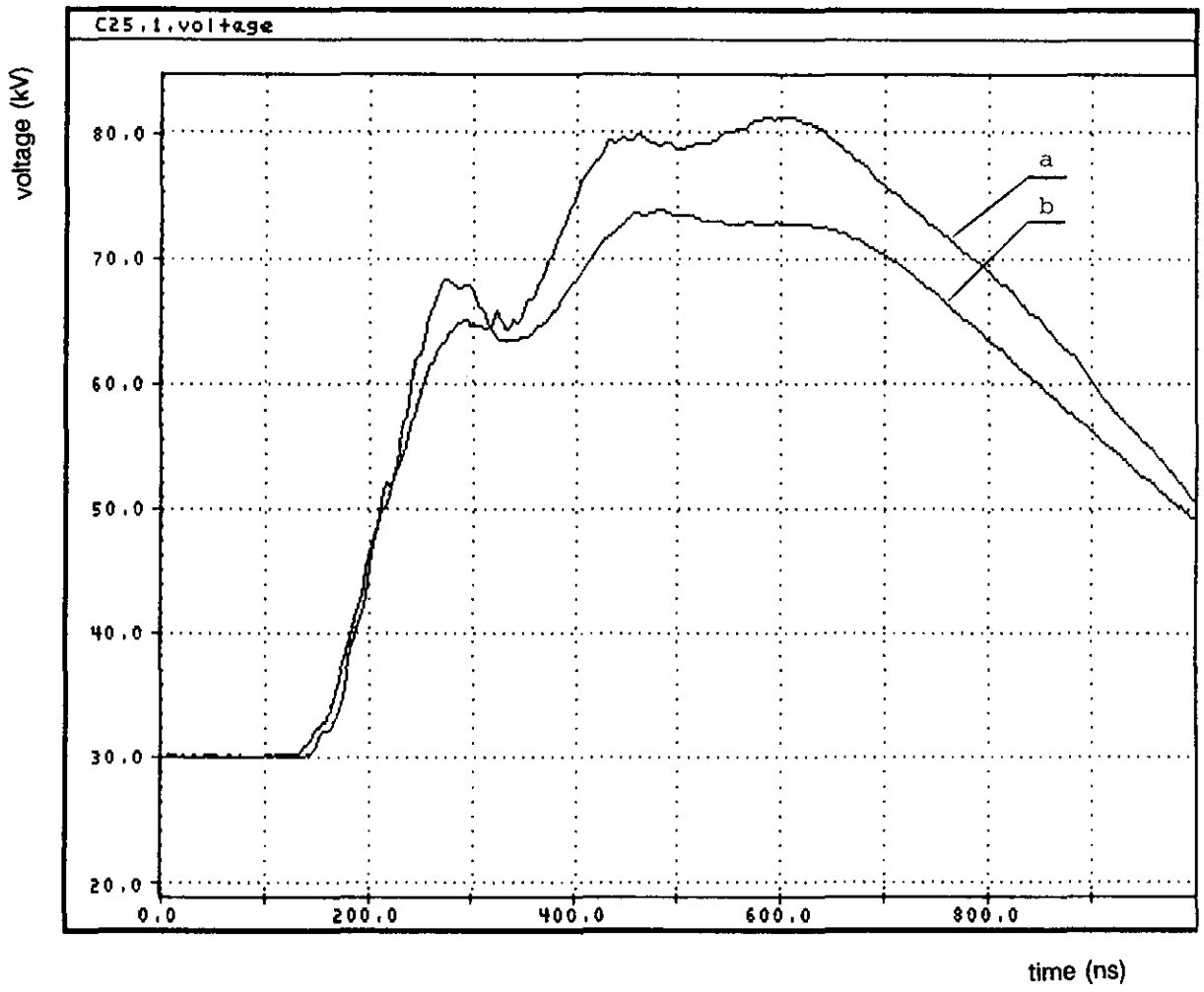

Figure 9a: Voltage waveform of the corona discharge in air for different peak voltages and a series inductance.
a: Vp = 80 kV, b: Vp = 60 kV, Li = 55 uH, Vdc = 30 kV.

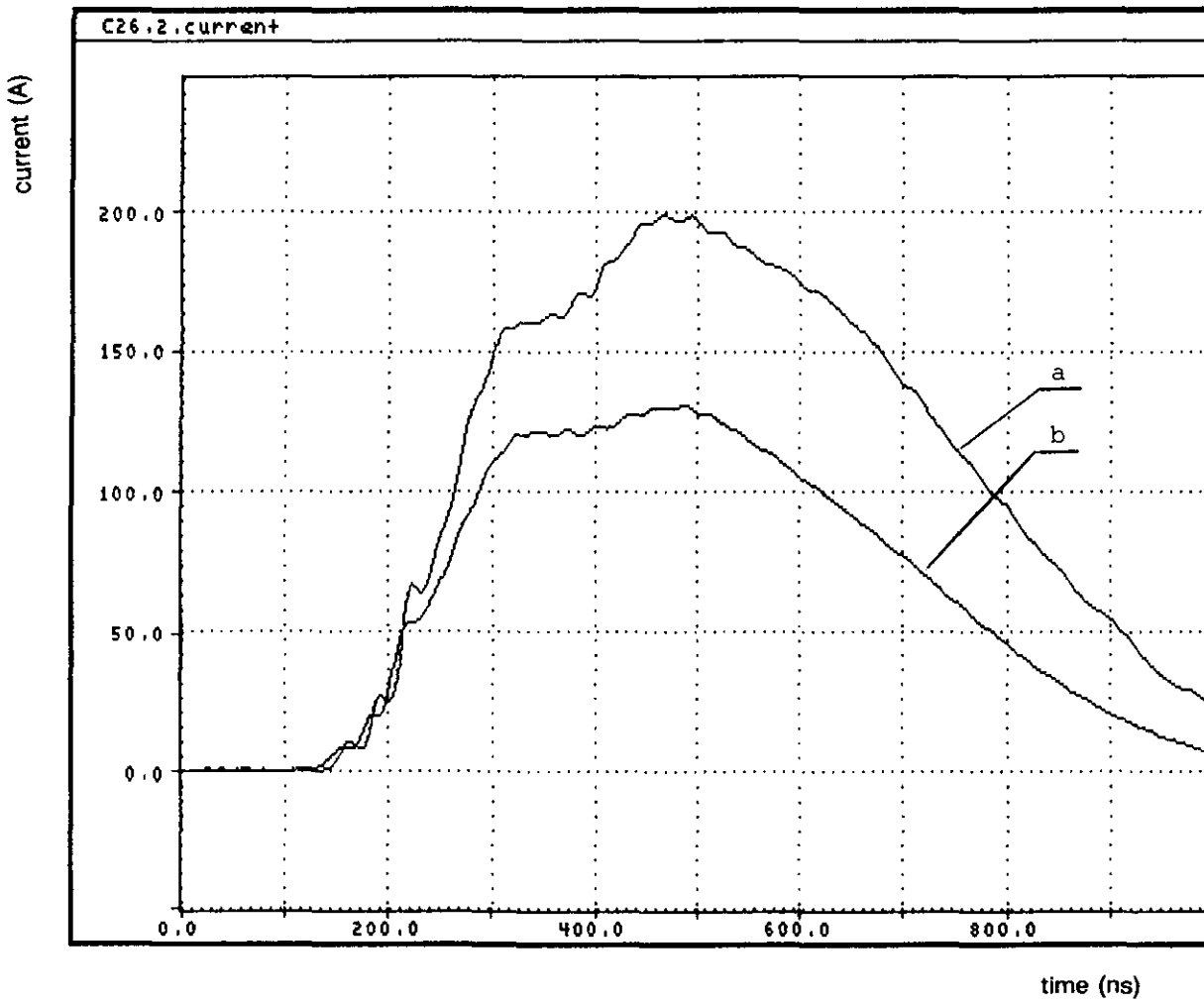

Figure 9b: Current waveform of the corona discharge in air for different peak voltages and a series inductance. a: Vp = 80 kV, b: Vp = 60 kV, Li = 55 uH, Vdc = 30 kV.

3.5 Effects of DC bias voltage level on the discharging properties

When streamer heads propagate roughly along the electric field, behind the head a plasma channel is formed with a electric field about 5 KV/cm in air. If the applied voltage is sufficient enough to sustain this field requirement, streamer heads can cross the gap and reach the cathode, otherwise, the heads would stop in the gap.

Once the streamer head has cross the gap and a plasma channel is formed between the electrodes, the energy conversion from the pulse supply to the reactor is supposed to become a resisitive type energy dispersion. The main interests to investigate the effects of DC bias level is to understand its effects on energy dispersion and conversion processes.

If considering the technology development, by using the DC bias voltage for replacing the pulse voltage, the same streamer intensity can be obtained, and high energy conversion efficiency can be also realized but without increasing the cost of the pulse voltage generator.

With different rise rate, DC bias level leads to different effects as observed with different pulse voltage. Figure 10 and figure 11 graphically illustrate the influence of DC bias level on the current and voltage waveforms under different rise rate.

(see figure 10 from data c-1)

Figure 10 indicates the effects of DC bias level on the current and voltage correspondence with larger rise rate.

(see figure 11 from data c-5)

Figure 11 indicates the effects of DC bias level on the current and voltage correspondence with smaller rise rate.

For fast rise rate as indicated in figure 10, it can be seen that with increasing the DC bias level, the total first peak voltage will be increased. It roughly indicates that the streamer starting voltage can be increased with the increasing the DC level. However, under the slow rise rate as indicated in figure 11, the first peak of the total voltage seems constant, which also roughly indicates that in this case the inception is almost constant.

Therefore, it can be concluded that the DC bias level can increase the streamer starting voltage (or called the inception value) under fast rise rate (The condition may be determined by the relative value of rise time with respect to the statistic time lag and the impendance of the circuit which limits the total current). However, the inception value is almost constant for different DC bias level under the slow rise rate. The streamer starting voltage is supposed to be determined by the rise rate of the pulse voltage, the electrode arrangements and gas compositions.

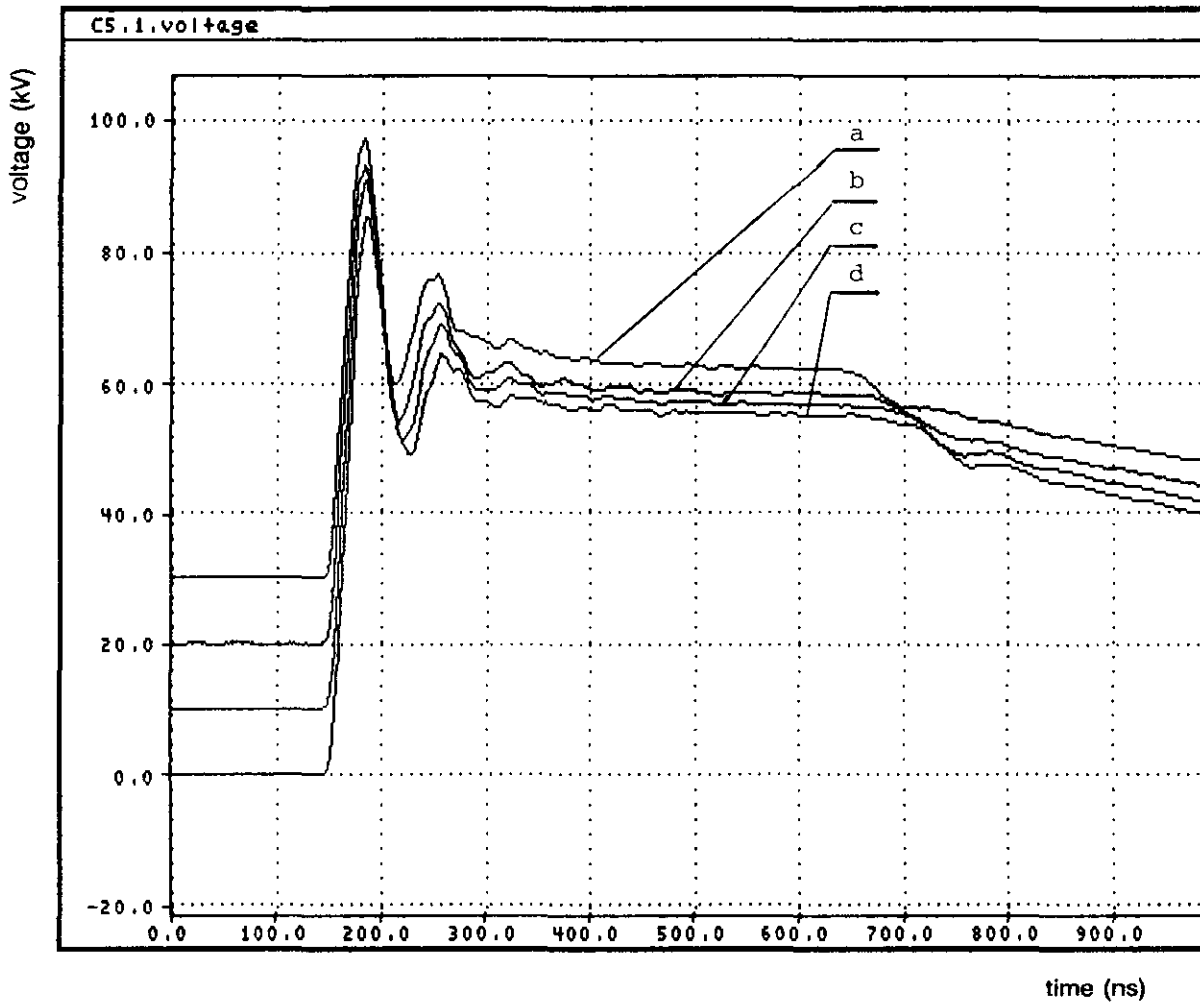

Figure 10a: Total voltage waveform of the corona discharge in air for different DC bias voltages and a series resistor.
a: Vdc = 30 kV, b: Vdc = 20 kV, c: Vdc = 10 kV, d: Vdc = 0 kV, R = 40 Ω and Vp = 80 kV.

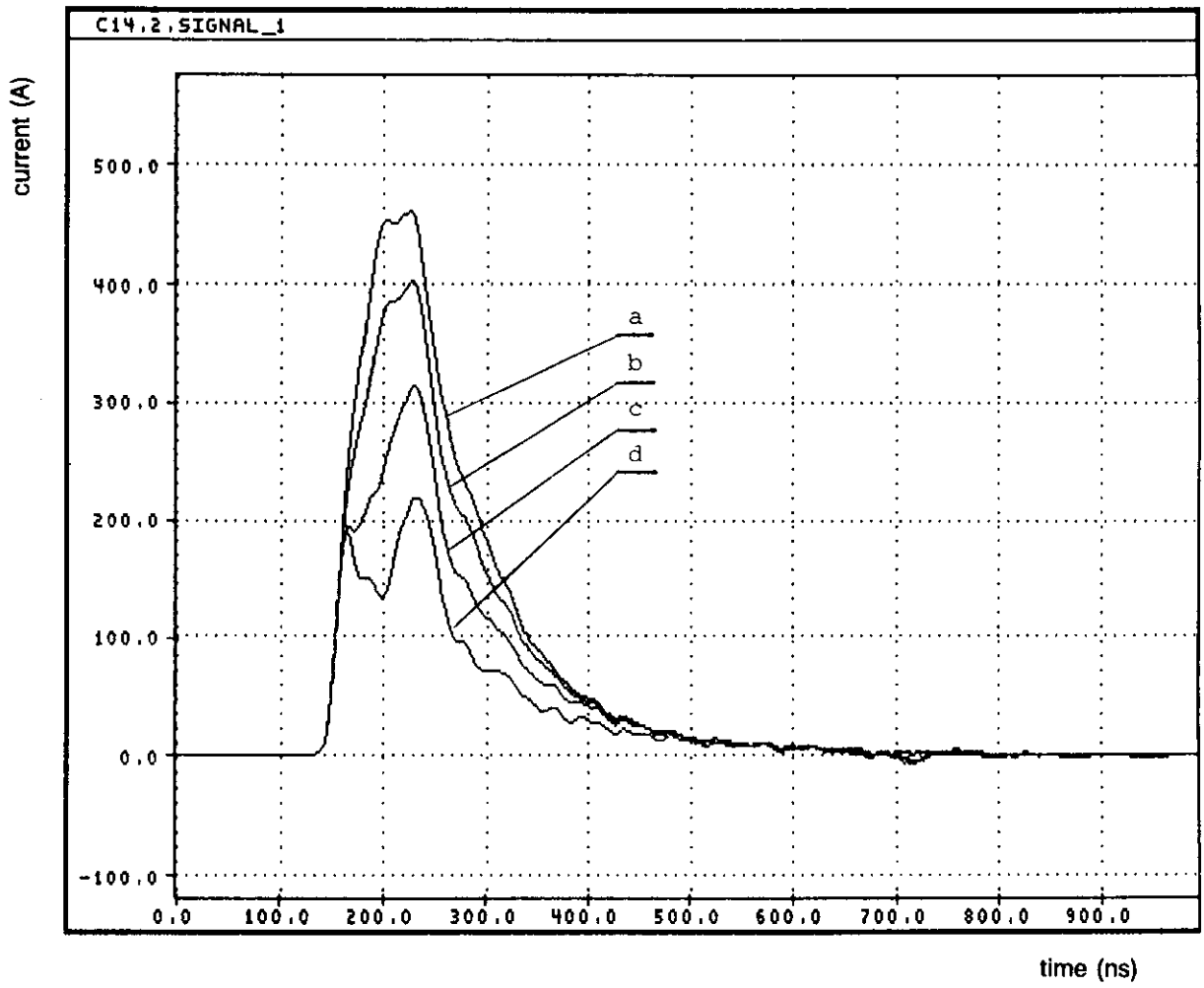

Figure 10b: Current waveform of the corona discharge in air for different DC bias voltages and a series resistor.
a: Vdc = 30 kV, b: Vdc = 20 kV, c: Vdc = 10 kV, d: Vdc = 0 kV, R = 40 Ω and Vp = 80 kV.

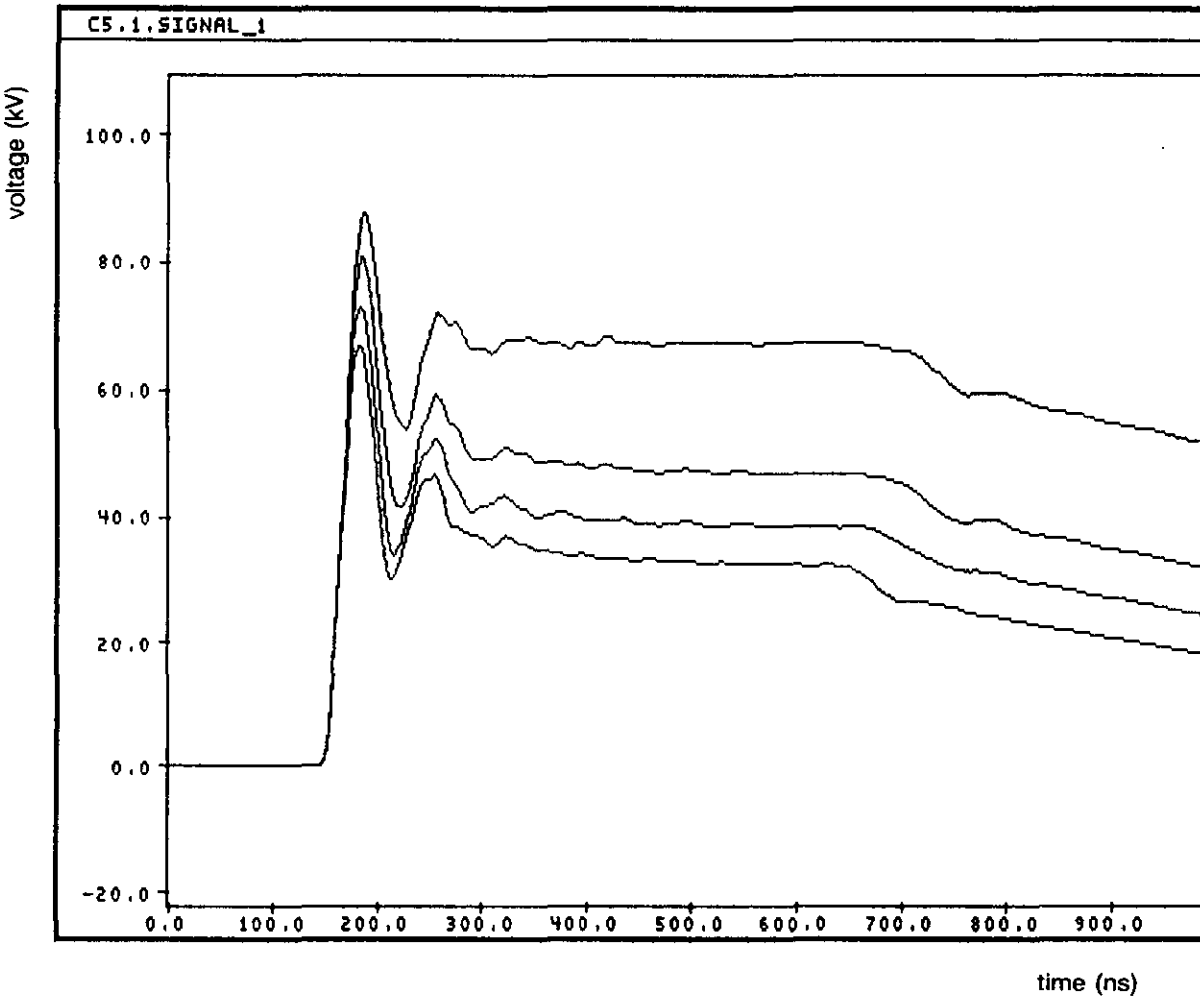

Figure 10c: Pulse voltage waveform of the corona discharge in air for different DC bias voltages and a series resistor.
a: Vdc = 30 kV, b: Vdc = 20 kV, c: Vdc = 10 kV, d: Vdc = 0 kV, R = 40 Ω and Vp = 80 kV.

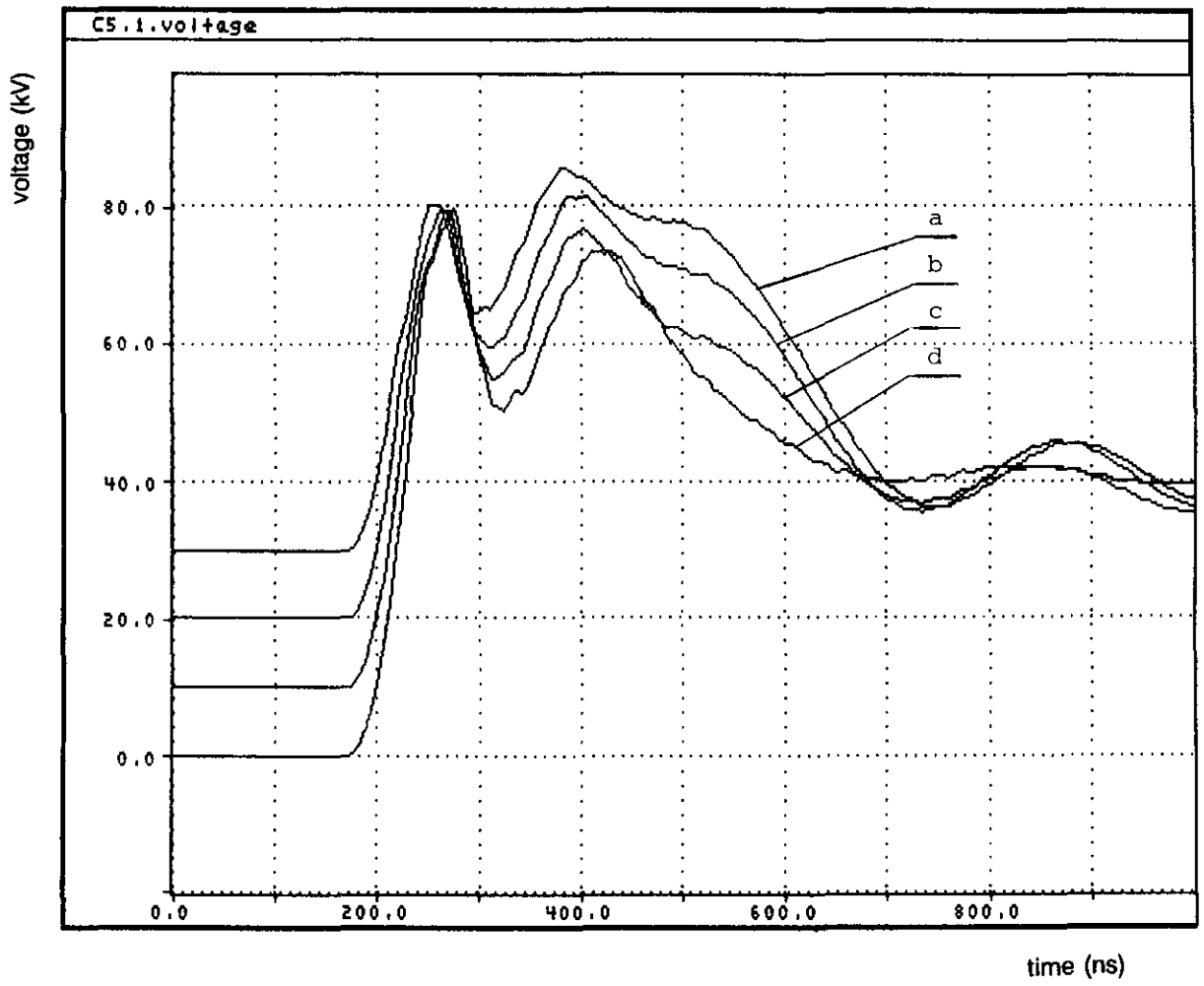

Figure 11a: Total voltage waveform of the corona discharge in air for different DC bias voltages and a series inductance.
a: Vdc = 30 kV, b: Vdc = 20 kV, c: Vdc = 10 kV, d: Vdc = 0 kV, Li = 17.5 uH and Vp = 80 kV.

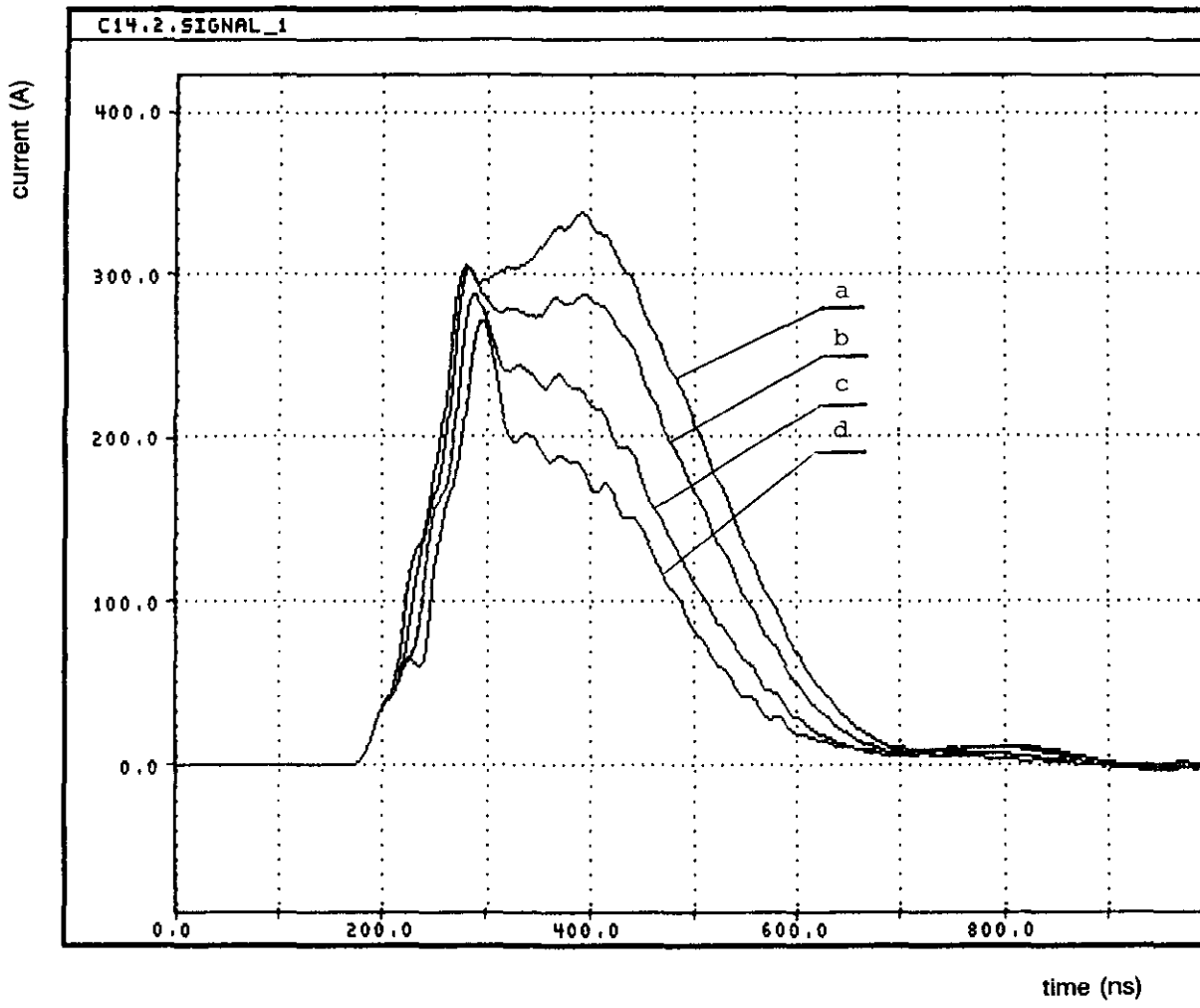

Figure 11b: Current waveform of the corona discharge in air for different DC bias voltages and a series inductance.
a: Vdc = 30 kV, b: Vdc = 20 kV, c: Vdc = 10 kV, d: Vdc = 0 kV, R = 40 Ω and Vp = 80 kV.

The voltage on the emitting wire after streamer quenching is referred to as the residual voltage. It can be easily seen from figure 10 and figure 11 that in any case the residual voltage is almost constant. It has also been noticed that the residual voltage level is mainly determined by the electrodes gap distance and the gas composition. The portion of the pulse voltage after streamer quenching is continuously decreased with increasing the DC bias level. If the DC bias voltage is increased to the residual voltage, the pulse voltage after streamer quenching can be reduced almost to zero.

Therefore it can be concluded that under the same pulse energy supply, with increasing DC bias voltage, a larger energy conversion from the pulse generator to the reactor can be obtained.

For the optimization of energization, the DC bias level should be evaluated according to the time dependent energy dissipation process. From the current oscillograms in figure 10 and figure 11, it can be concluded that with slow rise rate of pulse voltage the main effects of DC bias voltage will become to enhance the second part of energy or charge injection i.e. increase the secondary streamer intensity. For larger rise rate, the two parts could be enhanced simultaneously.

It is also supposed that the DC bias level could also lead to different enhancement on global chemical processes with different pulse rise rate.

3.6 Classification of current and voltage oscillograms and its corresponding streamer properties

Even just based on the above current and voltage oscillograms, it can been remarked that once streamers are produced a very complicated matching between pulse generator and the reactor occurs, which leads to different voltage and current correspondence.

From engineering point view, when producing pulse streamer for promoting chemical oxidations, following points can be used to evaluate the energization:

- the energy conversion efficiency from power source to the reactor
- maximum energy and charge injection per pulse
- streamer current duration
- peak current of corona streamer
- the percentage of the energy for streamer heads propagation

The main point is the active electrons production per unit energy injection and per unit discharging volume. Thus if regarding the two parts of the streamer, head and channel, increasing the active energy injection together with reducing the passive energy injection should be the principle procedures to optimise the energization.

From the current and voltage correspondence, we can divide the energization into

two types based on the voltage level V/p for primary streamer propagation and the voltage level V/s for the secondary streamer evaluation, which lead to produce different streamer structure.

- V/p is much larger than V/s
- V/p is very smaller that V/s

The first one corresponds to larger peak current but shorter duration, and the voltage and the current almost decraeses monotonuously after the peak value. The second corresponds to smaller peak current but its duration is much longer as indicated in fig. 6.

If considering streamer development, it can be easily concluded that for the first type much more energy or charge is dissipated during the primary streamers and the number of primary streamer is much larger together with limited intensity of secondary streamers.

On the contrary, for the second type, the secondary streamer is extremely enhanced and the main part of energy is transferred to the gas during the secondary streamer evaluation.

3.7 Observation of local light emission near the emitting wire, near the cathode and the propagation speed of primary streamers

Two quarts fibres are placed together with photo-multiplier in order to measure light emission and streamer propagation speed. One is placed to focus a small volume (4mm * 4mm) near the anode, the another is placed to focus a small part of cathode to detect the local light emission. The two photo-multipliers are sensitive in the range of 185 nm - 930 nm and have a 2 ns rise time.

Based on streak photogragh of streamer development, it is well known that once the voltage becomes larger than the streamer inception value, streamer develops along the field line with a weak light emission in the channel and bright emission around the head. Once the streamer has crossed the gap, a very strong light emission may be observed along the previous channel, which corresponds to the so called secondary streamer.

Therefore, it may be possible to detect the streamer duration and the evaluation of the streamer channel with the above local light measurements.

Figure 12 indicates typical light emission near the anode. The first part related to the first peak light emission corresponds to the primary streamers, while the second part is related to the secondary streamer.

It should be noticed that the signal duration is not limited by the measurement system, but it is due to the statistic time difference between different streamers as indicated in figure 13 and the size of the focussed region.

It has been observed that if the total voltage is lower, only the light emission corresponding to the primary streamer can be observed. Once the streamer has crossed the gap, the light emission related to the secondary streamers may be detected. If the voltage becomes very high, the two parts of light emission overlap at some times and at some emitting points as indicated in figure 14.

(see figure 12 from data c-3)

Figure 12. Typical light emission near the anode

(see figure 13 from data c-4)

Figure 13 illustrates the time difference of different primary streamers.

(see figure 14 from data c-4)

Figure 14. Special light emission near the anode when the primary and secondary streamers overlap.

As for as the light emission near the cathode as indicated in figure 15, it has been noticed that under the test conditions in this arrangement emission from the secondary streamers is rarely observed but light from the primary streamer always. This means that most of the secondary streamers stop propagation in the gap.

It has also been observed that streamers can be produced at different time and across the gap at different moment as indicated in figure 16.

(see figure 15 from data c-3)

Figure 15. Local light emission near the cathode.

(see figure 16 from data c-4)

Figure 16 illustrates the phenomena of streamers produced at different times.
a: near the anode, b: near the cathode.

When averaging the emission signal as indicated in figure 13 and figure 15, the average propagation speed for primary streamer can be evaluated as shown in figure 17. It can be seen that with increasing the applied voltage, the average speed is increased from 0.5 m/us to 3 m/us.

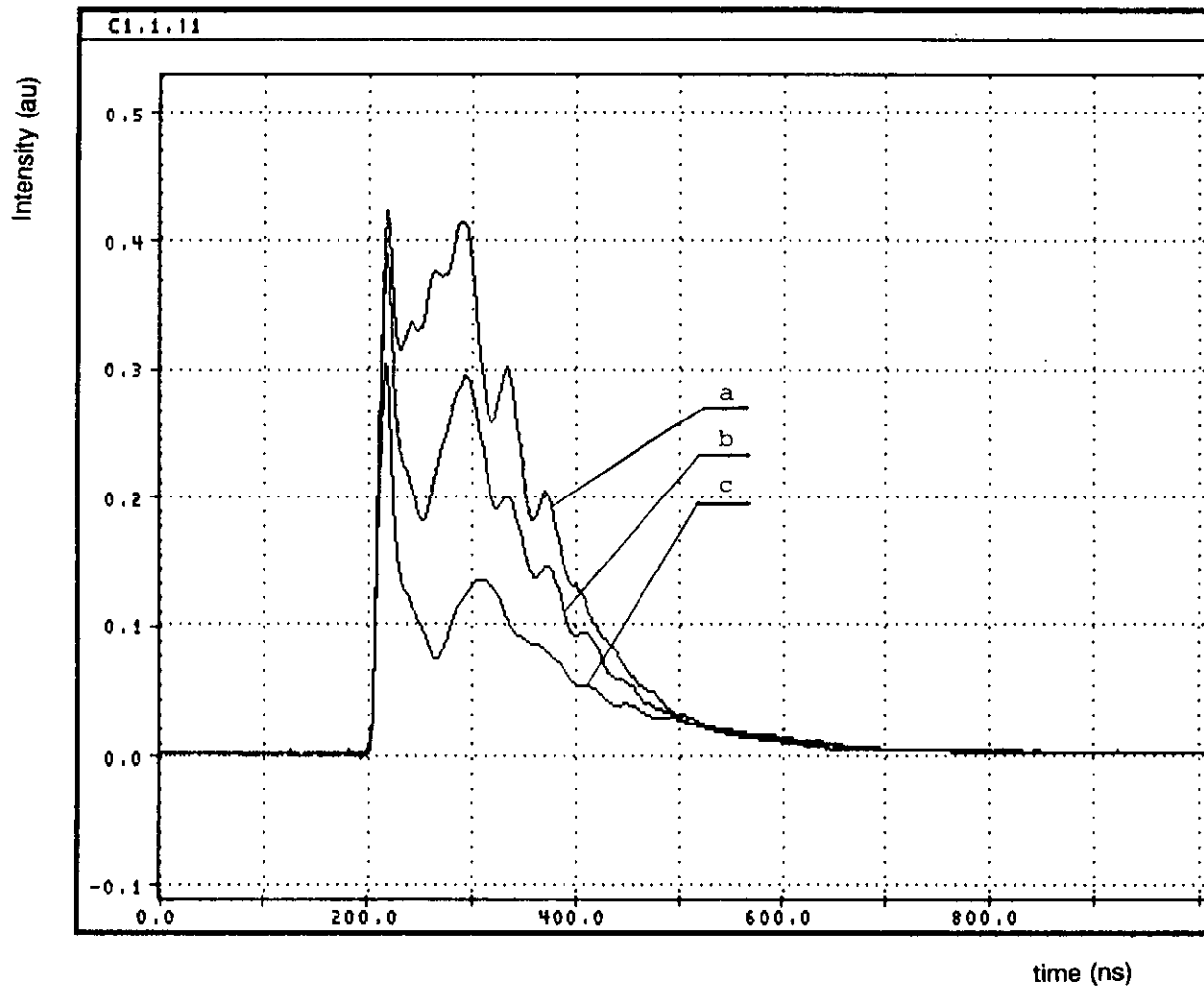

Figure 12: Local light emission of the corona discharge in air near the anode for different pulse voltages and a series resistor (typical form).
a: Vp = 80 kV, b: Vp = 60 kV, c: Vp = 40 kV, R = 100 Ω and Vdc = 30 kV.

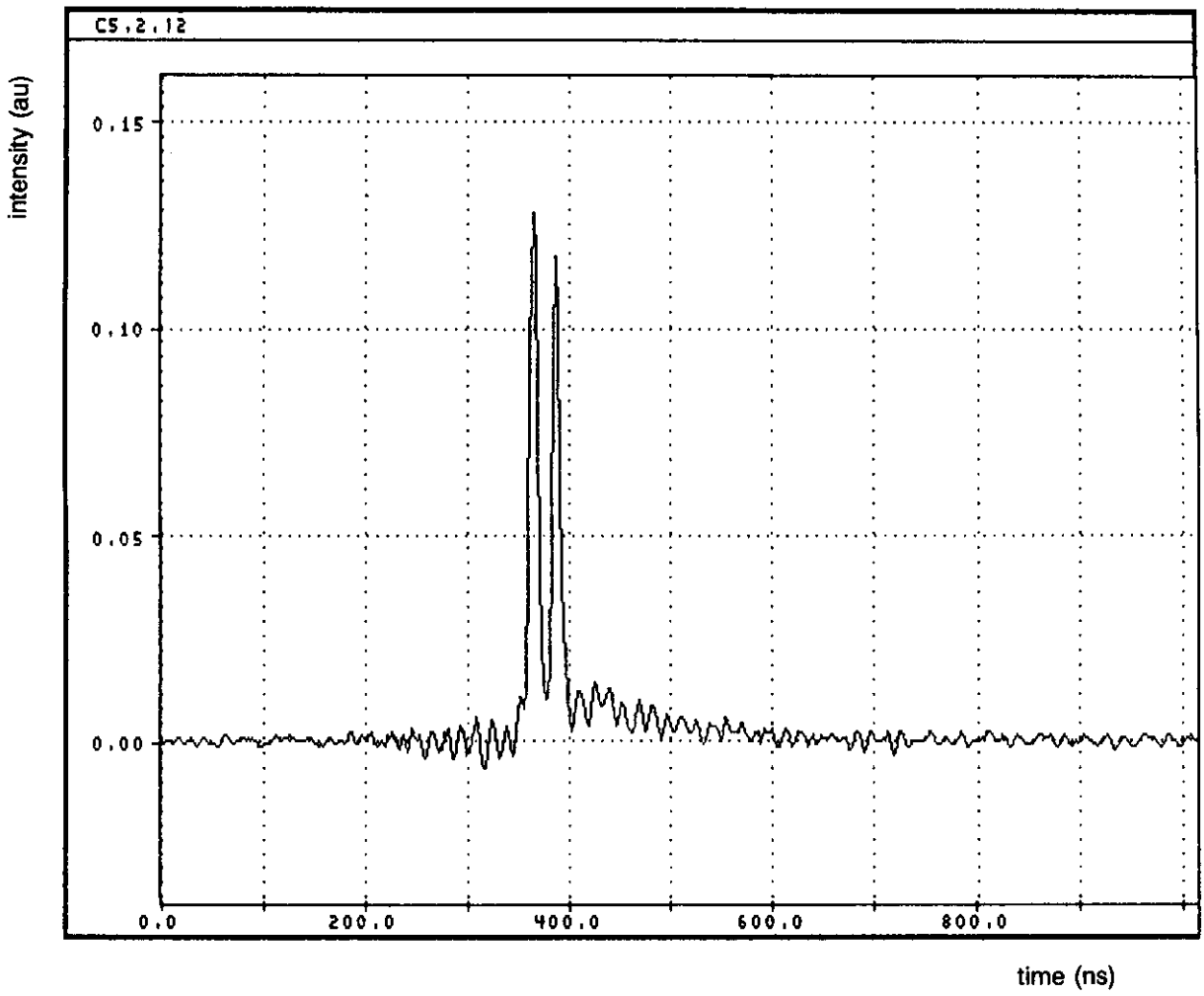

Figure 13: Local light emission of the corona discharge in air near the cathode with a series resistor.
Vp = 80 kV, R = 100 Ω and Vdc = 20 kV.

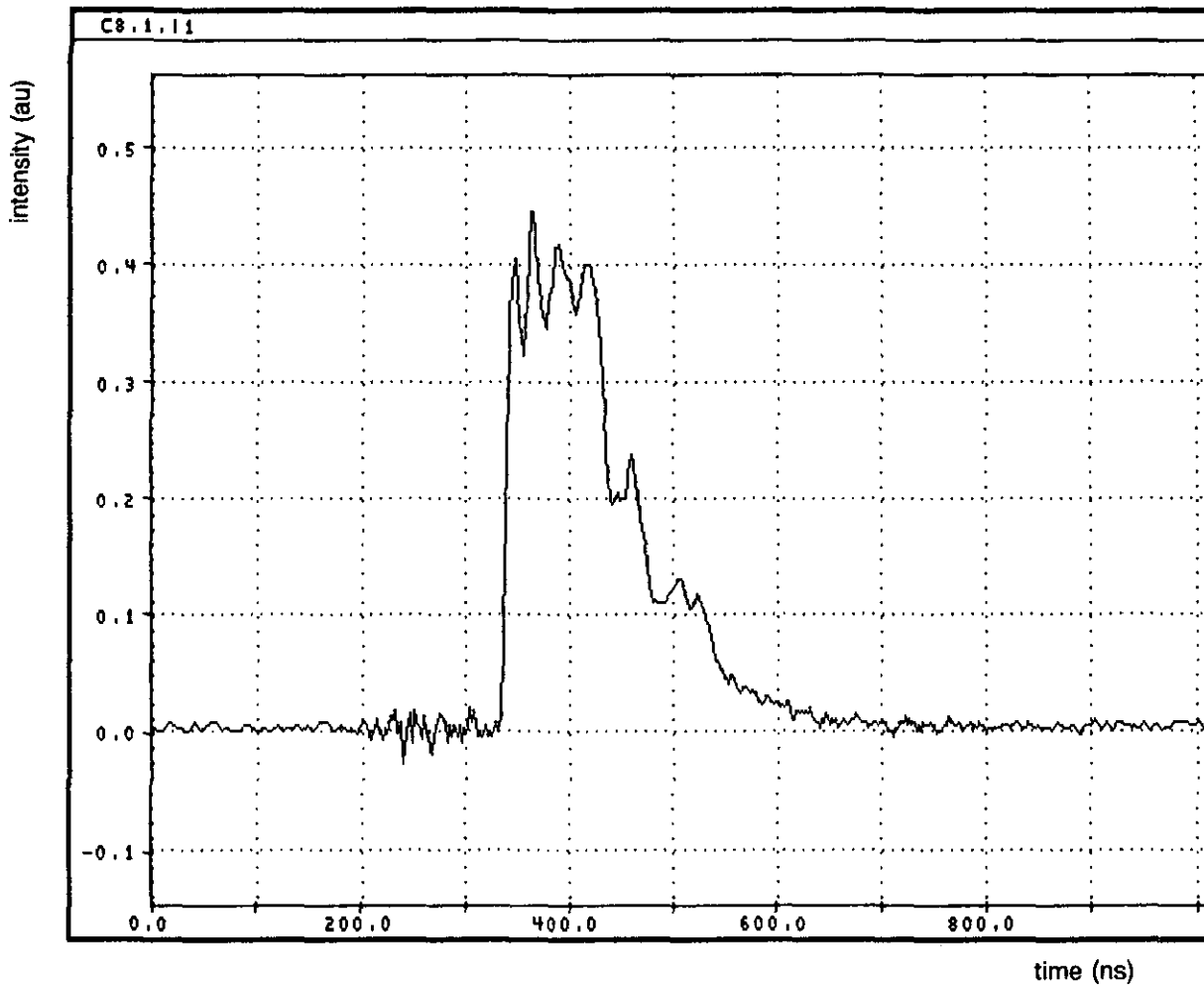

Figure 14: Special case of local light emission of the corona discharge in air near the anode with a series resistor: overlap of primary and secondary streamers.
Vp = 80 kV, R = 100 Ω and Vdc = 30 kV.

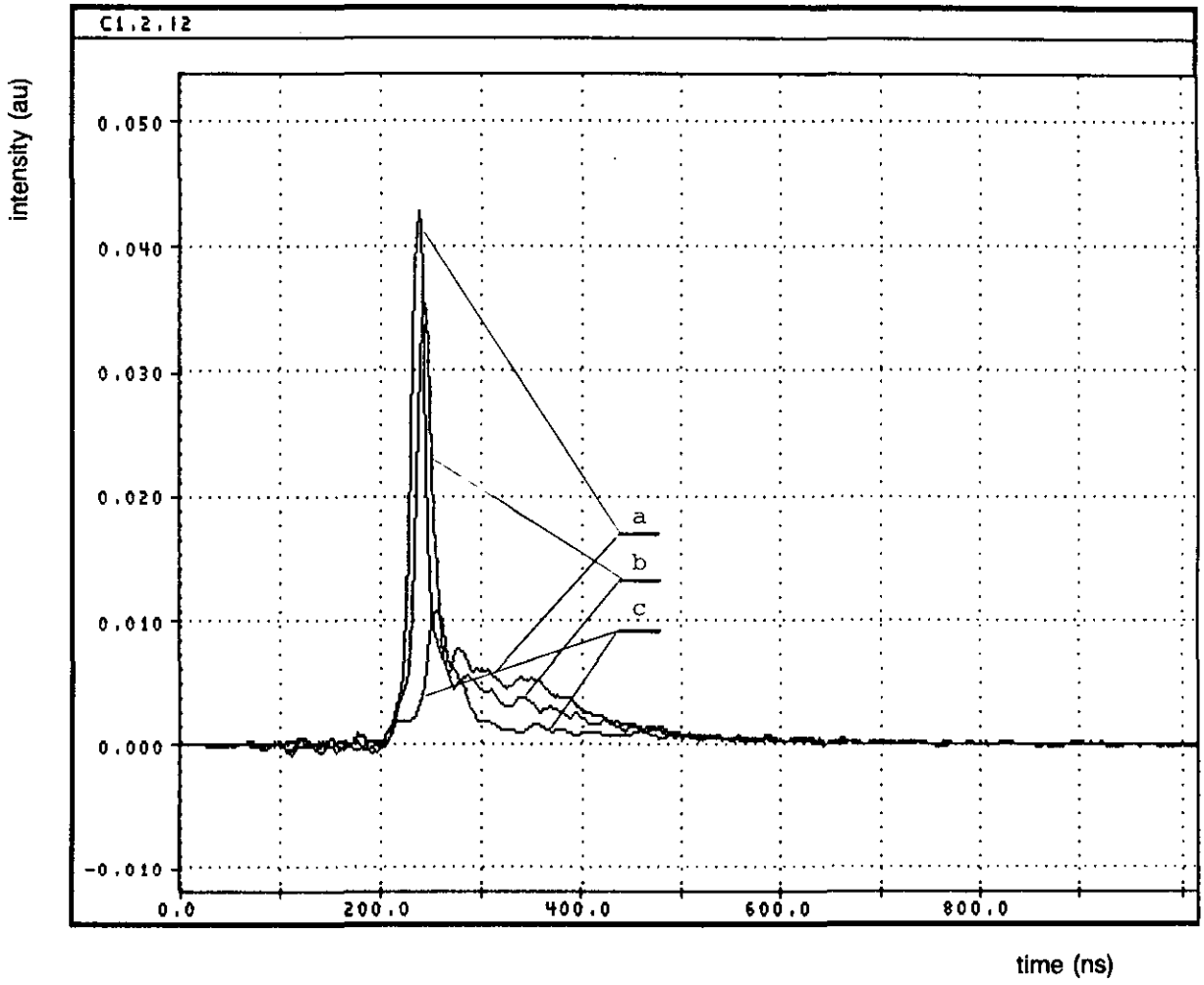

Figure 15: Local light emission of the corona discharge in air near the cathode for different pulse voltages and a series resistor.
a: Vp = 80 kV, b: Vp = 60 kV, c: Vp = 40 kV, R = 100 Ω and Vdc = 30 kV.

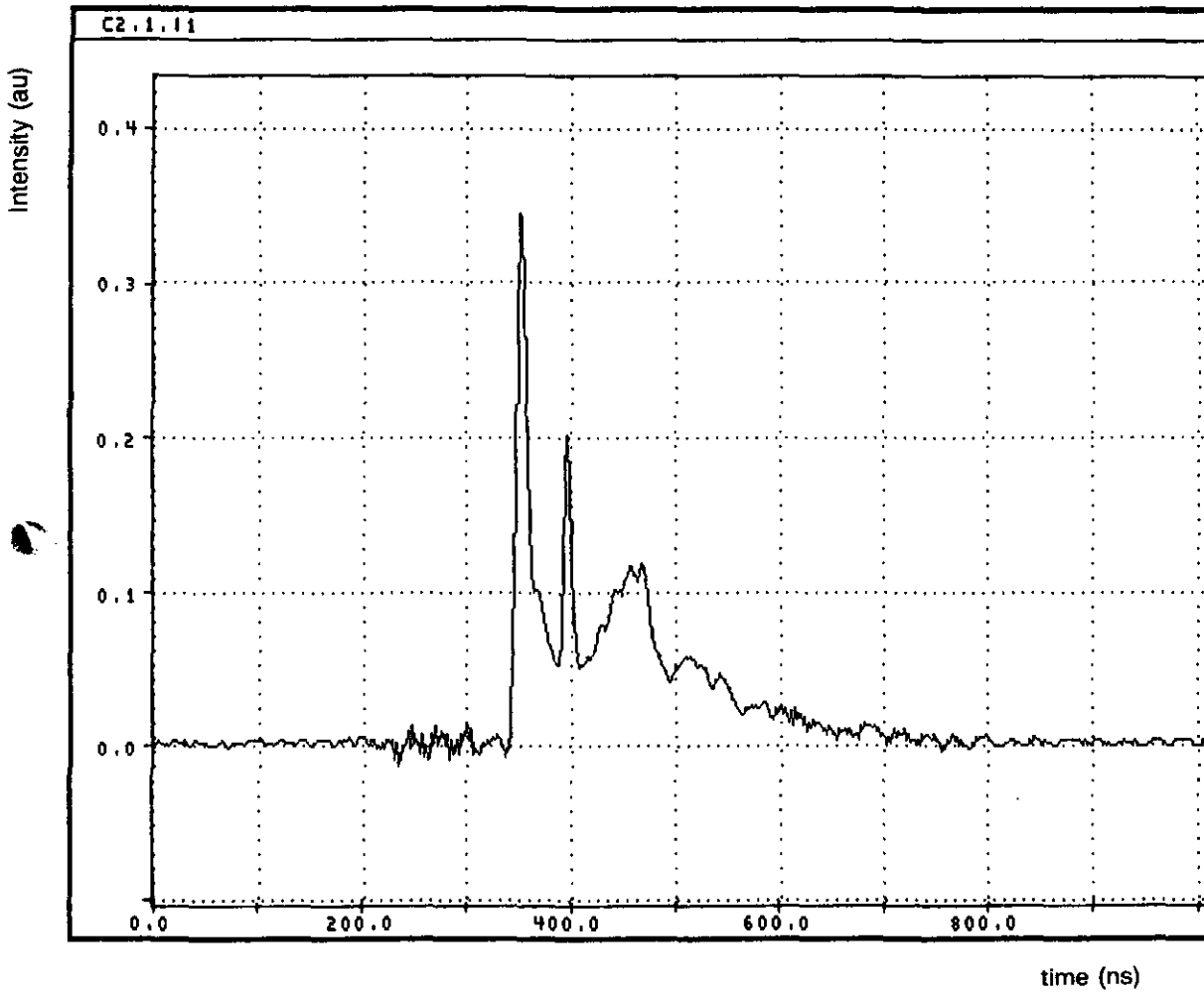

Figure 16a: Local light emission of the corona discharge in air near the anode with a series resistor.
Vp = 60 kV, R = 40 Ω and Vdc = 10 kV.

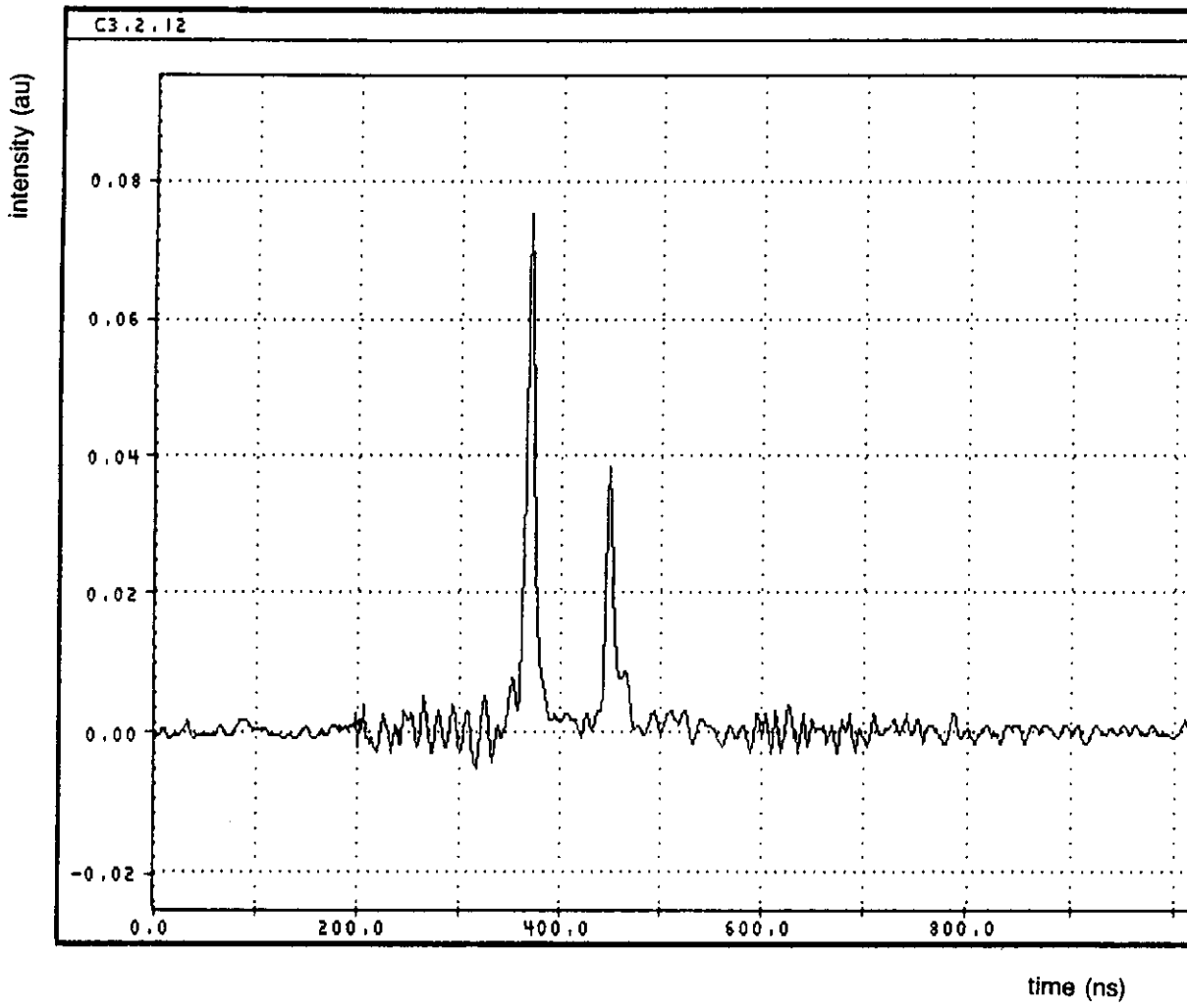

Figure 16b: Local light emission of the corona discharge in air near the cathode with a series resistor.
Vp = 80 kV, R = 40 Ω and Vdc = 10 kV.

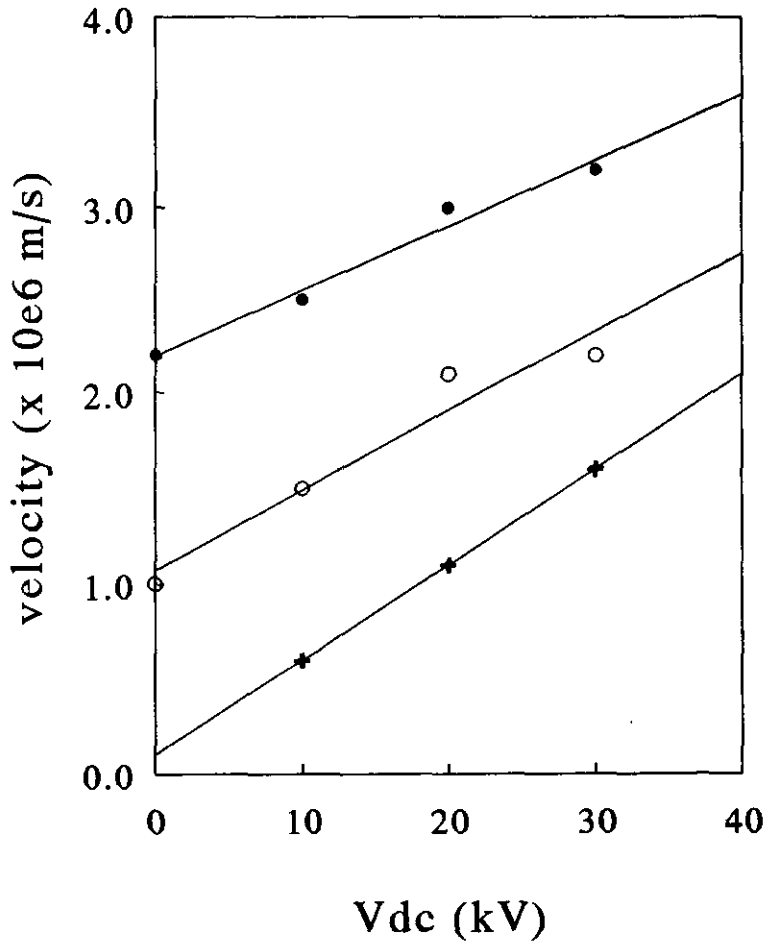

Figure 17: Average propagation speed of the primary streamers in air for different DC and pulse voltages.
+: Vp = 40 kV, ○ : Vp = 60 kV, ● : Vp = 80 kV, R = 100 Ω.

(see figure 17 from data c-3)

Figure 17 the dependence of the average streamers speed on the applied voltage. R = 100 ohm, Li = 0

Based on the light emission near the anode and the emission near the cathode, it was also observed that once the streamers reach the cathode, the light emission related to the secondary streamer near the emitting wire appear.

Therefore, it can be concluded that as the observed secondary streamer by DC corona in the shorter gap distance [1.5 cm - 2 cm], the pulse voltage also can lead to produce the secondary streamer in the range of 7.5 cm of gap distance once the primary streamer has crossed the gap.

From channel model, it was supposed that once the secondary streamer is across the gap, the corona would become spark. However, from the experiments, it has been observed that not only the primary streamer across the gap will not necessarily lead to the breakdown, but also the secondary streamer across the gap will not necessarily lead to the breakdown. The breakdown will be determined by the streamer intensity and the residual voltage after streamer quenching. A comprehensive model to describe this phenomena is still undeveloped.

3.8 Time resolved N2, positive N2 ions emission and estimation of average electron energy during the discharging periods

In order to evaluate the electron energy distribution and gas temperature during the streamer propagation and during the channel evaluation, the so-called SPS [Second Positive System] emission from N2 [C-B] and the so-called FNS [First Negative System from positive N2 ions [A-X] have been proposed and adopted for many years. The emission spectra along the emitting wire are measured with a quartz lens of 10 mm, which is placed 6 mm from the emitting wire. The methods are based on the two following hypothesis:

- excitation and ionization take place by electronic collisions from the fundamental level [N2-X];

- the population at the different levels follow the Boltzmann's law

However, due to the lack of reliable data, uncertainty of the cross sections, energy distribution fuctions and the detailed quenching mechanism, a comprehensive model, which takes into account the time scale and detailed quenching mechanism is still undeveloped. Therefore, it is very hard to evaluate the exact energy functions during the discharging periods.

However, if the two assumption can be valid, it is reasonable to believe that the relative emission intensity from nitrogen ions can be used to indicate the range of the average electron energy as used before by Hartmann. It is supposed that the average electron energy increases with increasing of the ratio of the reletive emission intensity of FNS/SPS.

Figure 18 and figure 19 indicate the SPS and FNS emission respectively near the emitting wire (6 mm away) with different applied voltage.

(see figure 18 from data c-8)

Figure 18 indicates typical SPS emission with different applied voltage.

(see figure 19 from data c-8)

Figure 19 indicates typical FNS emission with different applied voltage.

It can be seen that the ratio of FNS/SPS is about three times smaller during the second stage of discharging period [the so called secondary streamer]. The active electrons are only generated during the first stage.

If we suppose that during these test conditions the basic mechanism are the same, based on the ratio of the light intensity as shown in figure 20, it can be concluded that the average electron energy is increased with increasing the applied voltage and the average energy associated to the primary streamer is much larger than that associated to the secondargy streamers.

(see figure 20 from data c-8)

Figure 20 illustrates the influence of pulse voltage on FNS/SPS emission intensity of primary and secondary streamer.

If the quenching factor supposed by Spyrou [8] is still valid in this situations, the estimated electron energy near the emitting wire for the primary streamer and for the secondary streamer are about 10 - 12 eV and 3 - 5 eV respectively.

It is also supposed that the electron energy associated to the secondary streamer will decrease along the discharge channel from anode to cathode, and the so-called two region field controlled channel evaluation will stop at the time when the field reach the stability requirement.

From the field requirement and the applied voltage level during the secondary

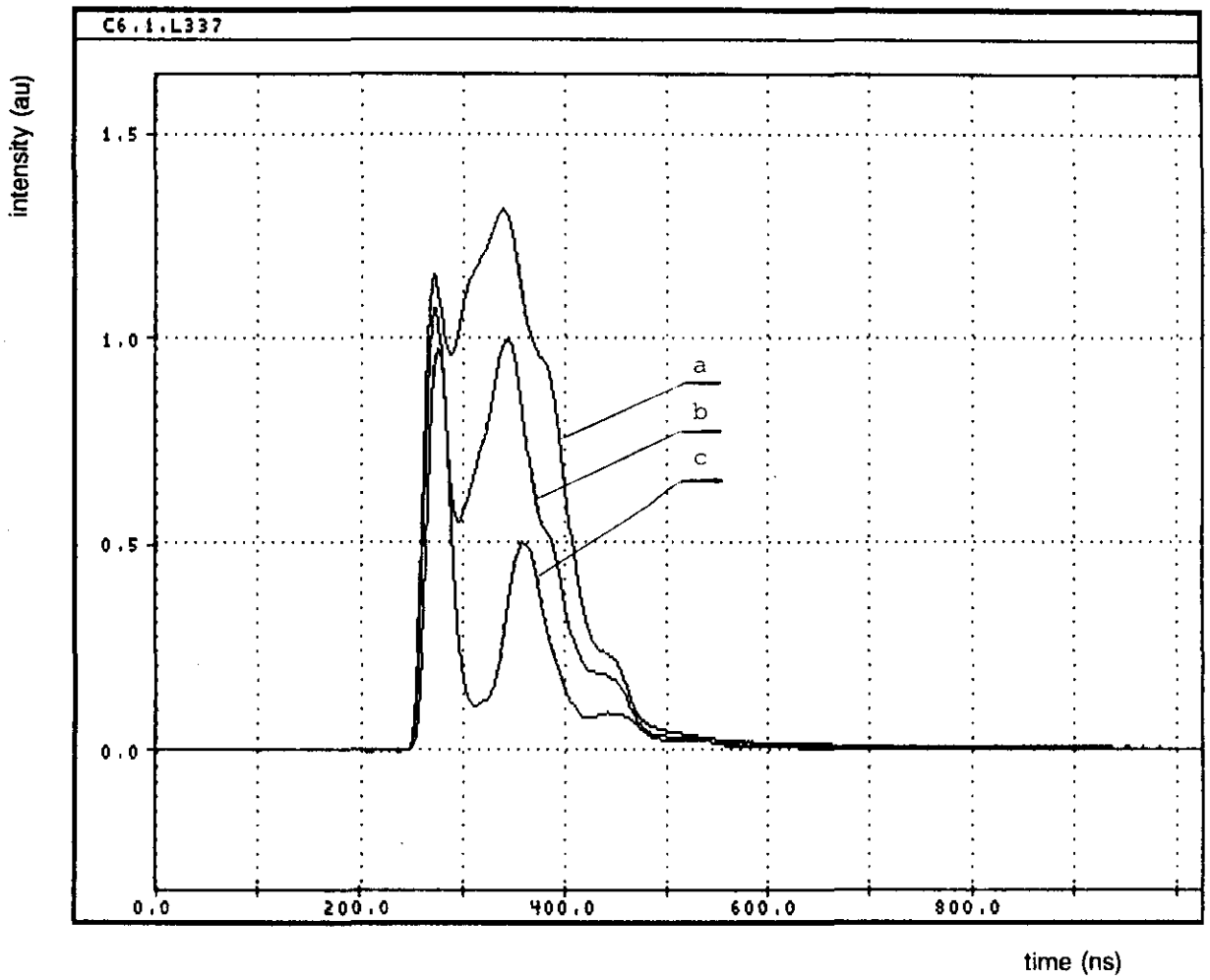

Figure 18: Maximum of spectral emission of N_2 SPS as a function of time for corona discharge in air under different peak voltages.
a: Vp = 80 kV, b: Vp = 60 kV, c: Vp = 40 kV, R = 0, Li = 0 and Vdc = 30 kV.

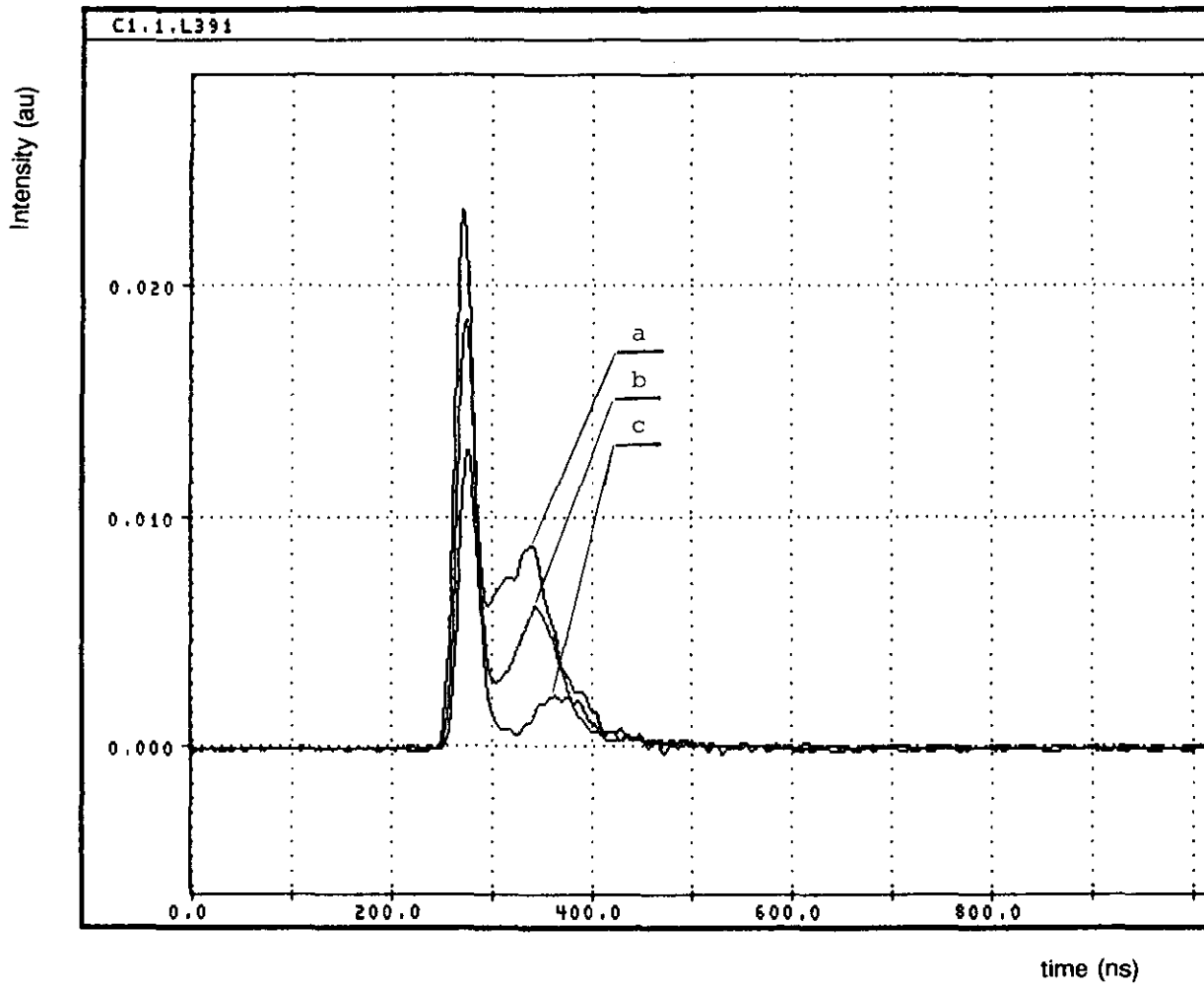

Figure 19: Maximum of spectral emission of N_2^+ FNS as a function of time for corona discharge in air under different peak voltages.
a: Vp = 80 kV, b: Vp = 60 kV, c: Vp = 40 kV, R = 0, Li = 0 and Vdc = 30 kV.

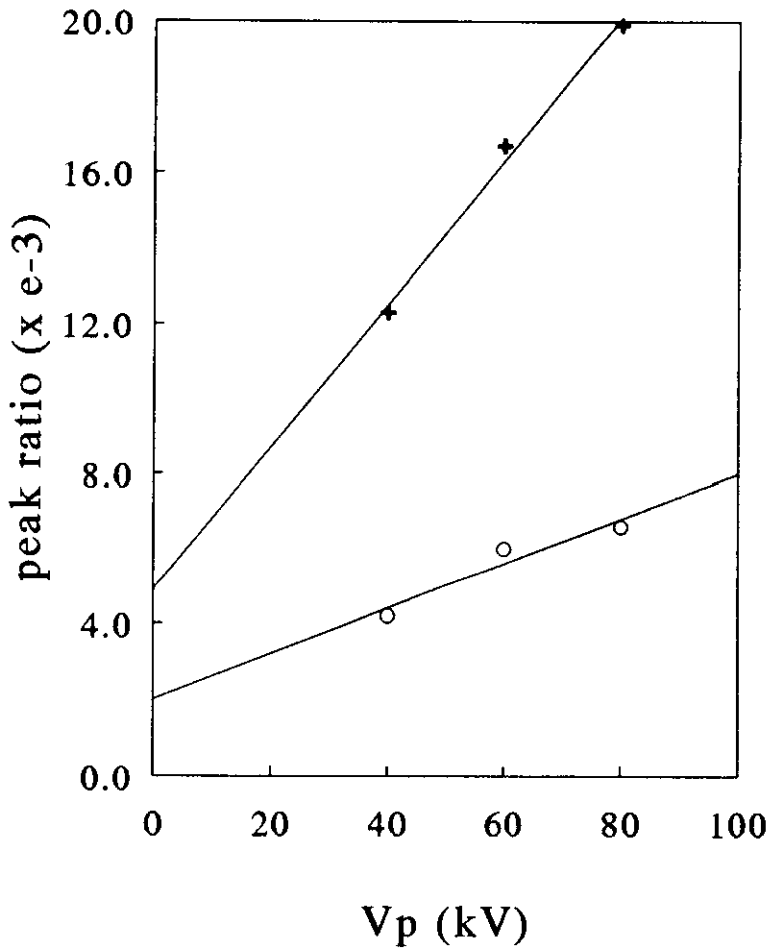

Figure 20: Ratio of FNS and SPS emission in air as a function of the peak voltage
+: primary streamers, ○ : secondary streamers

streamers development, it can be roughly estimated that the secondary streamer can be detected within 2-3 cm from the emitting wire with a decay of electron energy from 5 eV to about 1 eV.

As indicated in figure 18 and figure 19, the emission spectrum in figure 21 and figure 22 also show that the associated relative emission from the primary streamer is much stronger than that for the secondary streamers.

(see figure 21 from data c-6)

Figure 21. The typical spectrum near the SPS emission for primary and secondary streamers with different additional inductance

(see figure 22 from data c-6)

Figure 22 The typical spectrum near the FNS emission for primary and secondary streamers

3.9 Comparison of electrical properties of corona streamer in air and in flue gas

Both theoretical and experimental investigation on electron transport parameters in flue gas and in air have been conducted and the data have been often compared. A very good agreement has been obtained excepet for the attachment coefficient under the lower field.

However, the corona streamer current and voltage properties in flue gas is still uncertain and its correspondence to the pulse voltage generator is unknown.

Considering the practical operations, up to date, no direct experimental results demonstrate the difference or the similarity in electrical and optical properties and the associated streamer structures in flue gas and in air.

Comparing the gas composition, the main point is the O2 is replaced by CO2 and H2O in flue gas. If regarding the model by Gallimberti, the main part of energy conversion to the gas by corona streamer is releated to the N2 in air or in flue gas. Therefore, it is often supposed that no big difference exists in flue gas and in air.

During this investigation, the experiment was conducted several times with flue gas. Two typical parameters for the flue gas are indicated as following:

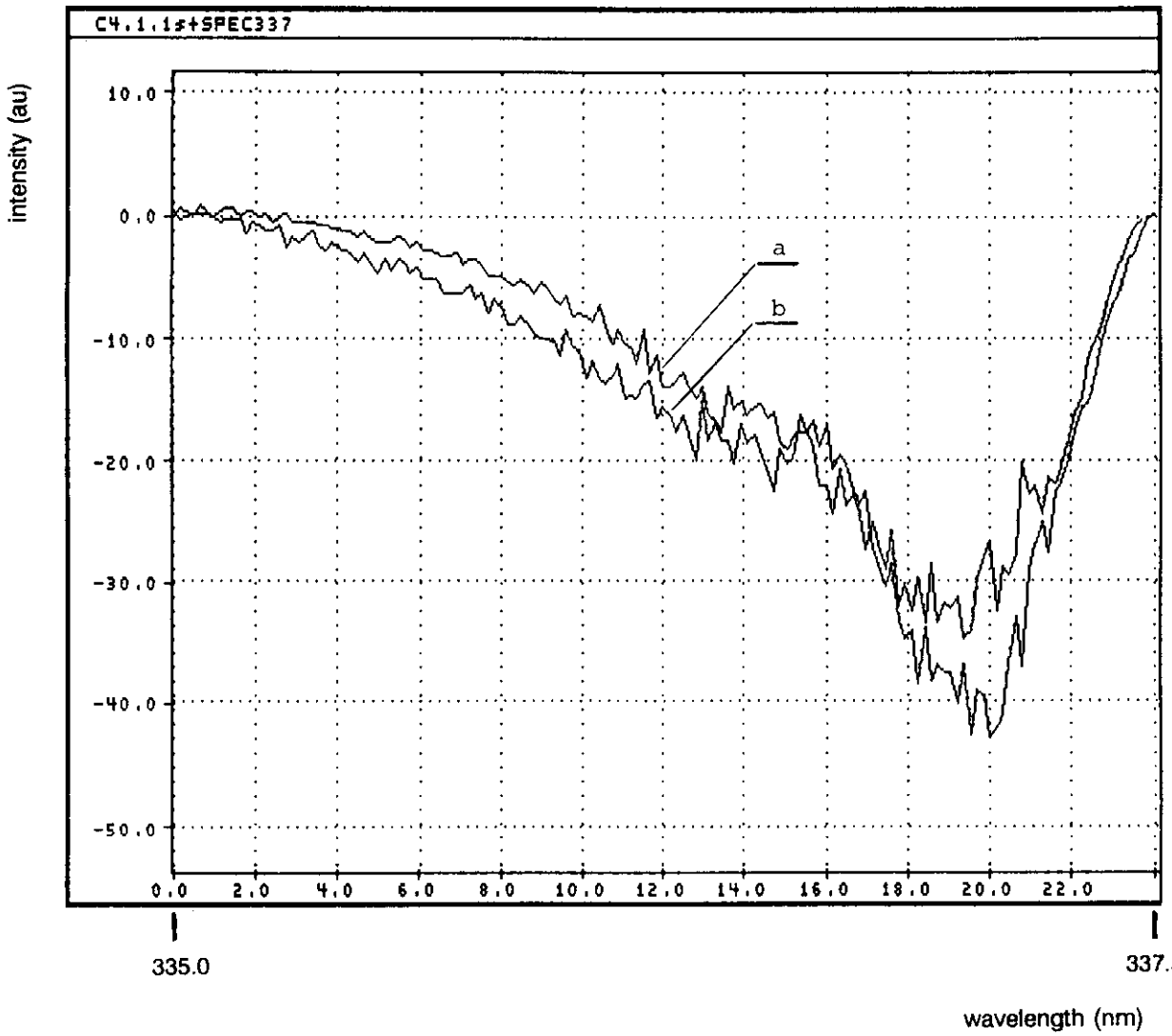

Figure 21a: Emission of N_2 SPS as a function of wavelength for primary streamers in air.
a: Li = 0, b: Li = 55 uH, Vp = 80 kV, Vdc = 30 kV.

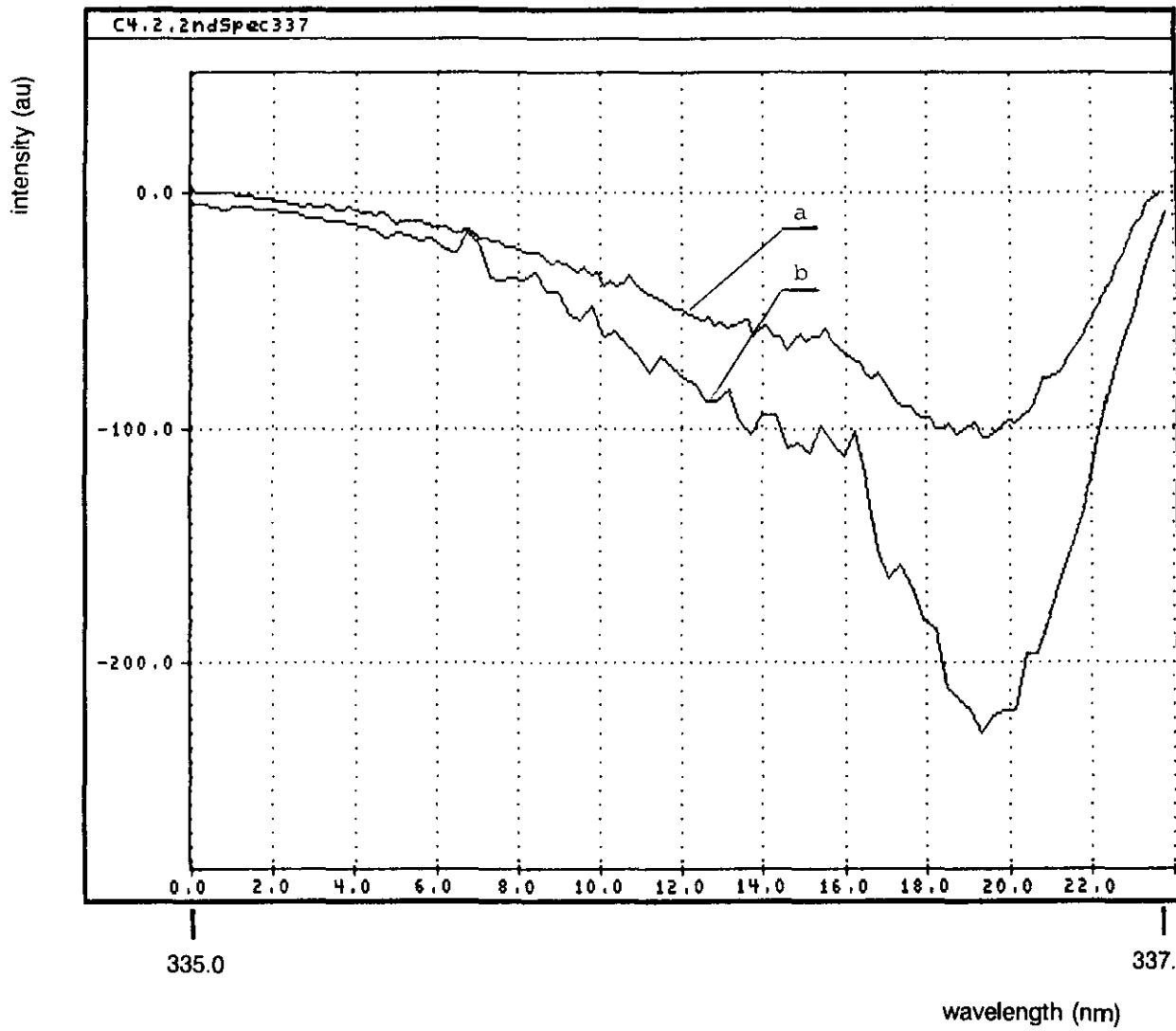

Figure 21b: Emission of N_2 SPS as a function of wavelength for secondary streamers in air.
a: Li = 0, b: Li = 55 uH, Vp = 80 kV, Vdc = 30 kV.

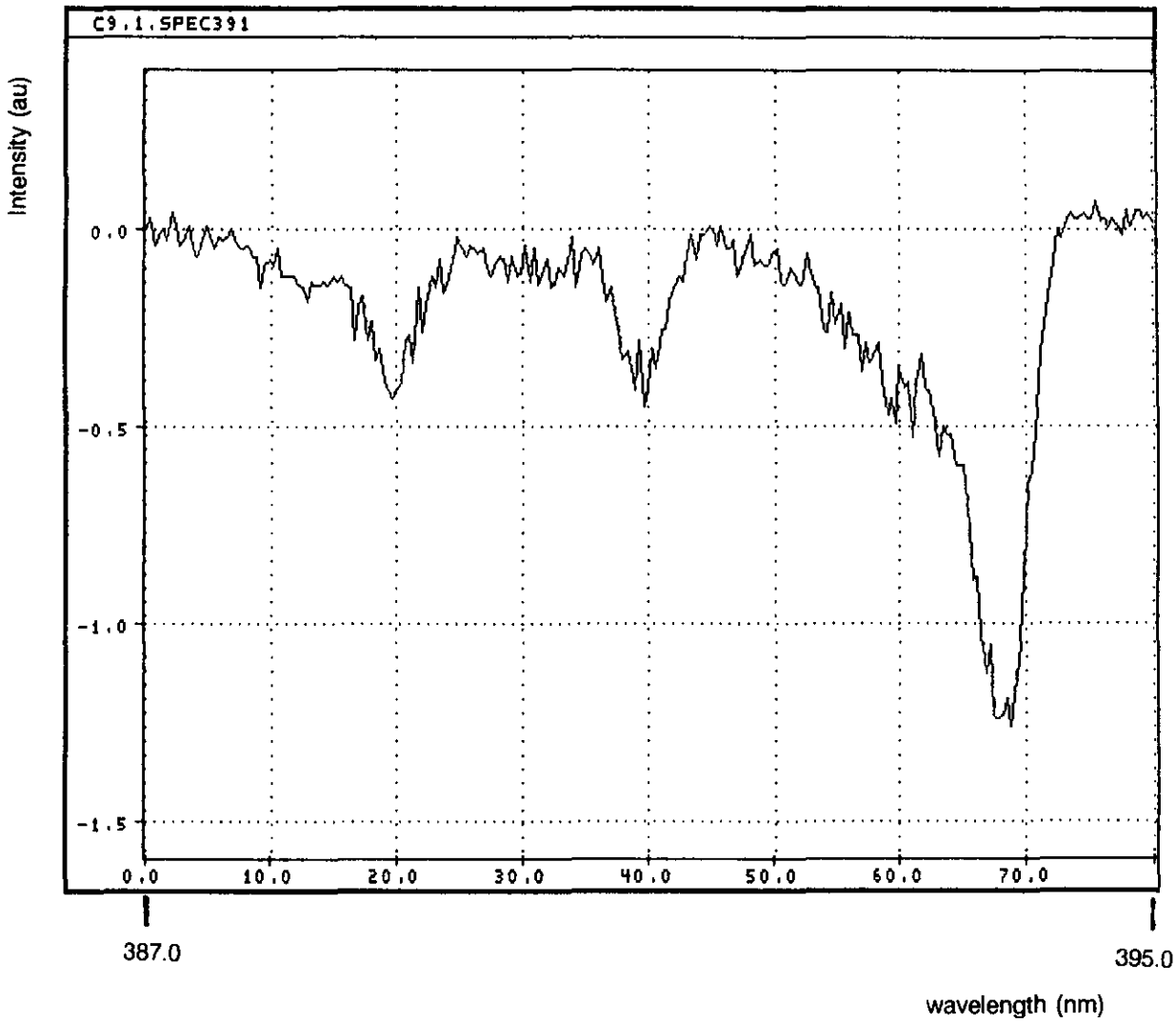

Figure 22a: Emission of N_2^+ FNS as a function of wavelength for primary streamers in air.
Li = 0, R = 0, Vp = 80 kV, Vdc = 30 kV.

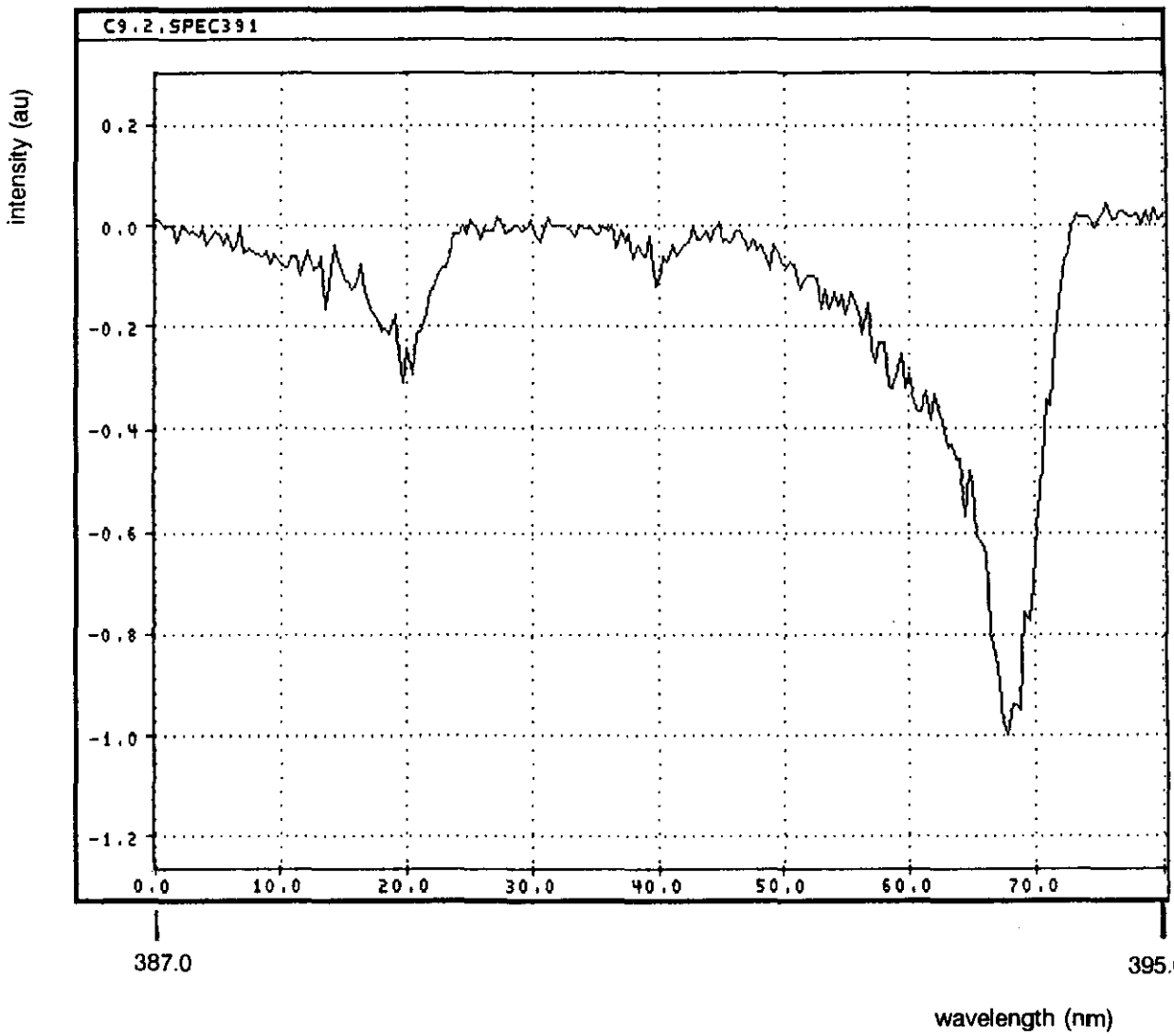

Figure 22b: Emission of N_2^+ FNS as a function of wavelength for secondary streamers in air.
Li = 0, R = 0, Vp = 80 kV, Vdc = 30 kV.

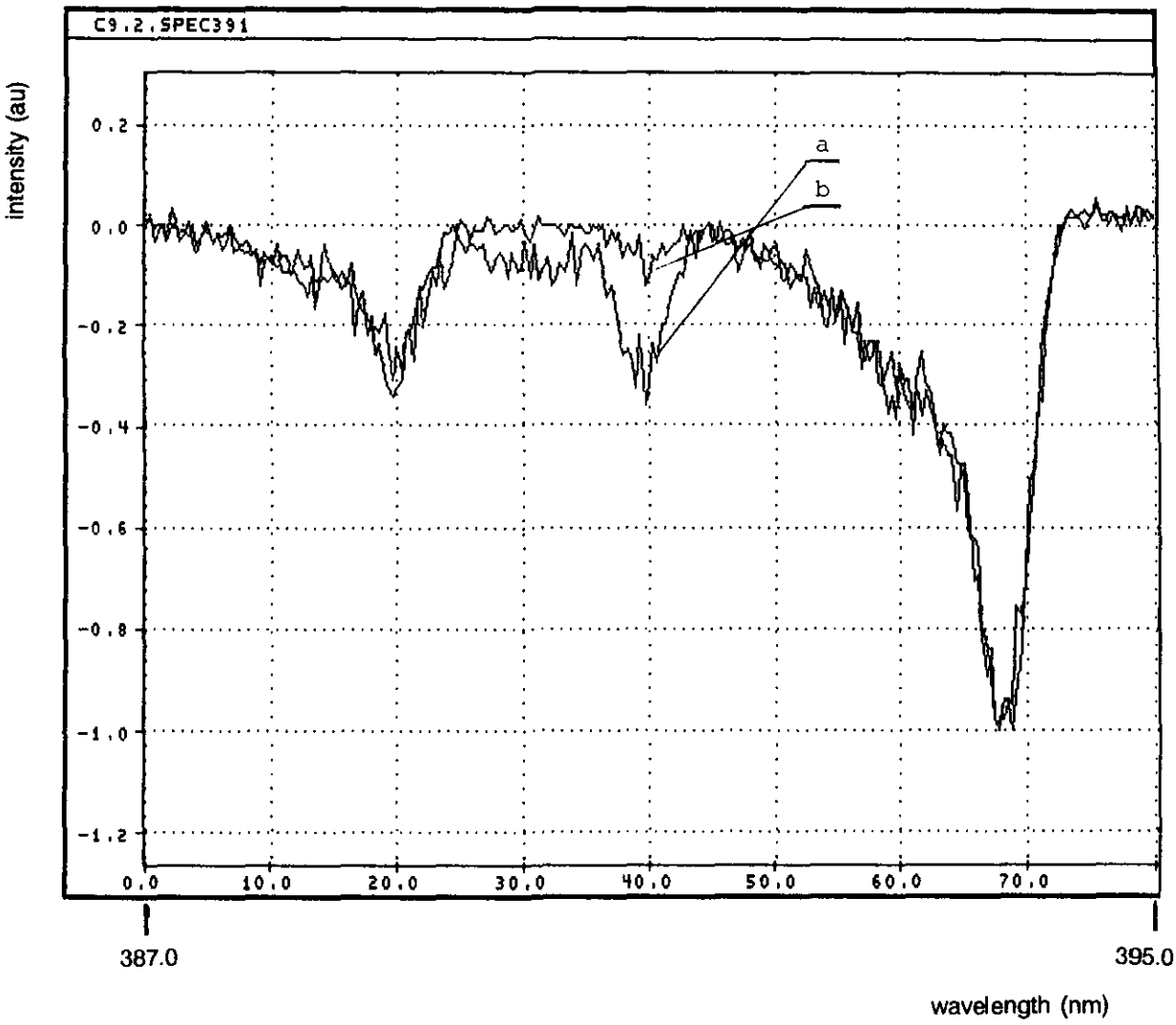

Figure 22c: Normalized spectra of SPS and FNS to compare primary (a) and secondary (b) streamers in air.
Li = 0, R = 0, Vp = 80 kV, Vdc = 30 kV.

Flue gas I

inlet temperatue : 160 C
outlet temperature :130 C
O2 - 10.5 %; CO2 - 5.8 %; H2O - 11 %;
NO - 28.4 ppm, NO2 - 0.4 ppm

Flue gas II

inlet temperature : 88 C
outlet temperature : 75 C
O2 - 15.2 %; CO2 - 3.2 %; H2O - 6.4 %;

Figure 23 indicates the typical comparison of the electrical properties of corona streamer in flue gas I, flue gas II and in air. It can be easily noticed that the peak corona current for flue gas is always smaller, but the residual voltage is larger. This means that the associated energy conversion to flue gas from the pulse voltage generator is smaller.

(see figure 23 from data c-91)

Figure 23 indicates the comparison of electrical properties
in flue gas and in air under the same power supply.

The energy difference becomes very obvious when the total applied voltage is smaller. If the energy obtained in these conditions is limited by the pulse voltage generator, very little difference has been observed.

When considering the current waveforms from the model, it can be concluded that the tendence of peak corona current shows a smiliar changing. But the current duration for flue gas is not so long as predicated by the model.

The reason for this phenomena is still not very clear, but at least two facts should be responsible. The first is that the attachment data used in the model is two or three times larger than the experimental results under the low field [9]. The second is the matching between the generator and the corona streamer can also influence the current duration.

Considering the influence of the damping resistor, the additional inductance, the peak pulse voltage and the DC bias voltage on the streamer properties in flue gas, similar tendence of the effects as observed in air on current and voltage oscillograms and the light emission have been observed from the experiments.

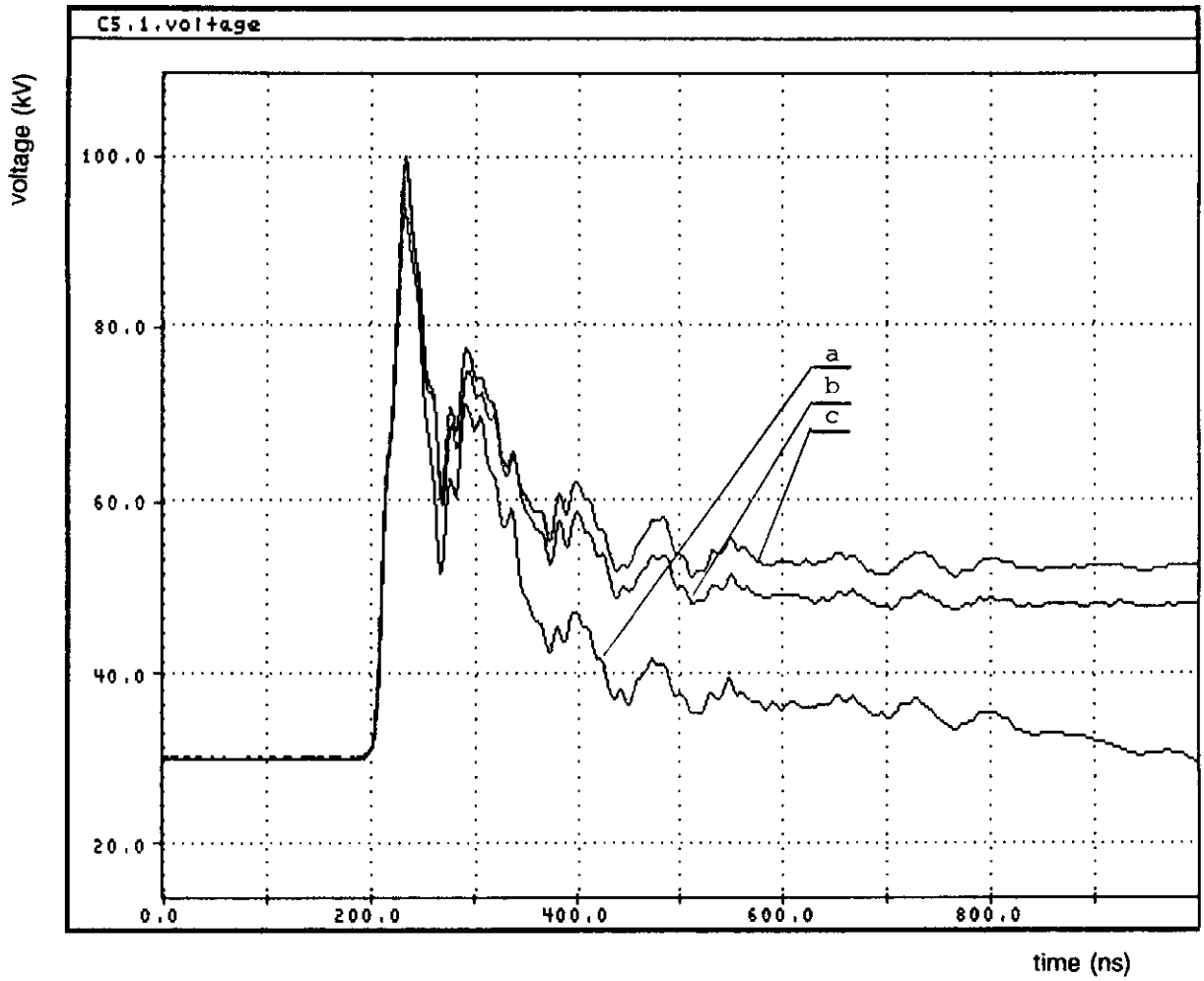

Figure 23a: Voltage waveform of the corona discharge in air and flue gas. a: air, b: flue gas I, c: flue gas II, Vp = 60 kV, Li = 0 uH, R = 40 Ω and Vdc = 30 kV.

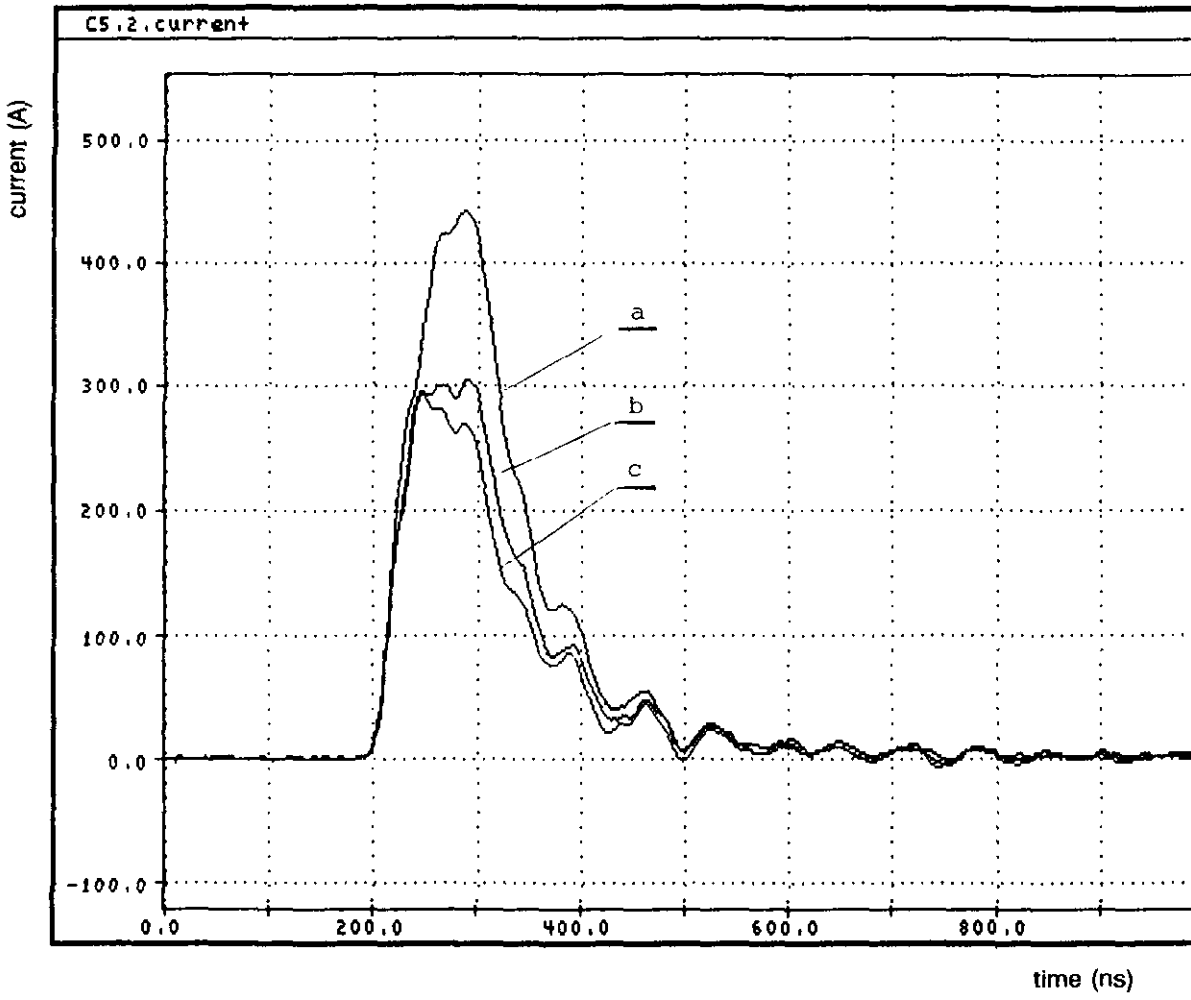

Figure 23b: Current waveform of the corona discharge in air and flue gas. a: air, b: flue gas I, c: flue gas II, Vp = 60 kV, Li = 0 uH, R = 40 Ω and Vdc = 30 kV.

3.10 Comparison of the SPS and FNS emission in air and in flue gas

The SPS and FNS light emission have also be measured with flue gas at the same position. Figue 24 and figure 25 show the comparison of SPS and FNS in flue gas I and in flue gas II with the emission in air respectively.

(see figure 24 from data c-92)

Figure 24. The comparison of light emission in flue gas I and in air. Vdc=30 KV, Vp=60 KV, Li=0, R=0

(see figure 25 from data c-92)

Figure 25. The comparison of light emission in flue gas II and in air. Vdc=30 kV, Vp=60 KV, Li=0, R=0

It was observed that the SPS emission in flue gas I and in flue gas II are very similar to the emission in air. However, the FNS emission in flue gas I is about 4 to 6 times stronger than in air for the primary streamer. As for as the flue gas II, the results are very similar to the air.

Generally speaking, the relative light emission intensity can be influenced by two factors, i.e. the energy distribution fuctions and the quenching processes. However, lack of data and uncertainty of quenching processes make it very hard to estimate the electron energy.

Considering the gas compositon in flue gas I and flue gas II and their emission intensity, only taking into account of gas composition seem to be not enough to explain the results. The effects of gas temperature on corona streamer seems not only just to reduce the gas density. Temperature may also play an important role in the evaluation of the importance of different quenching processes according to the associated activation energy.

As for the emission intensity of the secondary streamer, it can be concluded that the secondary streamer in flue gas may be extremely limited compared to the secondary streamer in air. This fact may be due to the larger attachment coefficient in flue gas, which leads to a higher electric field in the discharge channel when the primary streamer has crossed the gap. In air this field is ~ 5 kV/cm, near the anode the field has the critical value of ~ 25 kV/cm, the voltage across the gap is ~ 70 kV (see fig. 23a) so the secondary streamer can extend 1.5 cm into the gap. If the secondary streamer does not exist in flue gas than its electric field in the channel is ~ 8 kV/cm.

Therefore, we can conclude that the secondary streamer in flue gas is shorter and the corresponding electron energy is smaller when compared with that in air. While for the primary streamers, the associated electron energy may be larger than that in air.

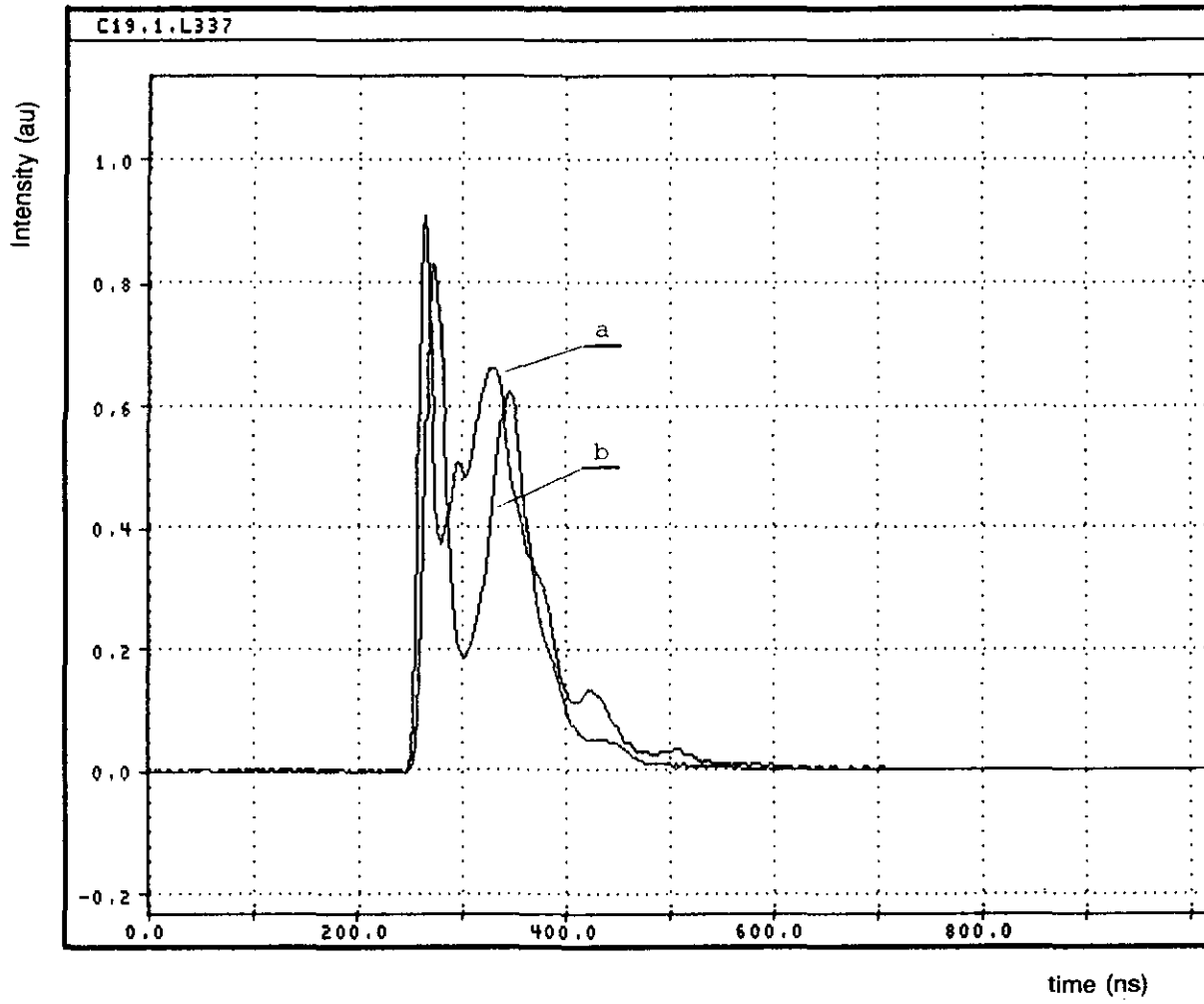

Figure 24a: Maximum of N_2 SPS emission as a function of time. a: flue gas I, b: air, Vp = 60 kV, Vdc = 30 kV, Li = 0.

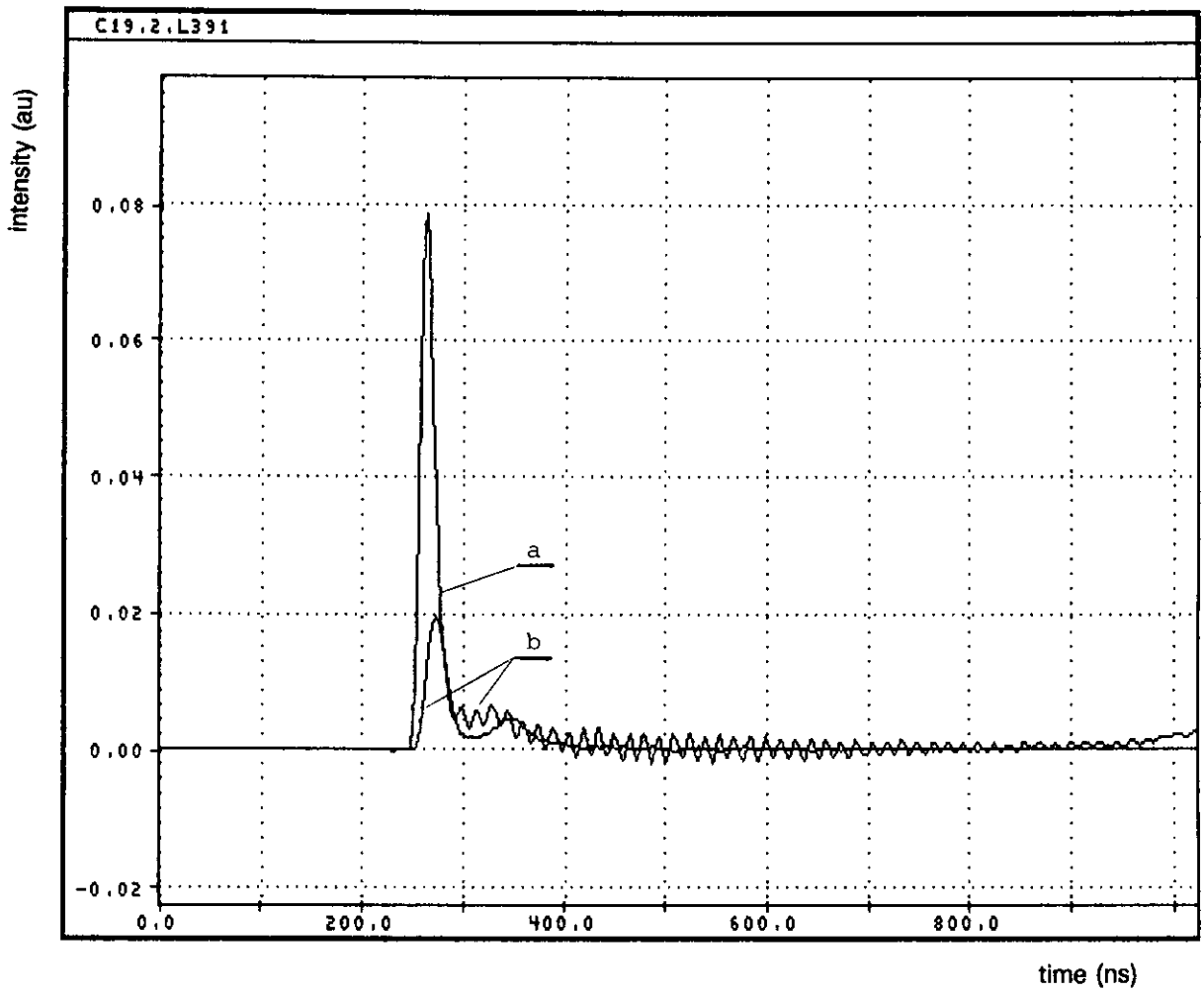

Figure 24b: Maximum of N_2^+ FNS emission as a function of time.
a: flue gas I, b: air, Vp = 60 kV, Vdc = 30 kV, Li = 0.

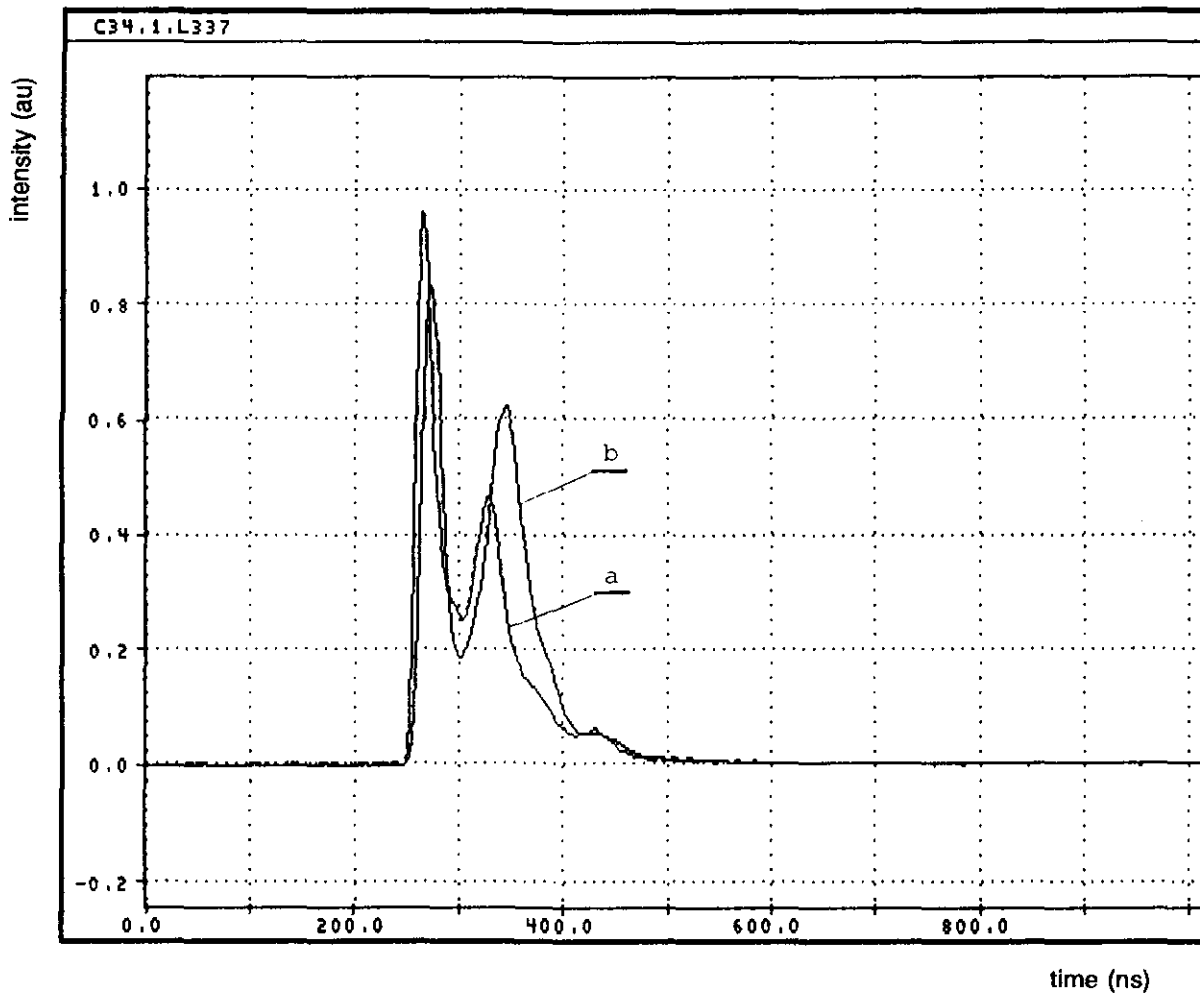

Figure 25a: Maximum of N_2 SPS emission as a function of time.
a: flue gas II, b: air, Vp = 60 kV, Vdc = 30 kV, Li = 0.

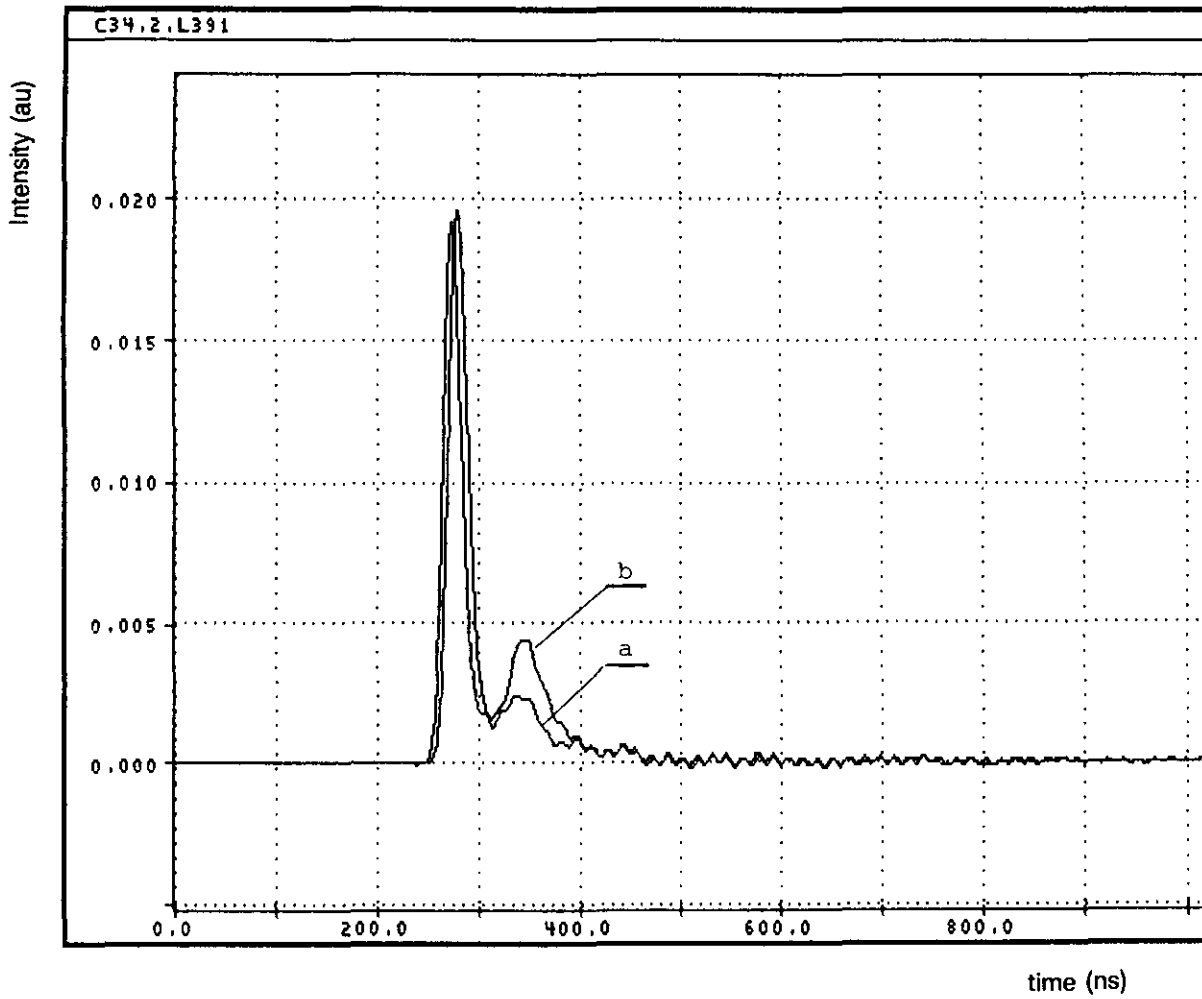

Figure 25b: Maximum of N_2^+ FNS emission as a function of time.
a: flue gas II, b: air, Vp = 60 kV, Vdc = 30 kV, Li = 0.

3.11 Optimization of energization for flue gas cleaning by pulsed streamer corona

If considering the pulse corona streamer as a active electrons generator, the promoted chemical reactions may be releated to the active electrons production and to the slow electrons production with respect to different chemical processes.

However, if concentrating on the active electrons production by pulse corona streamer, the main question releated to the energization for promoting the chemical oxidation is that what is the operation conditions in order to obtain the maximum active electrons production per unit energy injection. The question can be also expressed as what kinds of streamer structure is responsible for much more active electrons production per unit energy injection and per unit discharging volume.

As we known, pulse energization has been widely used in ESP for charging the fly ash in order to eliminate the back corona and to reduce the energy consumption. Several circuits for pulse generators have been proposed over the world for pulse corona in ESP. The energy intensity for charging fly ash is in the range several mJ per m emitting wire, which is much smaller than the energy density of corona streamer produced here for promoting chemical reactions. The corresponding different corona structure may lead to different requirement for the design of pulse voltage generator.

As we known, up to date, no direct experimental results have indicated the requirement of pulse generator for promoting chemical oxidation and no criterium is available for designing the pulse voltage generator.

If the total active electrons production per pulse is adopted as a target fuction to evaluate the energization process, it can be easily seen that only primary streamer is responsible for active electrons production. The optimal energization can be realized if the secondary streamer can be totally controled.

Based on the experimental results, it can be concluded that the secondary streamers are only produced if the voltage level is also very high when the primary streamer is across the gap. The typical results to show different primary and secondary streamer with different additional inductance are indicated in figure 26.

(see figure 26 from data c-92)

Figure 26. The influence of additional inductance on FNS and SPS light emission in air, Vdc=30 KV, Vp=60KV, a : Li=0, b: Li=11.2uH

If the light emission is directly proportional to the streamer number, it can be concluded that with reducing the rise rate of pulse voltage by increasing the additional inductance, the primary streamer number is decreased but the duration of the secondary streamer is enlarged.

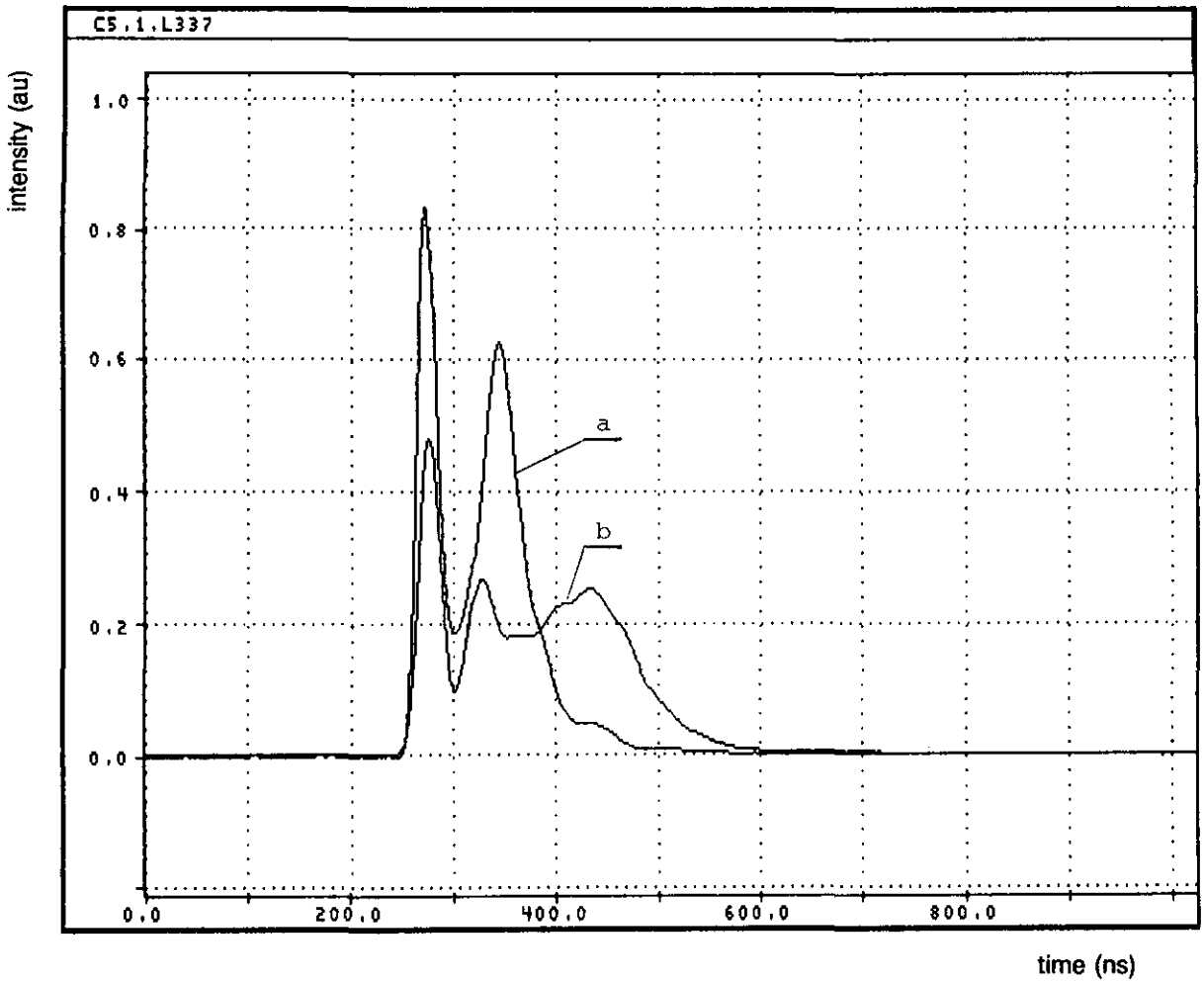

Figure 26a: Maximum of N_2 SPS emission in air as a function of time for different series inductance.
a: Li = 0 uH, b: Li = 11.2 uH, Vp = 60 kV, Vdc = 30 kV.

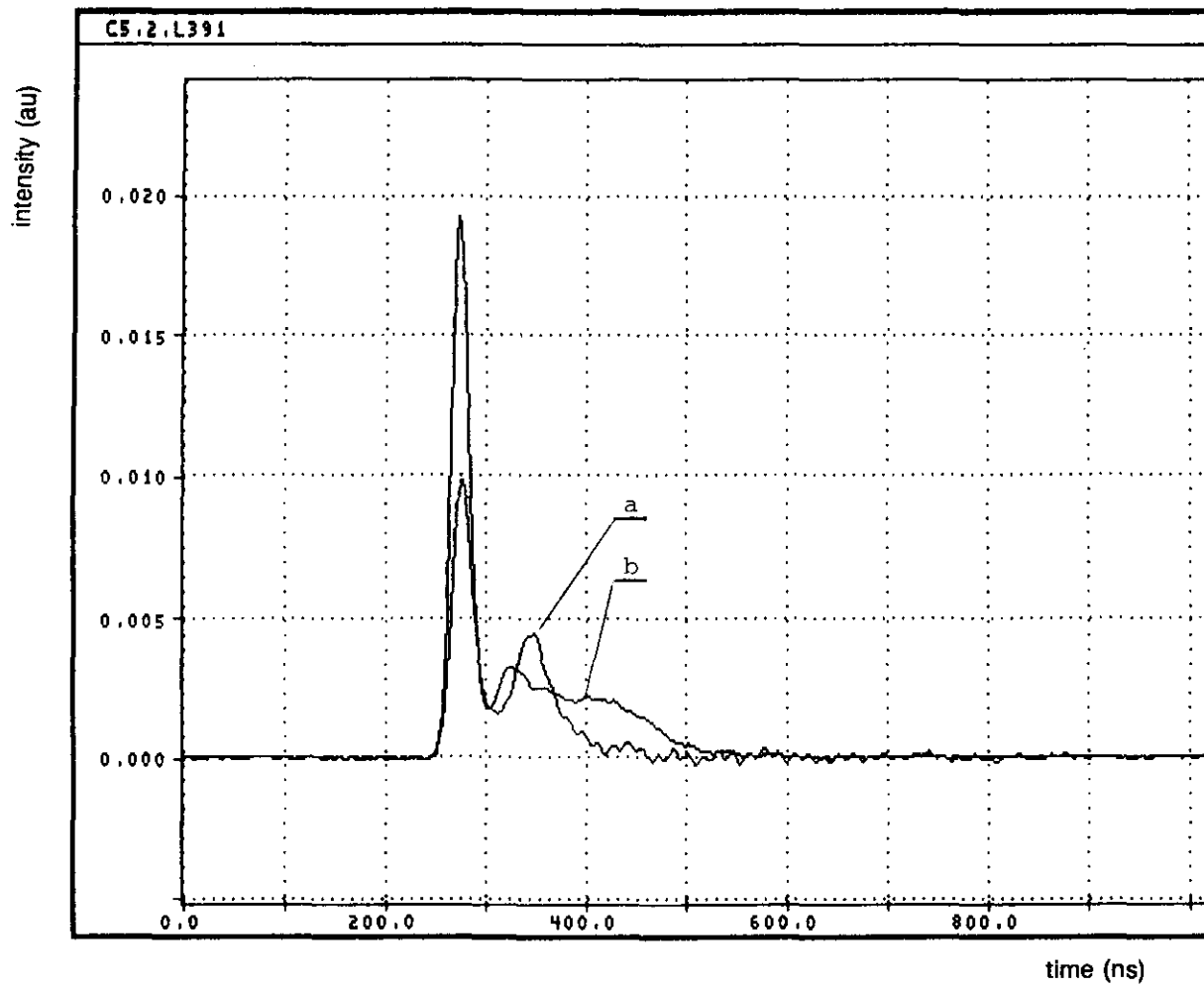

Figure 26b: Maximum of N_2^+ FNS emission in air as a function of time for different series inductance.
a: Li = 0 uH, b: Li = 11.2 uH, Vp = 60 kV, Vdc = 30 kV.

The energy conversion from the pulse generator to the reactor seems to be realized by two types of discharging structure.

- much more primary streamer and very limited secondary streamer
- very stronge secondary streamer and very limited primary streamer.

In principle, the control of secondary streamer can be obtained by means of optimising the DC bias level, the pulse voltage level, the emitting wire, the circuit parameters. It has also been observed that the primary streamers last from 30 ns to about 120 ns with different applied voltage. The energy releated to the primary streamers propagation can be changed at least up to 50%. With reducing the stored energy in the circuit and together with small inductance and a thicker emitting wire, the percentage can be even larger.

Considering the difference between flue gas and air, the secondary streamer in flue gas may be strongly limited as indicated by the normalized emission in figure 27.

Therefore, it can be concluded that when designing the pulse voltage generator for flue gas cleaning, the main criterium is to limit the secondary streamers evaluation.

(see figure 27 from data c-5)

Figure 27 indicates the normalized SPS and FNS light emission

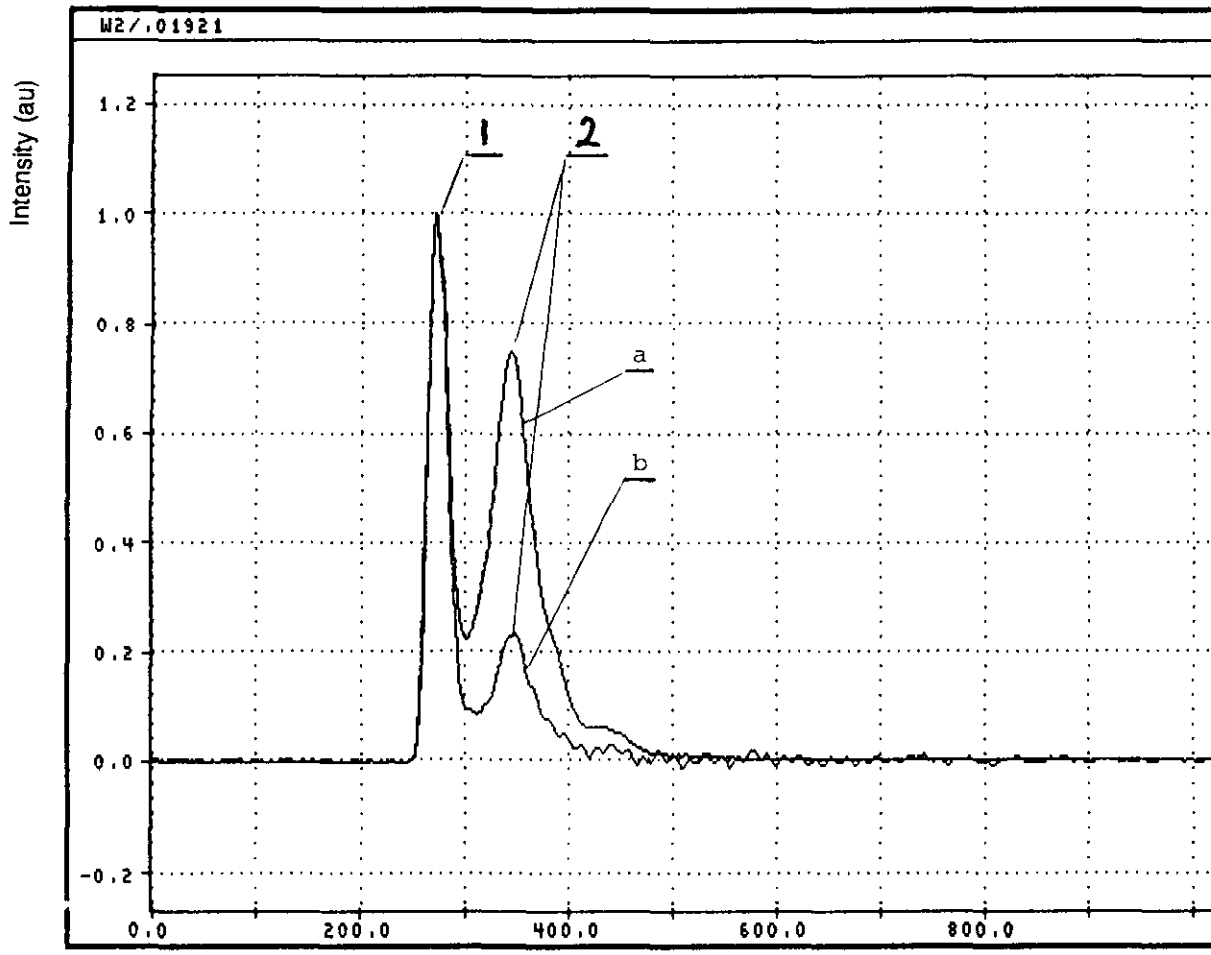

Figure 27a: Comparison of SPS (a) and FNS (b) emission in air for primary (1) and secondary (2) streamers.
Vp = 60 kV, Vdc = 30 kV, Li = 0, R = 0.

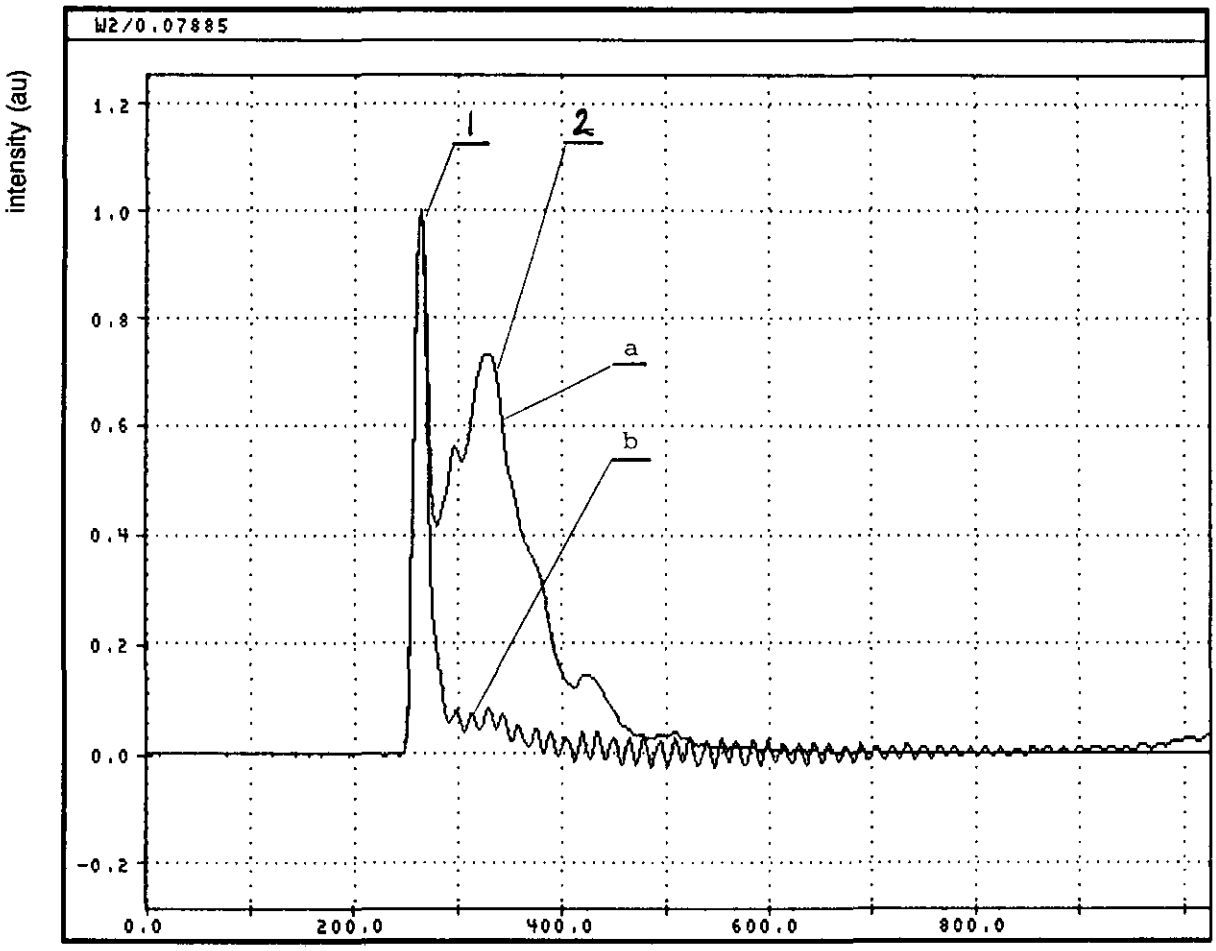

Figure 27b: Comparison of SPS (a) and FNS (b) emission in flue gas I for primary (1) and secondary (2) streamers.
Vp = 60 kV, Vdc = 30 kV, Li = 0, R = 0.

3.12 Preliminary experiment on flue gas cleaning efficiency

A cleaning experiment is performed to compare the capabilities of our facility with with results published in literature. The set-up is adapted in two ways, in the first place an NO injection system is added. This uses a nozzle of 0.1 mm diameter which provides a sonic flow of gas at an overpressure of 0.2 to 1 bar. The injection is perpendicular to the flow velocity at 2 m from the corona wire. Due to the strong turbulence of the flow mixing is expected to be sufficient. The flow is determined with a rotameter having a maximum capacity of 0.12 Sltr/min.

The second adaption is necessary to provide the required residence time of the gas in the discharge volume. The corona wire has a length of 1 m, so a gas velocity in the order of 1-5 m/s is required for a sufficient treatment of the gas. This implies a relatively low gas flow which has insufficient heat capacity to maintain the gas temperature above its condensation value. Therefore additional heating is required which is provided by electric heating tape, which consists of a resistive wire contained in silicon rubber. This tape can withstand 200 C, its total capacity is 800 W. It is wrapped around the cylinder from 1 m upstream the discharge downto the end of the discharge. By controlling the voltage on the tape the temperature of the cylinder can be regulated between 20 and 100 C.

The gas flow is determined by means of a pitot tube. The pressure difference is increased by surging the flow through a tube of 21 mm diameter. It was estimated that the flow in this tube is very turbulent and that viscosity plays no role, therefore the determination of the flow is straightforward and requires only the mass density of flue gas at the given temperature. The thickness of the boundary layer is the only remaining uncertainty. The accuracy of the flow used in the experiment decribed here, i.e. 10 m^3/hr, is estimated to be 10%.

The experiment is performed with an initial NO concentration of 290 ppm, for NO_2 48 ppm. The flue gas temperature is maintained at 70 C by means of the external heating. Due to the available ventilators and the safety requirements of the gas burner the gas composition was not (yet) real flue gas. It containes 2.1% CO_2, 4.2% H_2O, 17% O_2 and 77% N_2. The voltage pulses are made with the circuit as desribed in fig. 2, using 30 kV DC bias and 60 kV on the power supply of the pulse part. Largely due to the 10 Mohm coupling resistor this leads to a pulse of 40 kV on the wire when the repetition rate is increased to 30 Hz. This situation can be improved by replacing this resistor with a lower value type in combination with a large inductance. This will also allow higher repetition rates to be obtained, at least to 150 Hz. Now the rep rate is limited to 30 Hz.

The experiments are performed with a steady flue gas flow. The settling time for the NO detector, an electrochemical cell, is about 1 minute. The corona is switched on and off several times for periods of about 5 minutes. The concentrations of NO and NO_2 are reproducable within ± 3 ppm. NO decreased from 290 to 205 upon corona energization and simultaneously NO_2 increased from 48 to 76 ppm. This effect is also described by other authors, when the energy input is relatively low.

The voltage and the current of the pulsed used here are recorded and shown in fig. 28. The energy input per pulse is calculated to be 0.49 J. This leads to an energy input into the gas of 1.5 Wh/Nm^3 for an NO decrease of 85 ppm, which is almost a factor 3 lower compared to results presented up to now in literature. In most of these studies longer pulses have been used, this supports our ideas that the energy input into the secondary streamers is not used efficiently for the cleaning process.

This measurement must be repeated with a systematic variation of flue gas and power supply conditions. This will yield information about the optimum pulse shape and the maximum cleaning effect that can be achieved. If these results can be combined with the models of the gas discharge and the chemical process it can probably lead to a better understanding of the effects and provide means to optimize the whole cleaning process.

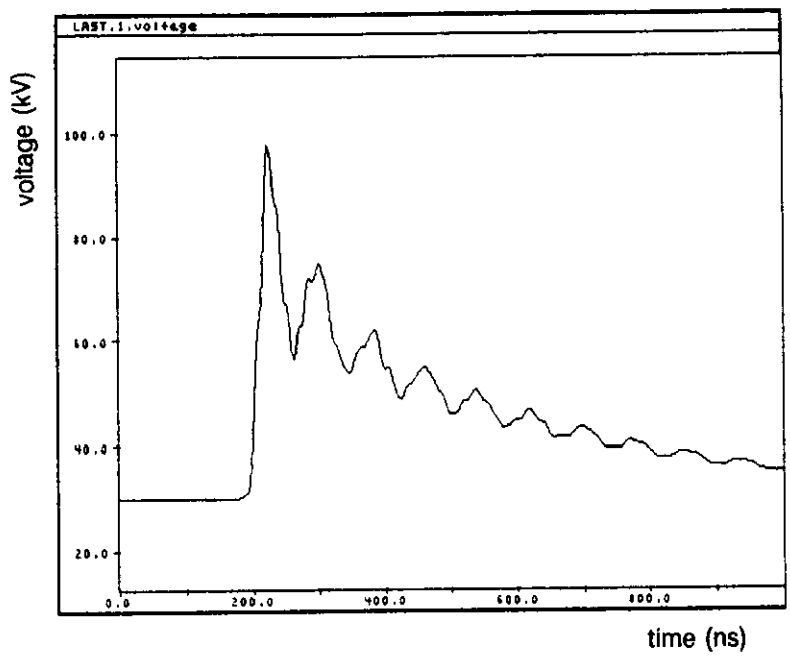

Figure 28 a: Voltage waveform of pulse used during cleaning experiment

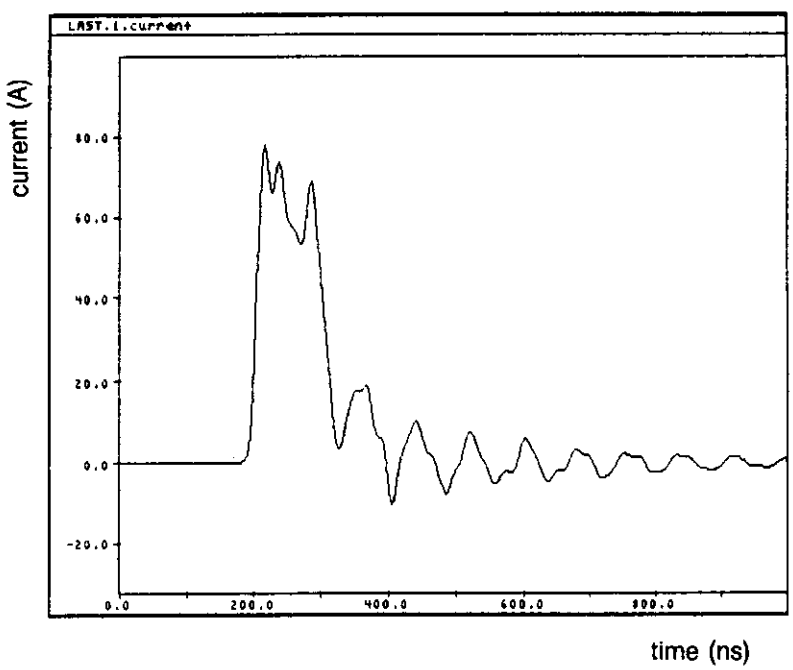

Figure 28 b: Current waveform of pulsed used during cleaning experiment

4. CONCLUSIONS AND SUGGESTIONS

Based on the experimental results obtained in air and in flue gas, following concluding remarks are summarized.

- The influence of electrical circuit on the pulse corona streamer has been demonstrated by means of electrical and optical measurements.

- With the current test conditions, the different streamer structure can be produced, which corresponds to different electrical and optical properties.

- The corona current is almost uniformuly distributed along the emitting wire and it can last from 100 ns to 600 ns with a maximum peak current of about 600 A. The obtained streamer intensity is limited by the power supply instead of the interface between streamers.

- The peak voltage can reach 110 KV with a 30 ns rise time, but without leading to breakdown. The maximum rise rate is supposed to be limited by the spark gap system instead of by the stray inductance of the electrode arrangements.

- The same energy conversion from the pulse voltage generator to the reactor can be realized with different streamer structure. Under the fast rise conditions, the main part of energy conversion is obtained by means of much more primary streamers. However, under the slow rise rate, the energy conversion is mainly realized by means of secondary streamers.

- Based on the light emission from the emitting wire and near the cathode, the average primary streamer speed is in the range of 0.5 m/us -3 m/us, which is increased with the increase of total applied voltage.

- The local light emission also indicates that the secondary streamer occurs when the primary streamer is across the gap, and its intensity strongly depends on the voltage level at that period. The primary streamer can be produced at different time. Roughly speaking the time difference between different streamers is in the range from 10 ns to 600 ns.

- The time resolved spectrum indicates that the average electron energy related to the primary streamer is much larger than that the energy associated to the secondary streamer. Both electron energies increase slightly with increasing applied voltage.

- If the channel is supposed to be a resistor with the same conductive current flow along the channel and theory of two-platform controlled electric field regions is also valid in this conditions, the secondary streamers are supposed to reach about 2 - 3 cm with a decay of electron energy from the emitting wire. This hypothesis seems to be very reasonable when it is compared with photos of corona streamer.

- The energy releated to the first primary streamers can be in the range of 30% - 50

% of the total injected energy. With reducing the stored energy in the pulse voltage generator, the percentage can become larger.

- Under the same power supply, the energy conversion to flue gas is smaller compared with the energy to air. The difference becomes much more obvious when the applied voltage is lower.

- The electron energy for the primary streamer is supposed to be larger in the flue gas than in air. However, the secondary streamer is limited in flue gas.

- Optimization of energization for promoting chemical oxidation by pulse corona can be realized by means of controlling the secondary streamer evaluation.

- The criterium for designing the pulse voltage generator for flue gas cleaning is to limit the secondary streamer evaluation together with enhancing the primary streamer number.

- The releation between the streamer structure and the chemical oxidation is need to be investigated in the future.

- For reducing the global energy consumption for De-SOx and De-NOx, two other stages are also recommded in order to enlarge the research possibility.

- For the experimental investigation, the limitation often arises from the power supply. Based on the size of this arrangements, the DC bias level should run in the range till 60 KV.

- The emitting wire can be designed with the maximum value of the DC bias level, its corresponding DC corona onset is set to be just larger than the DC base level.

- For the pulse repetition rate, the main limitation is due to the circuit; however, with modifying the charging and the discharging circuits, a high frequency is expected to be obtained.

- An NO reduction from 290 to 205 ppm has been observed in flue gas of 70 C using pulses with 40 kV amplitude, 30 kV DC bias and 30 Hz rep rate, simultaneously the NO2 concentration rises from 48 to 76 ppm.

- The energy consumption of the cleaning experiment is 1.5 Wh/Nm^3, with a current duration of 100 ns. This is about three times lower than results obtained elsewhere with longer pulses, this supports the theory that the primary corona is mainly responsible for the chemical activity.

5. REFERENCES

1. Civitano, L., et al.,
Flue gas simultaneous De/NOx and De/SO2 by impulse corona energization.
International Atomic Energy Agency, Vienna, IAEA-TECDOC-428, (1987), p. 55-84.

2. Matzing, H.,
Chemical kinetics of flue gas cleaning by electron beam.
Kernforschungszentrum Karlsruhe, Germany, 1989,
Report KfK 4494.

3. Potapkin, B.V. et al.,
Plasma-catalysis SO_2 oxidation in air.
Proc. 10th Int. Symp. on Plasma Chem., Bochum, August 1991.
Bochum: Int. Union of Pure and Appl. Chem., 1991, Paper 3.2-4.

4. Gallimberti, I.,
Impulse corona simulation for flue gas treatment.
Pure & Appl. Chem, vol. 60(1988), no. 5, p. 663-674.

5. Bastien, F. and E. Marode,
Breakdown simulation of electronegative gases in non-uniform field.
J. Phys. D: Appl. Phys., vol. 18(1975), p. 377-393.

6. Massimo Rea and Keping Yan,
Energization of pulse corona induced chemical processes.
NATO-Advanced workshop on Non-Thermal Plasma Techniques for Pollution Control, Cambridge, September 1992.
New York: Springer, 1993, to be published.

7. Creygton, Y. L. M. and E.M. van Veldhuizen,
Status report pulse positive corona for flue gas cleaning.
Division of Electrical Energy Systems, Faculty of Electrical Engineering, Eindhoven University of Technology, 1992.
Divisional Report EG/92/573.

8. Spyrou, N. and C. Manassis,
Spectroscopic study of a positive streamer in a point-to-plane discharge in air: Evaluation of the electric field distribution.
J. Phys. D: Appl. Phys., vol. 22(1989), p. 120-128.

9. Verhaart H.F.A.,
Discharge parameters in flue gas.
KEMA Scientific & Technical Report, vol. 7(1989), p. 377-383.
N.V. KEMA, Arnhem, The Netherlands.

Eindhoven University of Technology Research Reports ISSN 0167-9708
Coden: TEUEDE

Faculty of Electrical Engineering

(248) Hoeijmakers, M.J. and J.M. Vleeshouwers
DERIVATION AND VERIFICATION OF A MODEL OF THE SYNCHRONOUS MACHINE WITH RECTIFIER WITH TWO DAMPER WINDINGS ON THE DIRECT AXIS.
EUT Report 90-E-248. 1990. ISBN 90-6144-248-6

(249) Zhu, Y.C. and A.C.P.M. Backx, P. Eykhoff
MULTIVARIABLE PROCESS IDENTIFICATION FOR ROBUST CONTROL.
EUT Report 91-E-249. 1991. ISBN 90-6144-249-4

(250) Pfaffenhöfer, F.M. and P.J.M. Cluitmans, H.M. Kuipers
EMDABS: Design and formal specification of a datamodel for a clinical research database system.
EUT Report 91-E-250. 1991. ISBN 90-6144-250-8

(251) Eijndhoven, J.T.J. van and G.G. de Jong, L. Stok
THE ASCIS DATA FLOW GRAPH: Semantics and textual format.
EUT Report 91-E-251. 1991. ISBN 90-6144-251-6

(252) Chen, J. and P.J.I. de Maagt, M.H.A.J. Herben
WIDE-ANGLE RADIATION PATTERN CALCULATION OF PARABOLOIDAL REFLECTOR ANTENNAS: A comparative study.
EUT Report 91-E-252. 1991. ISBN 90-6144-252-4

(253) Haan, S.W.H. de
A PWM CURRENT-SOURCE INVERTER FOR INTERCONNECTION BETWEEN A PHOTOVOLTAIC ARRAY AND THE UTILITY LINE.
EUT Report 91-E-253. 1991. ISBN 90-6144-253-2

(254) Velde, M. van de and P.J.M. Cluitmans
EEG ANALYSIS FOR MONITORING OF ANESTHETIC DEPTH.
EUT Report 91-E-254. 1991. ISBN 90-6144-254-0

(255) Smolders, A.B.
AN EFFICIENT METHOD FOR ANALYZING MICROSTRIP ANTENNAS WITH A DIELECTRIC COVER USING A SPECTRAL DOMAIN MOMENT METHOD.
EUT Report 91-E-255. 1991. ISBN 90-6144-255-9

(256) Backx, A.C.P.M. and A.A.H. Damen
IDENTIFICATION FOR THE CONTROL OF MIMO INDUSTRIAL PROCESSES.
EUT Report 91-E-256. 1991. ISBN 90-6144-256-7

(257) Maagt, P.J.I. de and H.G. ter Morsche, J.L.M. van den Broek
A SPATIAL RECONSTRUCTION TECHNIQUE APPLICABLE TO MICROWAVE RADIOMETRY.
EUT Report 92-E-257. 1992. ISBN 90-6144-257-5

(258) Vleeshouwers, J.M.
DERIVATION OF A MODEL OF THE EXCITER OF A BRUSHLESS SYNCHRONOUS MACHINE.
EUT Report 92-E-258. 1992. ISBN 90-6144-258-3

(259) Orlov, V.B.
DEFECT MOTION AS THE ORIGIN OF THE 1/F CONDUCTANCE NOISE IN SOLIDS.
EUT Report 92-E-259. 1992. ISBN 90-6144-259-1

(260) Rooijackers, J.E.
ALGORITHMS FOR SPEECH CODING SYSTEMS BASED ON LINEAR PREDICTION.
EUT Report 92-E-260. 1992. ISBN 90-6144-260-5

Eindhoven University of Technology Research Reports ISSN 0167-9708
Coden: TEUEDE

Faculty of Electrical Engineering

(261) Boom, T.J.J. van den and A.A.H. Damen, Martin Klompstra
IDENTIFICATION FOR ROBUST CONTROL USING AN H-infinity NORM.
EUT Report 92-E-261. 1992. ISBN 90-6144-261-3

(262) Groten, M. and W. van Etten
LASER LINEWIDTH MEASUREMENT IN THE PRESENCE OF RIN AND USING THE RECIRCULATING SELF HETERODYNE METHOD.
EUT Report 92-E-262. 1992. ISBN 90-6144-262-1

(263) Smolders, A.B.
RIGOROUS ANALYSIS OF THICK MICROSTRIP ANTENNAS AND WIRE ANTENNAS EMBEDDED IN A SUBSTRATE.
EUT Report 92-E-263. 1992. ISBN 90-6144-263-X

(264) Freriks, L.W. and P.J.M. Cluitmans, M.J. van Gils
THE ADAPTIVE RESONANCE THEORY NETWORK: (Clustering-) behaviour in relation with brainstem auditory evoked potential patterns.
EUT Report 92-E-264. 1992. ISBN 90-6144-264-8

(265) Wellen, J.S. and F. Karouta, M.F.C. Schemmann, E. Smalbrugge, L.M.F. Kaufmann
MANUFACTURING AND CHARACTERIZATION OF GAAS/ALGAAS MULTIPLE QUANTUMWELL RIDGE WAVEGUIDE LASERS.
EUT Report 92-E-265. 1992. ISBN 90-6144-265-6

(266) Cluitmans, L.J.M.
USING GENETIC ALGORITHMS FOR SCHEDULING DATA FLOW GRAPHS.
EUT Report 92-E-266. 1992. ISBN 90-6144-266-4

(267) Józwiak, L. and A.P.H. van Dijk
A METHOD FOR GENERAL SIMULTANEOUS FULL DECOMPOSITION OF SEQUENTIAL MACHINES: Algorithms and implementation.
EUT Report 92-E-267. 1992. ISBN 90-6144-267-2

(268) Boom, H. van den and W. van Etten, W.H.C. de Krom, P. van Bennekom, F. Huijskens, L. Niessen, F. de Leijer
AN OPTICAL ASK AND FSK PHASE DIVERSITY TRANSMISSION SYSTEM.
EUT Report 92-E-268. 1992. ISBN 90-6144-268-0

(269) Putten, P.H.A. van der
MULTIDISCIPLINAIR SPECIFICEREN EN ONTWERPEN VAN MICROELEKTRONICA IN PRODUKTEN (in Dutch).
EUT Report 93-E-269. 1993. ISBN 90-6144-269-9

(270) Bloks, R.H.J.
PROGRIL: A language for the definition of protocol grammars.
EUT Report 93-E-270. 1993. ISBN 90-6144-270-2

(271) Bloks, R.H.J.
CODE GENERATION FOR THE ATTRIBUTE EVALUATOR OF THE PROTOCOL ENGINE GRAMMAR PROCESSOR UNIT.
EUT Report 93-E-271. 1993. ISBN 90-6144-271-0

(272) Yan, Keping and E.M. van Veldhuizen
FLUE GAS CLEANING BY PULSE CORONA STREAMER.
EUT Report 93-E-272. 1993. ISBN 90-6144-272-9